MASTERARBEIT | MASTER‘S THESIS

Titel | Title

Mortality and Temperature in Austria:
Regional and Demographic Patterns

verfasst von | submitted by

Christine Billinger BSc

angestrebter akademischer Grad | in partial fulfilment of the requirements for the degree of

Master of Science (MSc)

Wien | Vienna, 2026

Studienkennzahl lt. Studienblatt | Degree programme code as it appears on the student record sheet:	UA 066 945
Studienrichtung lt. Studienblatt | Degree programme as it appears on the student record sheet:	Masterstudium Global Demography
Betreut von | Supervisor:	Hon.-Prof. Dipl.-Geogr. Dr. Marc Luy Privatdoz.

Acknowledgements

I am sincerely grateful to my supervisor Hon.-Prof. Dipl.-Geogr. Dr. Marc Luy, Privatdoz., for his continued support throughout the thesis and for encouraging me to pursue the topic I was most interested in.

Another thank-you goes to my writing buddy, Chiara, who worked on her thesis alongside me. Sharing the highs and lows of the process made it more enjoyable – as did comparing the amounts of green peas in our meals.

The Lernbar crew deserves a mention for always being good at getting my mind off demography. A special mention goes to Matthias, who was a great help when it came to working with topographical data.

Thanks also to my demography colleagues and friends who supported me in the finalising process.

Finally, I want to thank my family: my brother for being my helpdesk when I first used an API, my parents for supporting me throughout my studies, and my sister for always supporting me, especially when I first moved to Vienna.

Table of Contents

List of Abbreviations

Abbreviation	Definition
API	Application Programming Interface
BLUP	Best Linear Unbiased Predictor
DLNM	Distributed Lag Non-Linear Model
ESP	European Standard Population
EU	European Union
MMT	Minimum Mortality Temperature

List of Figures

List of Tables

1 Introduction

Exposure to suboptimal temperatures has been identified as one of the leading risk factors of mortality globally, with more than 800,000 deaths in Europe annually (Brauer et al., 2024; Zhao et al., 2021). Cold- and heat-associated mortality differ in their underlying causes. Cold affects health outcomes primarily through indirect mechanisms, most notably through influenza and similar infections, but also through cardiovascular and respiratory complications (Ballester et al., 2016). Heat, by contrast, tends to affect the body more directly (Fastl et al., 2024).

In the past decades, there were by far more cold-related than heat-related deaths in Europe. This gap, however, is projected to converge. An analysis across European regions investigated the temperature-mortality relationship considering different scenarios of global warming. With an increase of 4 °C, heat- and cold-related deaths could become close to equal burdens (García-León et al., 2024).

In Austria, people aged 15 to 30 self-reported the highest heat burden across all income groups. Those aged 60 and over indicated below-average levels of stress, although this should not be confused with their actual health risk, which is typically higher for the older population. The heat burden was reported lower in rural regions, whereas in the capital, Vienna, around 60% of residents reported being strongly burdened by heat, independent of their income level (Statistik Austria, 2025f).

In 2024, the Austrian Federal Ministry of Social Affairs, Health, Care and Consumer Protection published an updated National Heat Protection Plan. This plan focuses on public early warning systems, behavioural advice, outreach to vulnerable populations and heat planning requirements for healthcare institutions. The planning of structural measures to reduce urban heat is largely left to the federal states, each of which have developed their own heat protection plans (Schmidt et al., 2024).

Health outcomes vary across Austria's federal states, with a visible east-west gradient. Western federal states, such as Vorarlberg, Tyrol and Salzburg, show lower mortality and higher life expectancy, while eastern federal states are disproportionately affected by cardiovascular mortality (Statistik Austria, 2025d; Stein et al., 2011). Heat exposure may add to this disparity, with eastern regions experiencing more heat days annually (Fastl et al., 2024).

As Austria's regional health disparities and climate exposure patterns emerge alongside an ageing population, which amplifies both cold- and heat-related mortality (Chen et al., 2024), the question of how temperature-related mortality differs across Austria's regions and age groups is becoming increasingly relevant for public health. Understanding these disparities is essential for targeted mitigation strategies. Such regional analyses remain rare in Central Europe. Janoš et al. (2024) characterised their countrywide study of temperature-related mortality in the Czech Republic as the first of its kind in the region. This thesis aims to address this gap in regional temperature-mortality research for Austria by combining daily temperature grid data with weekly mortality counts from March 2011 to March 2025. The relationship of mortality and temperature is analysed across federal states and by demographic subgroups, namely age and sex, modelling exposure-response curves and estimating minimum mortality temperatures, as well as attributable death fractions to non-optimal temperatures.

2 Literature Review

Analyses of the association between temperature and mortality have been conducted at multiple levels, from individual cities to entire continents (e.g., Ballester et al., 2011; Gallo et al., 2024; Hutter et al., 2007). Although different regions experience distinct temperature and weather patterns, some dynamics, like higher mortality being associated with extreme temperatures, are consistent across studies (Ballester et al., 2011; García-León et al., 2024).

This chapter provides an overview of existing literature on the temperature-mortality relationship. Factors known to affect this relationship include region, time, age, health conditions, sex, and socioeconomic differences (Achebak et al., 2019; García-León et al., 2024; Son et al., 2019). Additionally, the potential impact of climate change and population ageing on future health outcomes is taken into consideration, as both may shape the relationship (de Schrijver et al., 2022; García-León et al., 2024).

2.1 The Temperature-Mortality Relationship

The relationship between temperature and mortality has previously been compared with the shapes of different letters. It is mostly claimed that the relationship between daily temperature and death counts is U- or V-shaped (Achebak et al., 2019; Ballester et al., 2016; Conte Keivabu, 2022; Visser et al., 2022), in some more specific cases it can also be described as J- , reversed J- or slightly W-shaped (Cheng et al., 2019; Lowe et al., 2015; Masselot et al., 2023; Pascal et al., 2023). In all cases, it is clear that mortality is rising as temperature increases or decreases and there is a range of more comfortable temperatures in between, where mortality is at its lowest (Ballester et al., 2011). This point is called minimum mortality temperature (MMT) and ranges somewhere between 15 °C and 21 °C daily mean temperature in most analyses. This varies due to different geographic locations and demographic factors like sex and age (Achebak et al., 2019; Gallo et al., 2024; Vésier & Urban, 2023).

It is important to differentiate between cold- and heat-related mortality, since the causes of death in each case vary substantially. Cold temperatures are associated with indirect health effects, particularly ischemic heart disease, respiratory illnesses and strokes. The correlation between winter mortality and influenza is also well established. However, direct effects, such as hypothermia, also play a role (Ballester et al., 2016). In comparison, heat stress, defined as the point where the body feels strain from heat (Fastl et al., 2024), has an immediate risk of disease aggravation and homeostatic failures (Ballester et al., 2016). Heat is also linked to mental health issues and, particularly in older adults, it raises blood pressure, strains the heart and worsens diabetes control (Fastl et al., 2024). Evidence from an analysis with Swiss data suggests that rising temperatures may contribute to higher numbers of suicidal acts (Bär et al., 2022). In numbers, about 6.63% of deaths in European cities are attributed to cold temperatures, while only 0.69% are attributed to heat (Masselot et al., 2023). Since rural areas face similar cold risks but fewer heat-related deaths than cities (de Schrijver, Royé, et al., 2023), the cold-heat mortality gap may be even wider. Another analysis that focused on Europe, found that the cold-to-heat-related death ratio was 8.3:1 between 1990 and 2020 (García-León et al., 2024).

2.2 Factors influencing the Temperature-Mortality Relationship

Analyses of the temperature-mortality relationship by demographic groups and by health conditions reveal additional heterogeneity and highlight the most vulnerable subgroups (e.g., Achebak et al., 2019; de Schrijver et al., 2022; Janoš et al., 2024; Kollanus et al., 2021; Masselot et al., 2023). Further analyses document how these patterns change over time and project future developments (e.g., de Schrijver, Sivaraj, et al., 2023; García-León et al., 2024; Martínez-Solanas et al., 2021). Estimating future health burdens requires explicitly accounting for demographic change, particularly population ageing, as well as climate change scenarios, which will further influence this relationship (de Schrijver et al., 2022).

2.2.1 Regional Variation

Urban areas are usually hotter than rural areas, especially at night, due to scarce vegetation and the trapping of heat through concrete, asphalt and dense buildings. This is called the “urban heat island” effect. Measures to mitigate this effect include insulation and air conditioning, although they are not as widespread in poorer areas. Air pollution adds to rising health risks in cities, especially during heat waves. Although urban areas are more exposed to high temperatures, rural areas are usually less prepared for heat. Weaker infrastructure, reduced health care availability and different sociodemographic structure, such as lower education levels and a larger older population, can heighten mortality risks linked to temperature (Fastl et al., 2024).

Looking at Europe, there is high heterogeneity in the risk patterns of cold- and heat-related mortality across regions. Considering data from the last three decades, it was found that the risk of heat-related death is overall six times higher in Southern Europe compared to Northern Europe and the risk of cold-related death is 2.5 times higher in Eastern Europe than in the West of Europe. Austrian regions were part of this analysis and exhibited higher cold- than heat-related mortality (García-León et al., 2024).

An analysis looked at the association between seasonal mean winter temperature and mortality across Western, Southern and Central European countries. The authors found strong temperature-mortality links for most countries, including Austria. They showed that there are more deaths in harsher winters. Despite influenza, a key driver of winter mortality, occurring at similar levels as in the other analysed countries, the link was notably weaker for the United Kingdom, Belgium and the Netherlands (Ballester et al., 2016).

There is high heterogeneity within countries concerning the differences between cold- and heat-related deaths (García-León et al., 2024). For example, in a country-level analysis using data from the Czech Republic, high variation in temperature-related mortality trends was found across regions (Janoš et al., 2024).

2.2.2 Temporal Trends and the Influence of Climate Change

Temperatures are increasing due to climate change in Europe (Ballester et al., 2023) and extreme weather events are expected to happen more frequently (Ballester et al., 2011; Kollanus et al., 2021) with the degree of warming determined by carbon dioxide (CO_2) emission levels (Achebak et al., 2019). According to what is known about the relationship between temperature and mortality, this suggests that mortality will likely rise further in the future. Achebak et al. (2019) found that the risk of cardiovascular deaths due to warm and cold temperatures decreased for all age groups and sexes in Spain between 1980 and 2016. This might seem unintuitive at first, considering rising temperatures, but when analysing the effect over time, one also needs to consider other factors influencing the relationship, like the change in life expectancy, life quality, healthcare services and socioeconomic conditions, which explain the decrease.

It seems that as the mean temperature rises, so does the minimum mortality temperature (Achebak et al., 2019). Assuming that both winters and summers are getting warmer with climate change, winter mortality will reduce in the long run everywhere in Europe (Ballester et al., 2016), but heat-related mortality will increase (Ballester et al., 2023; Huber et al., 2024). Northern and Mediterranean Europe are likely to see the greatest temperature increases while Western Europe will be less affected (Fastl et al., 2024; Martínez-Solanas et al., 2021). Martínez-Solanas et al. (2021) suggested that heat-related mortality will become most threatening to Mediterranean Europe in the upcoming decades and García-León et al. (2024) propose that regional disparities could increase due to a warming climate. There are several possible scenarios, but Mediterranean regions are especially vulnerable to greenhouse emission trajectories (Martínez-Solanas et al., 2021). With a 3 °C increase in global warming by 2100 under current policies, the total number of temperature-related deaths is estimated to increase because of the rise in heat-related deaths. The cold-to-heat-related death ratio for the years 1991-2020 is at 8.3:1 and is predicted to change to 2.6:1 by 2100 under these circumstances (García-León et al., 2024). Not fully consistent with this projection, an analysis of Switzerland found that in several scenarios both heat- and cold-related mortality will increase across the country. Yet, it is in line with heat becoming a larger burden on health than cold (de Schrijver, Sivaraj, et al., 2023). Some evidence suggests that cold-attributable mortality risk has already declined over the past decades, but overall there is little research on exposure to cold temperatures and resulting health responses (Achebak et al., 2019).

2.2.3 Differences in Age Groups and the Influence of Population Ageing

Not only global warming, but also population ageing will likely increase the number of non-optimal-temperature-related deaths (Chen et al., 2024). In 2009, it was claimed that the population aged 60+ was expanding at a rate of about 1.9% per year in more developed countries. Back then, the European median age was almost at 40 and was projected to reach 47 in 2050 (United Nations, 2009). According to Eurostat, the median age in 2024 for the 27 member states of European Union was at 44.7 years, a decade earlier in 2014 it was already at 42.5 years. Among women, the median age was already above 46 years in 2024 (Eurostat, 2025).

Population ageing can be defined as “the process by which older individuals become a proportionally larger share of the total population” (United Nations, 2010). In an analysis that includes locations across 50 countries, it was concluded that between a fifth and a quarter of the increase in heat-related deaths will be due to population ageing in the upcoming decades, assuming that there are no changes in population adaptation. Although climate warming might lead to a decrease in cold-related deaths, this reduction will be largely offset by population ageing in 18 of 50 countries. Within Europe, Eastern Europe is facing the biggest increase in population ageing, whereas Northern and Western Europe are experiencing increases at a lower level. This analysis did not include Austria, but several regions from neighbouring countries (Chen et al., 2024). Another analysis, using Swiss data, compared observed excess deaths due to non-optimal temperatures with estimates for a hypothetical population without population ageing. Heat- and cold-related deaths would have been about 50% lower without population ageing (de Schrijver et al., 2022). Looking at all of Europe in the summer of 2022, the hottest on record for the continent, an age pattern is visible, as the heat burden rises with age, but exhibits sex-specific differences. Among those aged 0-64, males experienced more heat-related deaths, while in older age groups (65-79 and 80+) females show higher heat-related mortality (Ballester et al., 2023). Population ageing is increasing the number of temperature-related deaths as overall older adults are more vulnerable to non-optimal temperatures, particularly to heat (Chen et al., 2024; Masselot et al., 2023). This is due to lower physiological, behavioural, cognitive and social capacities (Fastl et al., 2024).

Bär et al. (2022) analysed Swiss data from 1995-2016 and studied the relationship between the number of suicides and ambient temperature. Unlike previously described papers, this analysis included people younger than 65 years and divided them into subgroups. This could be explained by the lack of strong effects of extreme temperature on individuals younger than 65 years (Conte Keivabu, 2022; Gallo et al., 2024). Suicide cases were separated into the age groups: younger than 35, between 35 and 65 and 65 and above. Overall, the most suicides occurred among people in the age group 35-64. Between 1995 and 2016, the total number of suicides slightly declined, although the rate increased among individuals aged 65 and above. It was found that suicide risk increases with rising temperatures, although it flattens at the highest temperatures. People under 35 experienced the largest increases in risk as temperatures rose. This pattern may be explained by the influence of psychological disorders that occur in early adulthood and are associated with heat stress (Bär et al., 2022).

2.2.4 Effects by Health Conditions

Extreme heat is linked to a range of harmful health effects, which raises morbidity and mortality. Especially cardiovascular diseases and respiratory causes are highly mentioned in that context. Most excess deaths due to heat occur on the first day of heat waves. This is often followed by a drop in mortality. Higher temperatures worsen cardiovascular risk factors and the resulting physiological changes, together with reduced physical activity during heat waves, increase the risk of ischemic heart disease, heart failure, arrhythmias and acute events like strokes. Dehydration risk grows when chronic conditions like cardiovascular, respiratory and renal diseases disrupt thermoregulation (Fastl et al., 2024).

A paper by Flynn et al. (2005) provides an in-depth description of why older adults tend to be more affected by heat exposure. Older patients often have worse temperature regulation, as some commonly prescribed medications can weaken heat-loss mechanisms such as sweating, further increasing their risk of overheating. Heat strokes occur when high core body temperature is accompanied by a dysfunction of the central nervous system. Older adults also face an increased risk of kidney failure as they have reduced ability to retain salt and water in their body when they are dehydrated. Ageing weakens the regulation of the renin-angiotensin-aldosterone system, reducing levels of renin and aldosterone, which in turn impairs kidney filtering, increases the likelihood of high potassium levels and can ultimately disrupt heart activity and cause arrhythmias. In older adults, dehydration can increase blood viscosity, which raises the risk of heart attacks and strokes and can cause brain and nervous system problems.

Some analyses of the temperature-mortality relationship examined cause-specific mortality. Finnish mortality data revealed that heat days are associated with increased cardiovascular and respiratory mortality. Among the residents of social care facilities, a weak association of temperature with deaths from mental and behavioural disorders was identified (Kollanus et al., 2021). An analysis of Swiss data suggests that higher temperatures are associated with an increasing risk of suicidal behaviour (Bär et al., 2022).

Based on a paper by Ballester et al. (2016), cold temperatures are affecting mortality rates in two main ways. There are indirect effects through cardiovascular and respiratory diseases and direct effects like hypothermia. Year-to-year winter temperature fluctuations can predict seasonal mortality in many European countries, where colder temperatures are associated with more deaths. Exceptions from this relationship are the United Kingdom, the Netherlands and Belgium, where adaptations to temperature, like better housing insulation, seem to weaken this link.

2.2.5 Differences by Sex

An analysis using data from Czech Republic found minimum mortality temperature at 16.2 °C for women and at 20.0 °C for males (Vésier & Urban, 2023). Women seem to be more vulnerable to heat than men. Their mortality risks increase significantly to even higher values in the age-group 85+ and among divorced individuals. Men have more capability to regulate their body temperature under heat stress. The socioeconomic gap between men and women, especially in combination with marital status, could also influence the vulnerability to non-optimal temperatures (Vésier & Urban, 2023). Janoš et al. (2024) used Czech data and found women being more vulnerable to heat than men, although the gender gap in the minimum mortality temperature was smaller with 17.6 °C for women and 19.3 °C for men.

Other analyses also found overall higher temperature vulnerability for women compared to men (Achebak et al., 2019; Ballester et al., 2023; Kollanus et al., 2021). Although the results become more diverse when filtering also by age group. Examining the effects of heat waves in Finland, an analysis showed that long heat waves are greater threats than short ones, with the largest and most significant differences observed for women aged 75 or above, suggesting that women are more vulnerable to heat (Kollanus et al., 2021). Ballester et al. (2023), looking at European data from 2022, the hottest summer on record, found a similar pattern, with women aged 80 and above being the most vulnerable and reporting more heat-related deaths than men in that age group. In contrast, men had higher numbers of heat-related deaths than women in the age groups 0-64 and 65-79 (Ballester et al., 2023). For deaths among people with cardiovascular diseases, higher fractions of heat-attributable deaths were found among women across all age groups, whereas attributable fractions for cold-related deaths were higher for men in every age group except for 60-74 (Achebak et al., 2019).

Physiological differences in males and women like the ability to regulate body temperature help explain these findings. Men tend to show higher drops in core body temperature in cold conditions, which can raise cold-triggered cardiovascular events (Graham, 1988). Women, in contrast, start sweating at higher temperatures compared to men so they cool down less effectively and become more vulnerable to heat (Mehnert et al., 2002). An analysis of Swiss data found that with rising temperature suicide risks increase more drastically for women than for men (Bär et al., 2022).

2.2.6 Education and Socioeconomic Status as Modifiers

Socioeconomic status is most commonly measured using education, income or occupation. While education reflects knowledge-based assets and shapes income and occupation, income most directly captures material resources and access to healthcare, and occupation indicates both earnings and social standing (Galobardes et al., 2007). In the context of temperature-related mortality, these parameters may shape vulnerability differently (Visser et al., 2022) and education alone might be insufficient to fully capture the socioeconomic position of an individual (Son et al., 2019). Education may rather shape risk perceptions of temperature, while income more directly reflects the availability of preventive measures such as air conditioning, as well as access to healthcare (Visser et al., 2022).

Overall, for all-cause adult mortality, each additional year of education is associated with a reduction of 1.9% in mortality risk (Balaj et al., 2024). In a systematic review of factors influencing the temperature-mortality relationship, most studies that included an education variable, found higher mortality risks for low or non-educated individuals. Some studies found no differences across education levels or even higher risks among the more educated (Son et al., 2019).

In an analysis of Dutch data, income data was used to measure the socioeconomic status. The lowest income group experienced higher excess mortality risks during warm periods compared to the highest income group. However, among institutionalised individuals, who share similar living conditions regardless of income, this gap was considerably smaller (Visser et al., 2022). This suggests that the disparity in heat-related mortality is driven by unequal availability of adaptation measures to those with lower socioeconomic status, such as cooling and housing quality, rather than individual-level factors.

An analysis using Spanish data used educational attainment to measure socioeconomic status. The authors found that the temperature-mortality relationship is U-shaped for individuals with low or medium socioeconomic status, whereas the association is flatter for individuals with high socioeconomic status. Individuals with low socioeconomic status face disadvantage when exposed to extreme temperatures, as they are more likely to be exposed, less resilient and less able to access support (Conte Keivabu, 2022). At a larger geographic scale, García-León et al. (2024) analysed European regions and found a positive association between regional income levels and mortality risks. It highlights importance of improving health infrastructure and planning of preventive measures.

Adaptation to warm and cold temperatures is suggested in several studies (Achebak et al., 2019; de Schrijver et al., 2022; Huber et al., 2024; Winklmayr et al., 2022). However, the specific mechanisms behind this trend are difficult to disentangle, as declining mortality risks might reflect improvements in healthcare and heat protection as much as the human body's adaptation to temperature over time (Achebak et al., 2019). For instance, education may play a role in adaptation processes, as populations across the world are becoming more educated over time (Lutz et al., 2014), and individuals with higher educational attainment appear to be less vulnerable to temperature-related mortality (Conte Keivabu, 2022).

3 Study Area: Austria

This chapter first gives an overview of Austria's geography and meteorological conditions, followed by a brief description of its healthcare system. The demographic structure of Austria is then outlined on the national level. The chapter concludes with a table summarising key figures for the analysis of the temperature-mortality relationship across all federal states, alongside remarks on the most relevant aspects and, where present, distinctive attributes of each federal state.

3.1 Geography and Climate

Austria is a landlocked country located in Central Europe. The republic of Austria is divided into nine federal states: Burgenland, Carinthia, Lower Austria, Upper Austria, Salzburg, Styria, Tyrol, Vorarlberg and Vienna. The largest one by population is Vienna, which is also the capital city of the country. The country is further divided into 94 districts and 2,093 municipalities (Statistik Austria, 2025e). Figure 1 shows a physical map of Austria, indicating its nine federal states and neighbouring countries.

Figure 1: Physical Map of Austria

Source: Guide of the World (n.d.)

The elevations of Austria range from the lowest point in Burgenland at 112 metres to the highest summit, the Großglockner, at 3,798 metres, which is close to the border of the federal states Carinthia and Tyrol (Own calculation using: Digitales Geländemodell – Höhenraster 5m Stichtag 31.12.2022). About 60% of Austria is covered by mountains, mainly the Eastern Alps. North of the Danube, in Upper and Lower Austria, is the Bohemian Massif. Most people live in flatter regions like the Alpine Foreland and the Vienna Basin along the Danube in the east, as well as in the Graz Basin in southern Styria (Austrian Federal Ministry for European and International Affairs, n.d.).

Austria's climate is mixed and shaped by its alpine geography. The west and north are usually wetter because of winds coming from the Atlantic. The eastern climate is drier with hotter summers and colder winters (Austrian Federal Ministry for European and International Affairs, n.d.). Austria's climate has shifted over the past 150 years. The average surface temperatures rose by almost 2 °C since 1880 (Balas et al., 2024). The warming has sped up over time and has been increasing by 0.5 °C every ten years since 1980. In 2024, Austria reached an average annual air temperature that is 3.1 °C above pre-industrial levels (1850-1900). Heat waves in Austrian cities now occur 50% more often and tend to last longer than in that period. In addition to changes in heat, Austria also faces other climate impacts. Snow cover lasts five to ten days less per decade and glaciers are melting faster. It is expected that most glaciers disappear in the next decades. Drought severity has also increased and could even double under higher warming, while summer floods increased as well. These climate trends are expected to continue in the coming decades (Huppmann et al., 2025).

3.2 Healthcare System and Causes of Death

Austria is among the highest healthcare spenders in the European Union (EU). In 2023, health spendings were 11.2% of the gross domestic product (GDP). It is mostly hospital-focused, while prevention spendings were just slightly above the EU average with 4.2%. The healthcare system is guided by the federal government, which sets the legal framework and oversees providers, while the nine federal states manage hospital planning and investment. It is funded through social health insurance, covering 99.9% of the population. Since 2020, the social health insurance has been organised through three main institutions: ÖGK, SVS and BVAEB (OECD & European Observatory on Health Systems and Policies, 2025).

Austria has a high density of physicians with about 5.5 per 1000 people, although they are not evenly distributed, with significantly lower density in rural areas. It is suggested that by 2030, more than 50 thousand additional nursing staff will be needed to meet demographic needs and replacement of retirees. The hospital bed capacity is, with 6.6 beds per 1000 people in 2023, well above EU average, even though it fell by about 10% between 2017 and 2023 (OECD & European Observatory on Health Systems and Policies, 2025).

Cardiovascular diseases are the leading cause of death in Austria (across 19 cause-of-death categories). However, their share declined from 42.3% in 2011 to 34.3% in 2024. Malignant neoplasms rank second, remaining roughly stable at 25%. Respiratory diseases increased over the same period from 5.3% to 6.2%. Mental and behavioural disorders showed the largest increase in both absolute and relative terms, rising from 941 deaths (1.2%) to 4,732 (5.4%) (Own calculation using: Statistik Austria, 2025b).

3.3 Demographic Structure

Austria's population has grown from almost 8.4 million inhabitants in 2011 to 8.8 million in 2018 and reached 9.2 million in 2025. This results in a total increase of 9.8% over 14 years (Own calculation using Statistik Austria, 2025a, 2025e). The total fertility rate stood at 1.3 children per woman in 2023, which is slightly lower than the EU's average of 1.4 (OECD & European Observatory on Health Systems and Policies, 2025).

Austria's demographic structure is characterised by moderate population growth and increasing population ageing. These trends have important implications for the country's vulnerability to the impacts of climate change, particularly heat-related health risks (Haas et al., 2019). The share of the population aged 65 and older has increased from 17.64% in 2011 to 20.22% in 2025 (calculated with Statistik Austria, 2025a). This places Austria below the EU average, which reached 22% in 2024. It is expected that the share of older adults will continue to rise to 28% in Austria by 2050 (OECD & European Observatory on Health Systems and Policies, 2025).

The growing share of older adults reflects changes in the size of the younger population as well as rising life expectancy. It rose for females by almost one year and for males by even more than one year from 2011 to 2024. Even though the pandemic has caused a decline in life expectancy in 2020, by 2023 it had surpassed the pre-pandemic peak of 2019 for both males and females in Austria. There is still a notable gender gap, as women are expected to live about 4.5 years longer than men (Statistik Austria, 2025d). Pronounced socioeconomic disparities are present in life expectancy. At age 35, highly educated individuals have considerably higher life expectancy, with a gap of more than six years among males and almost four years among females. However, the gender gap in life expectancy narrows with higher levels of education (Statistik Austria, 2023).

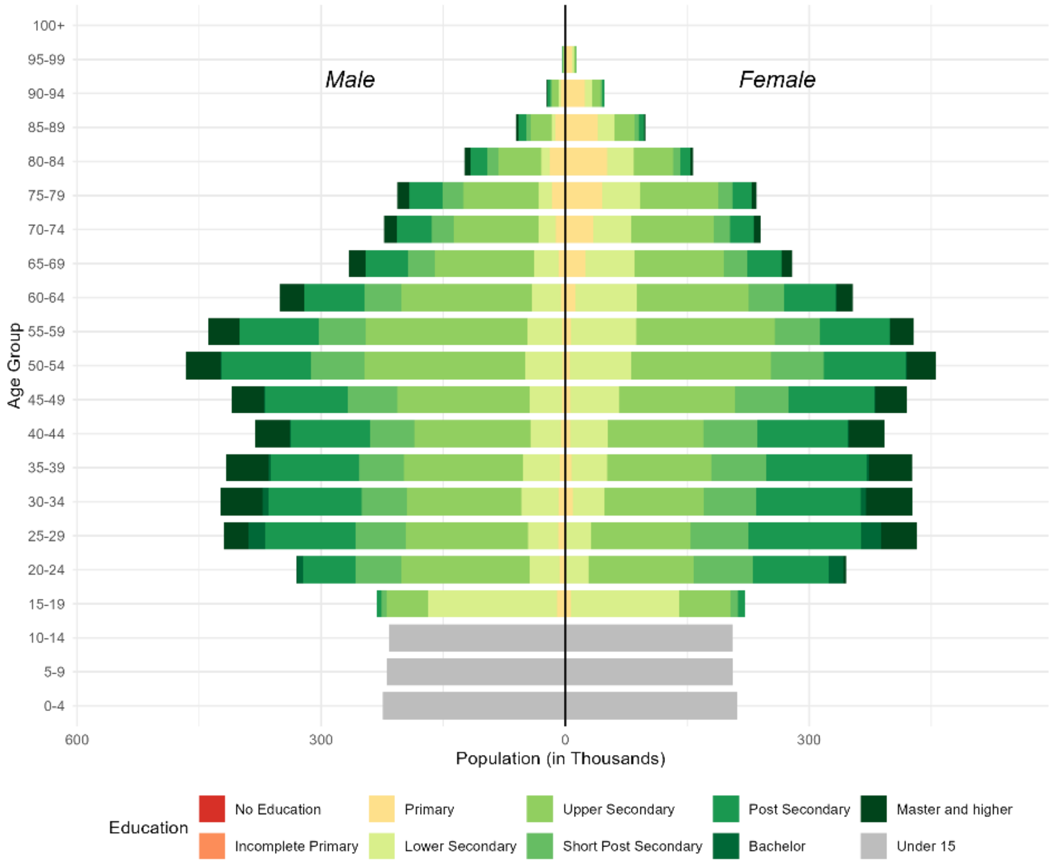

Figure 2: Population Pyramid for Austria in 2020 by Education

Notes: Austrian population (in thousands) by age, sex and educational attainment. Source: Own visualisation based on K.C. et al. (2024)

Figure 2 shows the population pyramid for Austria by educational attainment, using data from the Wittgenstein Centre Human Capital Data Explorer (K.C. et al., 2024). Although older age groups are larger in absolute size, educational attainment is higher among younger cohorts. Austria records no individuals in the categories of no education and incomplete primary education, and the share with only primary education is small for those under 65. The majority of the population under 65 has upper secondary education, and this share is increasing with each subsequent cohort. In the age groups under 30, the highest educational attainment categories show fewer individuals, which likely reflects the fact that many in these cohorts have not yet completed their education.

The progressive ageing of the population, throughout the years of the present analysis, is visible when comparing population pyramids. Figure 34, provided in the Appendix, shows the population structure for 2012 and Figure 35 shows the same for the year 2024. Figure 3 shows the structure mid-year population of 2018, which is the middle year of the analysed period.

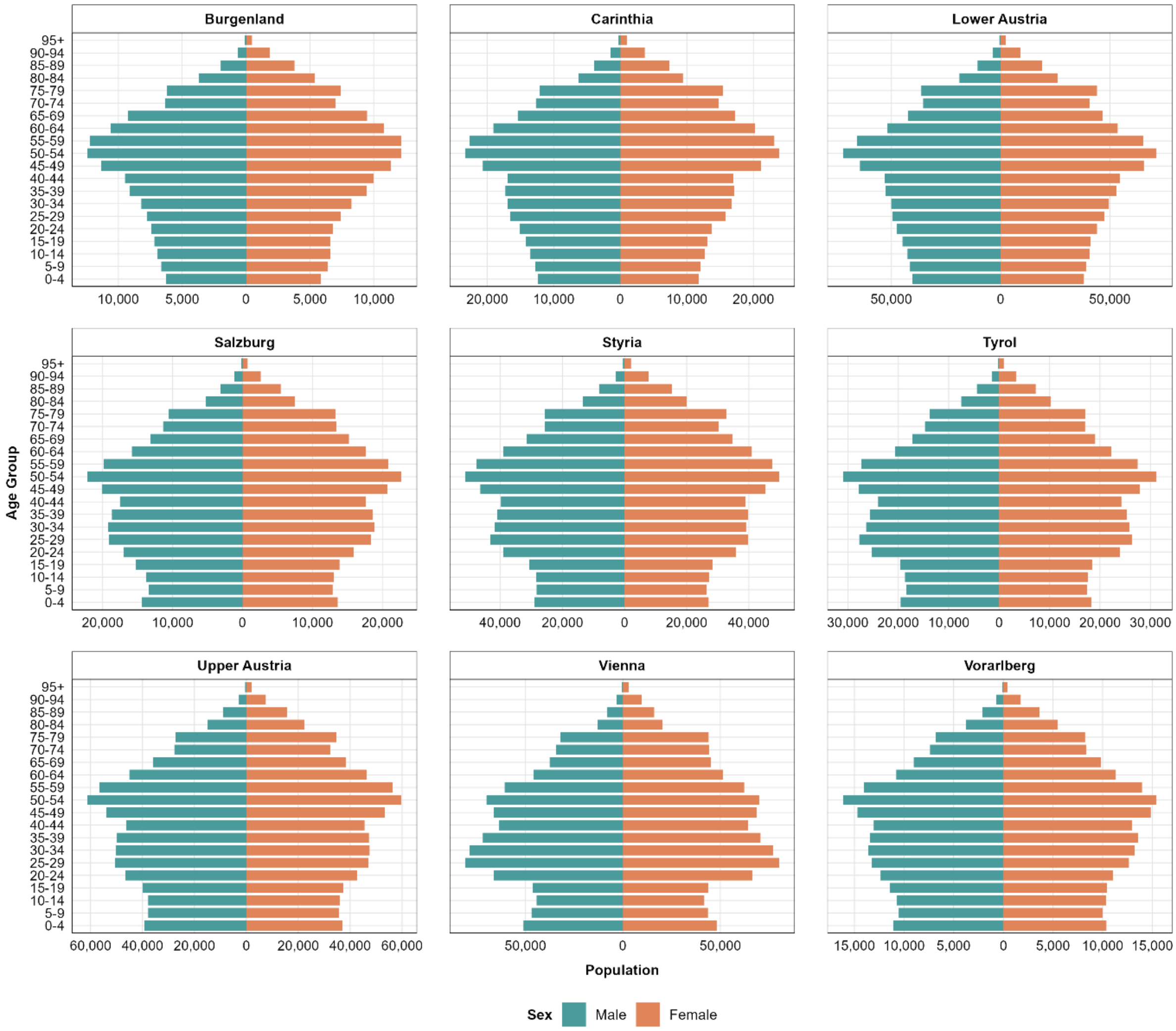

Figure 3: Population Pyramids by Federal State in 2018

Notes: Federal state-specific population by 5-year age group and sex. Source: Own visualisation based on Statistik Austria (2024b)

The population pyramids of 2018 reveal regional differences across federal states (Figure 3). Burgenland, Carinthia and Lower Austria share a similar structure with population numbers growing with age up to a peak at the 50-54 age group, which is the most populous in these regions. Salzburg, Styria, Tyrol, Upper Austria and Vorarlberg display a more uneven structure. Although they also have a peak at age group 50-54, a noticeable bump among young adults is also visible. Population sizes rise with age, then drop around the age of 30, before rising again toward the 50-54 peak. In these states the number of 0–4-year-olds is also slightly higher than the number of 5-9-year-olds. Vienna has the most distinct age pattern among all federal states, as it has a younger population. Like other states, it shows peaks among young adults and a populous 50-54 age group. However, the key difference is that Vienna's largest group is 25–29-year-olds. Vienna has the largest share of working-age residents compared to all other federal states.

3.4 The Federal States

While population pyramids provide a general overview of age structures, this only captures one aspect of variation across the federal states. To understand regional differences, it is necessary to look at additional indicators, which are explored in this section.

3.4.1 The Western Federal States

Looking at the numbers in Table 1, the western federal states Salzburg, Tyrol and Vorarlberg are dynamic in the demographic figures. All of them grew by about 10% between 2011 and 2025. After Vienna, Vorarlberg is the second-fastest growing federal state and the second most densely populated federal state. Salzburg became the sixth most populous federal state throughout the years by outpacing Carinthia's population.

Apart from Vienna, the west also has the youngest age profile compared to the rest of Austria. In 2025, the share of the population aged 65 and above was below 20% for Tyrol and Vorarlberg and also Salzburg is with 20.47% just above the threshold (Table 1). Life expectancy in these federal states is consistently higher compared to eastern and central federal states, as shown in Table 1. Tyrol led in life expectancy for both sexes in 2011 and 2024 and ranked second for both sexes in 2018, behind Salzburg for females and Vorarlberg for males. In 2018, Vorarlberg also had the smallest gender gap in life expectancy across all states and years of observation (Table 1).

3.4.2 The Central Federal States

The central federal states, with Carinthia and Styria in the south and Upper Austria in the north, are characterised by slower population growth (Table 1). With just 2.4% increase in population, Carinthia had the least relative population growth across the 14 years of observation, followed by Styria with an increase of 5.4%. Population density is also below the national average in these two federal states, as shown in Table 1. Upper Austria had higher population growth and ranks third in population density across all federal states.

Table 1: Geographic and Demographic Profile of Austrian Federal States (2011-2025)

(Federal) State		AUSTRIA	Burgenland	Carinthia	Lower Austria	Salzburg	Styria	Tyrol	Upper Austria	Vienna	Vorarlberg
Capital		Vienna[1]	Eisenstadt[1]	Klagenfurt am Wörthersee[1]	St. Pölten[1]	Salzburg (city)[1]	Graz[1]	Innsbruck[1]	Linz[1]	Vienna (city-state)[1]	Bregenz[1]
Area (km²)		83,883.87[1]	3,965.21[1]	9,536.83[1]	19,180.08[1]	7,154.48[1]	16,399.55[1]	12,648.46[1]	11,982.77[1]	414.82[1]	2,601.68[1]
Number of districts		94[1]	9[1]	10[1]	24[1]	6[1]	13[1]	9[1]	18[1]	23[1]	4[1]
Number of municipalities		2 093[1]	171[1]	132[1]	573[1]	119[1]	286[1]	277[1]	438[1]	(1)[1]	96[1]
Altitudinal range		112m – 3,797m[2]	112m – 882m[2]	326m – 3,797m[2]	131m – 2,075m[2]	376m – 3,660m[2]	188m – 2,995m[2]	450m – 3,785m[2]	222m – 2,994m[2]	132m – 543m[2]	392m – 3,304m[2]
Population on Jan. 1 (Population per km²)	2011	8,375,164[3] (99.8[4])	284,581[3] (71.8[4])	556,718[3] (58.4[4])	1,609,474[3] (83.9[4])	527,886[3] (73.8[4])	1,206,611[3] (73.6[4])	707,517[3] (55.9[4])	1,410,222[3] (117.7[4])	1,702,855[3] (4105.0[4])	369,300[3] (141.9[4])
	2018	8,822,267[3] (105.2[4])	292,675[3] (73.8[4])	560,898[3] (58.8[4])	1,670,668[3] (87.1[4])	552,579[3] (77.2[4])	1,240,214[3] (75.6[4])	751,140[3] (59.4[4])	1,473,576[3] (123.0[4])	1,888,776[3] (4553.2[4])	391,741[3] (150.6[4])
	2025	9,197,213[3] (109.6[4])	301,790[3] (76.1[4])	570,095[3] (59.8[4])	1,727,514[3] (90.1[4])	572,846[3] (80.1[4])	1,271,716[3] (77.5[4])	777,660[3] (61.5[4])	1,535,519[3] (128.1[4])	2,028,289[3] (4889.6[4])	411,784[3] (158.3[4])
Population aged 65+ (in %)	2011	17.64[3]	19.55[3]	19.22[3]	18.71[3]	16.59[3]	18.79[3]	16.20[3]	17.06[3]	16.89[3]	15.33[3]
	2018	18.67[3]	21.54[3]	21.39[3]	19.94[3]	18.47[3]	20.06[3]	17.76[3]	18.24[3]	16.45[3]	17.12[3]
	2025	20.22[3]	24.62[3]	24.10[3]	21.68[3]	20.47[3]	22.09[3]	19.80[3]	20.14[3]	16.48[3]	18.87[3]
Life expectancy at birth (male / female)	2011	78.08 / 83.43[5]	77.88 / 83.79[5]	78.41 / 83.44[5]	77.79 / 83.20[5]	78.97 / 84.04[5]	78.19 / 83.80[5]	79.33 / 84.38[5]	78.41 / 83.76[5]	76.98 / 82.29[5]	79.11 / 84.70[5]
	2018	79.29 / 84.01[5]	79.02 / 83.62[5]	78.81 / 84.11[5]	79.09 / 83.75[5]	80.34 / 85.04[5]	79.51 / 84.58[5]	80.37 / 85.02[5]	79.69 / 84.42[5]	78.18 / 82.73[5]	80.53 / 84.71[5]
	2024	79.84 / 84.32[5]	79.62 / 83.98[5]	79.55 / 84.88[5]	79.55 / 83.99[5]	80.53 / 85.36[5]	79.94 / 84.80[5]	81.06 / 85.54[5]	80.20 / 84.48[5]	78.96 / 83.21[5]	80.72 / 85.05[5]

Notes: The altitudinal range is given in meters above sea level. Altitudinal range, population per km² and population aged 65+ (in percent) are based on own calculations using the data sources indicated in the footnotes. The share of the population aged 65+ was derived from the population on January 1 of the respective year.

[1] (Statistik Austria, 2025e)
[2] (Own calculation based on Bundesamt für Eich- und Vermessungswesen, 2022)
[3] (Own calculation based on Statistik Austria, 2025a)
[4] (Own calculation based on Statistik Austria, 2025a, 2025e)
[5] (Statistik Austria, 2025d)

Population ageing is most pronounced in central Austria. Carinthia has the second highest share in population aged above 65, reaching 24.62% in 2025 (Table 1). Styria is also above the Austrian average in this figure. Upper Austria has a younger population compared to them, being close to the Austrian average across all years. As Table 1 shows, life expectancy is about average among Austrian levels in all three central federal states. Styria stands out for having one of the highest female life expectancies in 2024.

3.4.3 The Eastern Federal States

The easternmost federal states are Burgenland, Lower Austria and Vienna. Burgenland is the least populous federal state, and Lower Austria is the largest federal state by area. Both are below the national average in population growth and have comparatively low population density (Table 1).

Burgenland has the oldest population structure across federal states. According to Table 1, almost a quarter of its population is more than 64 years old. Lower Austria's population ageing is at a similar level as the national average. Life expectancy is on the lower end across federal states (Table 1).

Despite Vienna being geographically enclosed within Lower Austria, the two federal states diverge across most demographic indicators (Table 1). This is likely due to Vienna being a city-state and the capital of Austria with a distinct demographic structure, while Lower Austria is characterised by more rural areas. Vienna is the smallest federal state by area, but the most populous, having surpassed 2 million inhabitants in 2025, making it also the most densely populated federal state. Table 1 further shows that its population grew by 19.1% from 2011 to 2025, which is by far the largest increase across the federal states in that period. Vienna has the smallest proportion of people aged 65 and above, and this proportion has remained almost stagnant at about 16.5% throughout the observed period. It also has the lowest life expectancy for both males and females, although it did increase throughout the observed period (Table 1).

4 State of Knowledge and Research Objectives

This chapter reviews the existing evidence on temperature-related mortality in Austria, focusing on regional differences and relevant influencing factors. It aims to outline key patterns already found in Austria and concludes with the definition of the research question and its sub-questions.

The relationship between mortality and temperature has become increasingly important in recent years, especially due to the major trends of climate change and population ageing. Climate change is changing weather patterns, which has direct consequences for human health. As Fastl et al. (2024) pointed out, temperature changes related to climate change can increase the risk of a variety of diseases. Populations of developed countries are getting older, which results likely in an increase in size of a more vulnerable population group. De Schrijver et al. (2022) showed in their analysis of Swiss data that older adults are more sensitive to both heat and cold. Their findings suggest that population ageing has been responsible for more than half of heat-related mortality in recent decades. Adding these two trends together suggests that temperature-related deaths likely rise in the next decades, making research on this topic increasingly relevant to research on human health.

Looking at the distribution of mortality and diseases in Austria, analyses using data from previous decades found differences across Austria's federal states (Rásky et al., 2015; Stein et al., 2011). Vorarlberg, Tyrol and Salzburg, western federal states, had the lowest death rates and a tendency of healthy lifestyles, whereas Vienna had the largest share of potentially preventable deaths. Other federal states with high prevention potential were Burgenland, Styria and Carinthia, which are located in the southeast of Austria (Rásky et al., 2015). After examining three common cardiovascular risk factors, diabetes, hypertension and obesity, a clear east-west gradient across Austria was found. The prevalence and risk factors as well as cardiovascular mortality are higher in eastern and lower in western federal states. Psychological distress and low social support are strongly linked factors, but the regional differences could not be fully explained. Cultural and lifestyle differences are seen as probable contributors (Stein et al., 2011). Overall, cardiovascular diseases remain the leading cause of death in Austria and are more common in this country compared to EU average (OECD & European Observatory on Health Systems and Policies, 2025).

Burtscher et al. (2021) analysed deaths using age-standardised rates over a 10-year period and found that living at altitudes above 1,000 metres was associated with about 20% lower all-cause mortality compared to mortality at altitudes below 250 metres. This difference is primarily caused by deaths from circulatory diseases, such as cardiovascular diseases and cancers. The authors assume that the adaptation of bodies to lower oxygen levels at altitude, along with colder temperatures and more sun exposure explain why people at moderate heights tend to live longer. As Austria's western federal states are predominantly mountainous while eastern regions are characterised by lower elevations, these results tie in with an east-west variation.

Looking at the most recent values for life expectancy at birth, an east-west gradient can be observed as well. Male life expectancy exceeds 80 years only in the western states of Vorarlberg, Tyrol and Salzburg as well as Upper Austria, located in the north-centre. Tyrol leads with 81.06 years, while Vienna has the lowest value of 78.96 years. Female life expectancy follows a similar pattern, with Tyrol leading at 85.54 years, followed by Salzburg and Vorarlberg. Those are the only three states exceeding 85 years in female life expectancy. Vienna has the lowest female life expectancy at 83.21 years, with just slightly higher values for the eastern federal states Burgenland and Lower Austria (Statistik Austria, 2025d).

Austria shows an uneven spatial pattern of heat exposure. Between 1991 and 2020 the mean number of annual heat days in Austria ranged from 0 to 27.5 days. Heat days are defined as days with a maximum temperature of at least 30 °C. The greatest exposure is in eastern, less mountainous areas of Austria, affecting both urban and rural areas. The smallest numbers of heat days are found at weather stations located in more mountainous areas. Zero heat days were just found for stations more than 1,400 metres above sea level. A significant correlation was found between number of heat days and population density of municipalities in Austria. This relationship held at the district level and also remained after excluding the densely populated capital city Vienna (Fastl et al., 2024).

The regional differences in health outcomes seem to mirror climate exposure to some degree. Given Austria's ageing population and vulnerability to temperature extremes rising with age, it is important to understand how mortality and temperature are associated across Austria's regions and age groups. Leading to the research question:

How does the association between mortality and temperature vary regionally and are there age- and sex-specific differences in Austria?

Three sub-questions to answer this:

1. What is the pattern between mortality and temperature in Austria?
2. How does the association differ across Austria's federal states?
3. Does the temperature-mortality association differ by age group and sex?

5 Data

Data was downloaded from several sources. This chapter deals with the downloading, cleaning and linking of multiple datasets. It first describes how mortality and demographic data were collected, cleaned and combined. This is followed by a description of how meteorological data was retrieved, processed and combined to acquire the final population-weighted temperature values.

Demographic data was downloaded from Statistics Austria to the extent available. Since 2020, population records available to Statistics Austria include non-binary gender categories, but the numbers are very small. For most analyses non-binary entries are reclassified as either male or female using a standard rule (Schuster, 2025). This is the case for all datasets used in this analysis.

5.1 Mortality Data

For mortality data the dataset "Gestorbene in Österreich (ohne Auslandssterbefälle) ab 2000 nach Kalenderwoche und Altersgruppe" (translated "Deaths in Austria (excluding deaths abroad) from 2000 by calendar week and age group") (Statistik Austria, 2025c) was selected. Due to export limitations, the data was downloaded in 46 separate files and reassembled in one dataset afterwards. This dataset contains weekly absolute death counts. To match the meteorological data, the counts for March 2011 to March 2025 were downloaded. This dataset includes the variables calendar week, 5-year age groups, sex (male/female), federal state and total number of deaths. Federal state and sex had a "not classifiable"-category that contained only zeros for the period considered and was therefore excluded. Values for 2024 and 2025 in the dataset are preliminary.

The dataset "Bevölkerung zu Jahresbeginn ab 2002" (translated "Population at the beginning of the year from 2002") (Statistik Austria, 2025a) was used to obtain annual population counts from 2011 to 2025. The variables in the dataset are year, 5-year age group, sex (male/female), federal state and total population. Again, the dataset included a notes variable that was entirely empty as well as "non classifiable" categories for federal state and sex that contained only zeros and were therefore removed.

To obtain population estimates for all dates present in the mortality data, the annual values, indicating population on January 1, were linearly interpolated. This produced continuous weekly population estimates for each combination of federal state, age group and sex. Since the population data ends on January 1, 2025 and the mortality data continues until March 2025, the population values for the beginning of the year 2025 were held constant for the remaining weeks. The mortality and population datasets were then joined, not only to calculate age-specific death rates, but also to include the population variable for later statistical modelling purposes.

5.2 Meteorological Data

A density dataset was downloaded from Eurostat, “1 square km grid data from the Austrian population census 2021” (Statistik Austria, 2024a). Included in this data set are coordinates of the 1 x 1 km raster and the total number of people living in that square kilometre. The spatial distribution of population density across Austria is visualised in Figure 20 in the Appendix.

Additionally, a shapefile was downloaded from the Austrian Federal Office of Metrology and Surveying called “Verwaltungsgrenzen (VGD) BEV Stichtag 01.10.2024” (translated “Administrative boundaries, reference date October 1, 2024”) (Bundesamt für Eich- und Vermessungswesen, 2024). Included in this dataset are all Austrian administrative borders. For this analysis the borders are reduced to the nine federal states’ borders (Figure 21 in the Appendix). This shapefile was then converted to the same coordinate reference system as the density data, and they are joined so that every coordinate in the 1 x 1 km raster receives a federal state value. A total of 35,394 people, representing 1.8% of density values, living at the border to neighbouring countries, could not be assigned to a federal state. The biggest issues are at the borders of Vorarlberg, but also in Salzburg, Upper Austria and Styria. Most values of these could be added manually, as it was very clear where they belonged. Among those not manually assigned, the majority have a population density of zero, which would exclude them from the analysis regardless.

Figure 4 shows each coordinate where population density data is available. The unknown values are the black points at the border, which were not overlapping with the shapefile. The black rectangles mark the areas, where values were manually assigned to the respective federal state, as these border regions had sufficiently high population density and a clearly identifiable federal state affiliation.

In the end, 3,042 people, living close to the border, are cut off in total. As an additional check, after the manual assignment, the number of coordinates in the 1 x 1 km raster is compared to the actual area of each federal state in square kilometres, taken from a publication of Statistik Austria (2025e). The values differ by less than 0.6% for each federal state. Finally, the data is transformed to the same coordinate reference system as the meteorological data, so that they can be merged later.

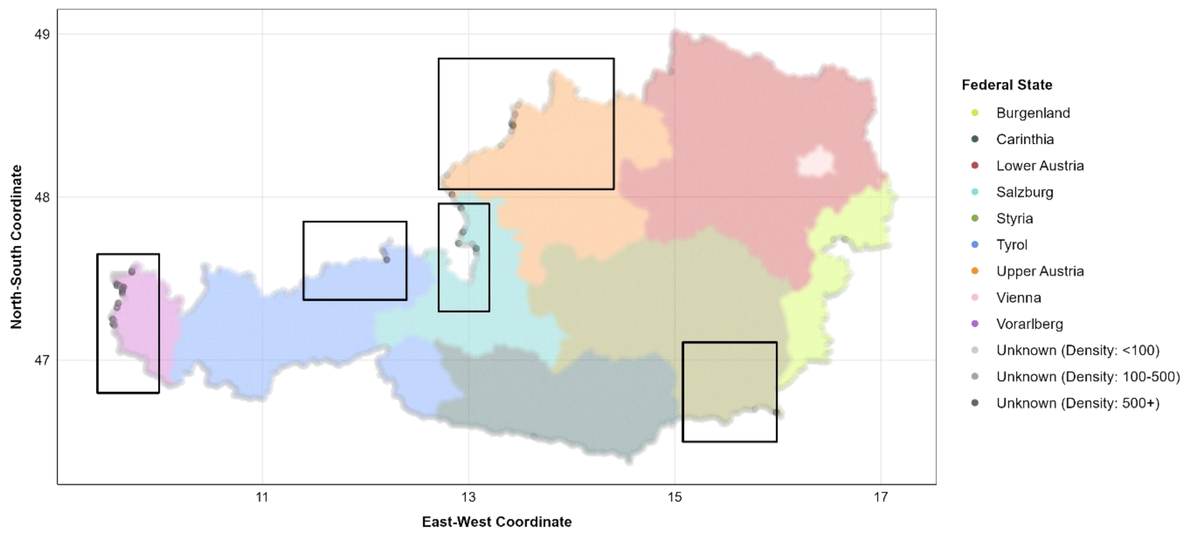

Figure 4: Population Density Grid Data Availability and Manual Border Assignment

Notes: The figure shows the spatial availability of population density grid data and assignments of the data points to federal states based on shapefile borders. Darker values of the unclassified variable in border regions indicate a high density of unassigned grid data. The black rectangles indicate, where unclassified grid points were manually assigned to the corresponding federal state. Source: Own visualisation based on Statistik Austria (2024a) and Bundesamt für Eich- und Vermessungswesen (2024)

Meteorological data was downloaded from GeoSphere Austria, namely “INCA Stundendaten” (translated “INCA hourly data”) (GeoSphere Austria, 2021), using GeoSphere’s API in R. It is stored as NetCDF files, each file containing hourly measurements for one single day for the time span March 2011 to March 2025. The dataset is gridded at 1 km x 1 km resolution and extends beyond Austria’s borders (Figure 22 in the Appendix). It contains the variables time, longitude, latitude, air temperature at 2 metres height and relative humidity in percent. The INCA analysis and nowcasting system merges station observations, remote sensing, numerical weather prediction models and a high-resolution terrain model to produce the best possible estimates on this 1 km grid.

To merge the density and meteorological datasets, a mapping data frame was generated from a single meteorological file to associate each density grid cell with its corresponding meteorological grid cell. Since the meteorological grid shifts position every hour, each single hour only covers 2 km x 1 km. To obtain the full 1 km x 1 km grid, pairs of consecutive hours were combined. As the data is aggregated to daily resolution in the following step, any bias resulting from the hourly grid shifts is expected to be largely mitigated. Although both layers were projected on a common coordinate reference system, they did not perfectly align (Figure 23 and Figure 24 in the Appendix). Euclidean distances between grid cells were therefore computed and each density cell was assigned to the nearest meteorological cell.

All meteorological files were handled sequentially, applying the same procedure to each file. For each file, daily statistics were computed for every grid cell: mean, variance, minimum and maximum for both temperature and relative humidity values. These were then linked to the density data using the previously constructed mapping data frame. A right join was used to preserve all density records. As a result of this, meteorological grid cells that were not the nearest neighbour to any density cell were excluded from the resulting dataset. This approach ensured that density records were neither replicated nor lost and automatically removed meteorological observations located outside Austria's borders. The initial and resulting matched data is visualised for a single day in Figure 22 and Figure 25 in the Appendix. In the next step, the dataset was restricted to populated areas and cell-level statistics were aggregated to the federal state-level for each day by computing population density-weighted means, variances, minima and maxima for again both temperature and relative humidity. The resulting data frame therefore includes the variables federal state, date and mean, variance, minimum and maximum of temperature and relative humidity. Population density-weighting of meteorological values such as temperature has been applied in previous studies and proved more effective than simply using data from single weather stations (de Schrijver et al., 2021).

A closer look at the resulting data frame reveals recurring issues on nine dates. On those dates either

- the temperature variance was zero for all federal states,
- every federal state recorded a minimum of - 9.99 °C with relative humidity missing for the same date,
- or no values were recorded at all for any federal state.

These same rows also appear as extreme outliers in temperature variance. These problems account for 81 rows in total, representing nine dates with nine federal states each. The calculations for those dates were rechecked and found to be correct. Because these values are unrealistic and probably caused by measurement or processing errors, the nine dates were removed from further analysis. The excluded dates are August 26-29, 2011, October 24, 2023, May 5-6, 2024 and November 2-3, 2024.

6 Methodology

The relationship between mortality and temperature in Austria is analysed across federal states, sex and age groups. This is done using distributed lag non-linear models (DLNM) in a two-stage time-series regression. In the first stage, the data is stratified by federal state, age group and sex. A separate model is fitted for each subgroup. In the second stage, a multivariate meta-analysis is done across all previously fitted models. This pools information across federal states and demographic groups and thereby borrows strength from related subgroups, producing the best linear unbiased predictors (BLUPs) for each combination. The resulting estimates are aggregated on three different levels:

- The National level,
- the Federal state level and
- the Population subgroup level (by sex and age group).

Pooling these estimates through meta-analysis enables an analysis of the overall temperature-mortality association as well as vulnerable regions and populations. At each level, temperature-attributable mortality is calculated, which refers to the number of deaths statistically associated with temperatures below or above the temperature optimum. To get comparable baseline estimates, the minimum mortality temperature (MMT) is also calculated across all models.

This chapter first outlines the methodological foundation, followed by a description of how the data was structured for the regression analysis. The first and second stage of the analysis are then described in detail, including a brief overview of each of the three pooling levels. After that, it is explained how predictions, minimum mortality temperature and attributable mortality was computed. The chapter closes with a description of the assumption checks performed and the computational environment used.

6.1 Methodological Foundation

The methodological approach for this analysis was primarily based on a paper by Basagaña and Ballester (2024). They developed methodological approaches to handle temporally aggregated data in the analysis of temperature-mortality relationships. They compared various combinations of temporal resolution. It included daily temperature data combined with daily, weekly or monthly mortality counts as well as weekly temperature data combined with weekly mortality counts. By applying the different approaches to data from Paris and the French region Aveyron, they could not only validate their approach and find weaknesses between the combinations, but also consider weaknesses of the approaches in different regional settings.

The analysis using Parisian data revealed that using weekly mortality counts with daily temperature data leads only to small losses in in precision when estimating the exposure-response relationship compared to daily mortality and temperature data. In the lag-response relationship, some biases were present at the 99th percentile when using only five years of data. The minimum mortality temperature calculations became unbiased when using at least 20 years of data. Cold-attributable mortality was underestimated when using only 10 years of weekly mortality data, while heat-attributable mortality showed more accurate values. Weekly and daily mortality data, both combined with daily temperature data, lead to similar results overall. Analyses using regional data from Aveyron, which was sparser, showed larger biases, particularly when using monthly mortality counts, which introduced more substantial biases in all analyses (Basagaña & Ballester, 2024).

For most other published studies that analyse the temperature-mortality relationship, daily mortality data was available (e.g., Achebak et al., 2019; de Schrijver et al., 2021; Janoš et al., 2024; Masselot et al., 2023; Schifano et al., 2012). The methodological paper by Basagaña and Ballester (2024) is therefore particularly relevant, as it demonstrates that the analytical methods developed for daily mortality can be applied to weekly data without violating model assumptions, while preserving daily temperature heterogeneity despite the weekly aggregation of mortality counts. The mathematical foundation is the property that the sum of independent Poisson variables follows a Poisson distribution with summed parameters. Therefore, expressing the likelihood for weekly outcomes in terms of the daily model parameters allows to analyse the daily temperature-mortality relationship using weekly data.

Basagaña and Ballester (2024) did not include further variables such as age group and sex, which will be included in this analysis. To account for heterogeneity introduced by geographic and demographic differences in the temperature-mortality relationship, the approach used in this analysis combines the approach of Basagaña and Ballester (2024), by pairing weekly mortality data with daily temperature, with the approaches of two further papers, which had daily mortality data, but stratified their results by geographic and demographic variables. Achebak et al. (2019) used Spanish data and analysed the temperature-mortality relationship by province, age group and sex, while controlling for long-term trends via splines. The main difference from the present analysis is that they had daily mortality counts and a larger study period with data from 1980 to 2016. A further methodological reference was Masselot et al. (2023), which analysed regional and age-specific variation in the temperature-mortality relationship across European cities, also using daily mortality counts. They additionally included further city-specific characteristics, which was not included in the present analysis.

6.2 Data Structure for Regression Analysis

The obtained datasets include daily meteorological data as well as weekly mortality counts, which are broken down by federal state, age group and sex. They are joined so that weekly death values are duplicated for every day of the respective week. Dividing the mortality counts into pseudo-daily values was considered but rejected for two reasons. First, count data models require whole numbers, meaning that dividing the weekly mortality counts would require rounding the resulting daily counts, which introduces loss of heterogeneity in the mortality data. This is particularly problematic for combinations of federal state, sex and age group with already sparse counts, such as the youngest age group (0-39) in Burgenland or Vorarlberg, where the mean weekly count of deaths is below 1 for both sexes. Second, this loss is unnecessary, given that all results are expressed as relative measures, such as relative mortality and attributable fractions, and therefore never refer to absolute counts. In this way, the heterogeneity of daily temperature data that is essential for lagged effects is preserved, while respecting the weekly resolution of the mortality data.

Although the mortality data provides values for 5-year age groups, these are aggregated into larger age groups due to data sparsity issues, especially in younger age groups. The five resulting categories are 0-39, 40-59, 60-74, 75-89 and 90+ years. These combined age categories help increase the number of deaths per stratum to capture age-related vulnerability. Counts for the youngest age group remain relatively low in small federal states. This leads to imprecise results after Stage 1 analysis, but in Stage 2 of the analysis, this issue is partially mitigated by pooling estimates, thereby borrowing strength across subgroups.

To make the methodology easier to follow, the coloured boxes appearing throughout this section walk through the process in a simplified form, using the data from a single federal state (Salzburg), two age groups (0-59 and 60+) and a reduced timespan, starting with Monday, January 1, 2018 and reduced dimensions for the cross-basis matrix (3 knots for the temperature dimension and 3 knots for the lag dimension instead of 4 and 5).

EXAMPLE

After joining the weekly mortality data with the daily temperature data, Table 2 shows, what the data frame looks like using the reduced data. The highlighted line marks, where the first week ends and the second one begins.

Table 2: Mortality and Temperature Data after Merging (Reduced Example)

Date	Week ID	Federal State	Sex	Age Group	Temperature	Total weekly deaths	Population
2018-01-01	356	Salzburg	Female	0-59	2.27	1	207,111
2018-01-01	356	Salzburg	Female	60+	2.27	55	75,154
2018-01-01	356	Salzburg	Male	0-59	2.27	4	210,418
2018-01-01	356	Salzburg	Male	60+	2.27	35	59,918
2018-01-02	356	Salzburg	Female	0-59	2.07	1	207,111
2018-01-02	356	Salzburg	Female	60+	2.07	55	75,154
2018-01-02	356	Salzburg	Male	0-59	2.07	4	210,418
2018-01-02	356	Salzburg	Male	60+	2.07	35	59,918
[…]	[…]	[…]	[…]	[…]	[…]	[…]	[…]
2018-01-07	356	Salzburg	Female	0-59	0.66	1	207,111
2018-01-07	356	Salzburg	Female	60+	0.66	55	75,154
2018-01-07	356	Salzburg	Male	0-59	0.66	4	210,418
2018-01-07	356	Salzburg	Male	60+	0.66	35	59,918
2018-01-08	357	Salzburg	Female	0-59	1.59	1	207,110
2018-01-08	357	Salzburg	Female	60+	1.59	42	75,181
2018-01-08	357	Salzburg	Male	0-59	1.59	7	210,417
2018-01-08	357	Salzburg	Male	60+	1.59	43	59,944
[…]	[…]	[…]	[…]	[…]	[…]	[…]	[…]

Notes: This table shows a reduced subset of the merged dataset, filtered to Salzburg, starting from January 1, 2018, stratified by sex (female, male) and aggregated age groups (0-59, 60+). The coloured line indicates the switch from the first to the second week. Week ID is a self-created variable that assigns a sequential number to each calendar week across the study period. Temperature refers to the population density-weighted daily mean temperature in °C. The total number of deaths is reported by calendar week, so all days within the same week share the same mortality value. Population refers to the population count as of January 1 of the respective year and is linearly interpolated across the weeks of the year until the next available annual figure. Source: Own computation based on Bundesamt für Eich- und Vermessungswesen (2024), GeoSphere Austria (2021), Statistik Austria (2024a), Statistik Austria (2025a) and Statistik Austria (2025c)

As mortality values are broken down by two age categories and two sexes, there are four rows for each day, each showing the same temperature and the corresponding death count for each demographic subgroup. Since the meteorological data is at the daily level, the weekly mortality counts are duplicated for each day of the respective week, which is why within the first week, the same four death values repeat.

6.3 Stage 1 Analysis

The temperature-mortality relationship is modelled using a distributed lag non-linear model (DLNM) fitted with quasi-Poisson regression. This allows to capture not only the relationship on the day of the temperature exposure but also delayed patterns (Gasparrini et al., 2010). Quasi-Poisson specification is chosen to account for the mild under- or overdispersion, which is present in the data (Table 20 in the Appendix). In Stage 1, the data is stratified by federal state, age group and sex, resulting in 90 subsets (9 federal states, 5 age groups, 2 sexes). For each subset, a separate model is fitted to estimate the subgroup-specific temperature-mortality relationship.

6.3.1 Formula for Distributed Lag Non-Linear Model

The model fitted for each subset is a distributed lag non-linear model with quasi-Poisson regression, with the following formula.

$$\text{(weekly) death count} \sim \text{quasi-Poisson}(\mu, \phi)$$

$$\log(\mu) = \alpha + \beta \cdot cb(\text{temperature}, 0 - 21) + \theta \cdot ns(\text{date}, \text{df} = 112) + \text{ offset}(\log(\text{population}))$$

where μ is the expected value of the weekly death count, ϕ describes the dispersion parameter, α is the intercept, β is a vector of coefficients for the cross-basis matrix *cb*, and θ is a vector of coefficients for the natural spline *ns* of date.

temperature is included as a cross-basis matrix to model a non-linear association and to capture delayed effects with lags of 0-21 days. The cross-basis function *cb* is necessary to model not only the non-linear effect of temperature, but also the temporal distribution across days, since temperature may not only be associated with mortality on the day of exposure, but also for days after. This approach follows the distributed lag non-linear model (DLNM) framework proposed by Gasparrini et al. (2010), which combines exposure-response and lag-response functions into a single cross-basis structure. The exposure-response dimension of the cross-basis is modelled with a natural cubic spline with three internal knots at the 10^{th}, 75^{th} and 90^{th} percentile of temperature distribution. The lag-response dimension is also modelled with a natural cubic spline with internal knots placed evenly distributed on the logarithmic scale, with a maximum lag of 21 days to capture direct as well as delayed effects. The internal knots for the exposure-response and the lag-response dimensions were defined using the full dataset and then applied to each data subset's model to ensure comparability. The placements of internal knots followed the recommendations from the paper by Basagaña and Ballester (2024).

ns(date, df = 112) is a natural spline function of date that controls for seasonality as well as long-term trends in mortality. 112 degrees of freedom result from the multiplication of 8 times 14, because it is recommended to use 8 degrees of freedom per year of observation (March 2011-March 2025) (Achebak et al., 2019; Basagaña & Ballester, 2024). This is particularly important for years when the COVID-19 pandemic influenced the number of deaths directly (Yu et al., 2021).

log(population) (the logarithm of *population*) is included as an offset term to control for the population at risk. The population is defined as the annual average population of the specific subgroup in each year. The offset changes the model so that instead of modelling death counts, death rates are modelled. Since separate models are fitted for each demographic and regional subgroup, this controls for the changes in subgroup's population size over time.

EXAMPLE

The data is split into subsets, so that each combination of federal state, age group and sex has its own data frame. Table 3 displays the data of the subset for Salzburg (federal state), 60+ (age group) and females (sex).

Table 3: Mortality and Temperature Data for Females aged 60+ in Salzburg (Reduced Example)

Date	Week ID	Federal State	Sex	Age Group	Temperature	Total weekly deaths	Population
2018-01-01	356	Salzburg	Female	60+	2.27	55	75,154
2018-01-02	356	Salzburg	Female	60+	2.07	55	75,154
2018-01-03	356	Salzburg	Female	60+	2.71	55	75,154
2018-01-04	356	Salzburg	Female	60+	3.15	55	75,154
2018-01-05	356	Salzburg	Female	60+	4.81	55	75,154
2018-01-06	356	Salzburg	Female	60+	3.38	55	75,154
2018-01-07	356	Salzburg	Female	60+	0.66	55	75,154
2018-01-08	357	Salzburg	Female	60+	1.59	42	75,181
2018-01-09	357	Salzburg	Female	60+	4.79	42	75,181
[…]	[…]	[…]	[…]	[…]	[…]	[…]	[…]

Notes: This table shows a reduced subset of the merged dataset, filtered to Salzburg's females aged 60+, starting from January 1, 2018. The coloured line indicates the switch from the first to the second week. Week ID is a self-created variable that assigns a sequential number to each calendar week across the study period. Temperature refers to the population density-weighted daily mean temperature in °C. The total number of deaths is reported by calendar week, so all days within the same week share the same mortality value. Population refers to the population count as of January 1 of the respective year and is linearly interpolated across the weeks of the year until the next available annual figure. Source: Own computation based on Bundesamt für Eich- und Vermessungswesen (2024), GeoSphere Austria (2021), Statistik Austria (2024a), Statistik Austria (2025a) and Statistik Austria (2025c)

Using this data, the cross-basis matrix for temperature is calculated, which captures the possible lags in the relationship between mortality and temperature. A cross-basis takes in temperature values from the 21 days preceding the day of exposure and summarises the relationship between mortality and temperature across both the lag and temperature dimensions.

In this simplified example, the cross-basis uses 3 knots for the temperature dimension and 3 knots for the lag dimension, as opposed to 4 and 5 respectively in the full analysis. The higher number of knots allows for greater flexibility, as it introduces more temperature categories beyond cold, medium and hot, and more lag groupings beyond simply recent and distant.

For a single day of observation, the 3x3 dimensional cross-basis describes the temperature distribution for the corresponding death count, which are the 21 days before, using three lag dimensions (L1-L3) and three temperature dimensions (V1-V3). A single day therefore has 9 values, corresponding to the 3x3 combinations of temperature and lag components. Using the reduced dataset for a single day (January 22, 2018), the resulting values are shown in Table 4.

Table 4: Cross-basis values for January 22, 2018 in Salzburg (Reduced Example)

	L1 (Intercept)	**L2** (Lag Dimension 1)	**L3** (Lag Dimension 2)
V1 (Temperature Dimension 1)	0.37	0.79	0.61
V2 (Temperature Dimension 2)	1.69	4.17	1.46
V3 (Temperature Dimension 3)	-1.35	-3.34	-1.16

Notes: To compute the values displayed in the table, a reduced data subset, filtered to Salzburg's females aged 60+, starting from January 1, 2018 was used, although for other demographic subsets of Salzburg the results are the same, since this is solely based on the temperature data. Source: Own computation based on Bundesamt für Eich- und Vermessungswesen (2024), GeoSphere Austria (2021) and Statistik Austria (2024a)

Values for the cross-basis matrix are available from the 22nd day onwards, as the preceding days do not have sufficient data to summarise the full 21-day lag period. Using the reduced dataset, the resulting cross-basis matrix is displayed in Table 5. The cross-basis is identical across demographic subgroups within the same federal state, as it is solely based on temperature.

Table 5: Cross-Basis Matrix for Salzburg (Reduced Example)

Date	V1.L1	V1.L2	V1.L3	V2.L1	V2.L2	V2.L3	V3.L1	V3.L2	V3.L3
2018-01-01	NA	NA	NA	NA	NA	NA	NA	NA	NA
2018-01-02	NA	NA	NA	NA	NA	NA	NA	NA	NA
2018-01-03	NA	NA	NA	NA	NA	NA	NA	NA	NA
[…]	[…]	[…]	[…]	[…]	[…]	[…]	[…]	[…]	[…]
2018-01-21	NA	NA	NA	NA	NA	NA	NA	NA	NA
2018-01-22	0.37	0.79	0.61	1.69	4.17	1.46	-1.35	-3.34	-1.16
2018-01-23	0.30	0.80	0.60	1.68	4.17	1.45	-1.35	-3.34	-1.15
2018-01-24	0.24	0.81	0.59	1.68	4.17	1.45	-1.35	-3.34	-1.15
2018-01-25	0.19	0.82	0.55	1.68	4.18	1.44	-1.35	-3.34	-1.14
2018-01-26	0.19	0.79	0.50	1.68	4.18	1.43	-1.35	-3.35	-1.14
2018-01-27	0.22	0.70	0.40	1.68	4.18	1.45	-1.35	-3.35	-1.15
2018-01-28	0.20	0.70	0.31	1.68	4.18	1.44	-1.35	-3.35	-1.15
2018-01-29	0.16	0.76	0.30	1.68	4.18	1.44	-1.35	-3.35	-1.15
2018-01-30	0.15	0.80	0.26	1.68	4.18	1.43	-1.35	-3.35	-1.14
2018-01-31	0.19	0.78	0.11	1.68	4.19	1.44	-1.35	-3.35	-1.16
2018-02-01	0.24	0.75	0.05	1.68	4.19	1.43	-1.35	-3.36	-1.15
2018-02-02	0.30	0.73	0.09	1.68	4.18	1.44	-1.35	-3.35	-1.16
2018-02-03	0.35	0.69	0.12	1.69	4.17	1.44	-1.36	-3.34	-1.16
2018-02-04	0.39	0.64	0.17	1.71	4.14	1.45	-1.37	-3.32	-1.17
[…]	[…]	[…]	[…]	[…]	[…]	[…]	[…]	[…]	[…]

Notes: The table displays the cross-basis matrix resulting from a 3x3 dimensional setting, using the reduced dataset filtered to Salzburg, starting from January 1, 2018. Each row represents a single day, and the nine columns correspond to the combinations of three temperature dimensions (V1-V3) and three lag dimensions (L1-L3). Values are available from January 22, 2018 onwards, as the preceding 21 days do not provide sufficient data to compute the full lag period. The cross-basis is identical across demographic subgroups within the same federal state, as it is solely based on temperature data. The highlighted row corresponds to the values displayed in Table 4. Source: Own computation based on Bundesamt für Eich- und Vermessungswesen (2024), GeoSphere Austria (2021) and Statistik Austria (2024a)

Once the cross-basis matrix is created, the distributed lag non-linear model (DLNM) is fitted using the formula defined in chapter 6.3.1. After fitting, standard errors are recalculated and clustered by week, as the model assumes independence of observations. Table 6 displays the model results after recalculation of standard errors for females aged 60+ in Salzburg from the reduced dataset.

Table 6: Stage 1 DLNM Results for Females Aged 60+ in Salzburg (Reduced Example)

Predictor	Estimate	Standard Error	p-value	
(Intercept)	-7.42	0.18	0.00	***
cb_v1.l1	0.01	0.04	0.77	
cb_v1.l2	-0.06	0.02	0.00	***
cb_v1.l3	0.04	0.03	0.09	.
cb_v2.l1	-0.02	0.11	0.86	
cb_v2.l2	-0.02	0.06	0.76	
cb_v2.l3	0.10	0.07	0.12	
cb_v3.l1	-0.03	0.05	0.47	
cb_v3.l2	-0.02	0.02	0.48	
cb_v3.l3	0.03	0.02	0.07	.
ns(date, df = 8)1	-0.02	0.06	0.76	
ns(date, df = 8)2	-0.12	0.09	0.17	
ns(date, df = 8)3	0.10	0.08	0.22	
ns(date, df = 8)4	-0.03	0.09	0.77	
ns(date, df = 8)5	0.01	0.09	0.89	
ns(date, df = 8)6	0.05	0.07	0.44	
ns(date, df = 8)7	0.04	0.14	0.79	
ns(date, df = 8)8	0.14	0.07	0.04	*

*Notes: **Significance codes: *** < 0.001; ** < 0.01; * < 0.05; . < 0.1**. The table displays the results of the Stage 1 analysis: Distributed lag non-linear model (DLNM), fitted to the reduced dataset, which starts with January 1, 2018, for females aged 60+ in Salzburg using reduced cross basis dimensions with 3x3. Standard errors have been recalculated using clustering by calendar week. The highlighted values in the Estimate column correspond to the cross-basis coefficients reproduced in Table 8. Source: Own computation based on Bundesamt für Eich- und Vermessungswesen (2024), GeoSphere Austria (2021), Statistik Austria (2024a), Statistik Austria (2025a) and Statistik Austria (2025c)*

Since all predictors, both cross-basis values and the natural spline capturing temporal trends, are part of spline functions, they cannot be interpreted individually. Their significance values are also not individually interpretable, as the spline terms function as a package rather than as independent predictors. The model is fitted separately for each combination of federal state, age group and sex, resulting in 4 models in this simplified example.

The resulting cross-basis estimators are saved as displayed in Table 7, showing the cross-basis estimators for each model. Model 2 in Table 7 mirrors the results shown previously in Table 6. The corresponding variance-covariance matrices for these estimators of each model are saved as a list of matrices. The meta-predictors are also saved, where age is included as a numeric value, representing the midpoint of each age group. For the oldest age group, the life expectancy at the corresponding age is used.

Table 7: Cross-Basis Estimates and Meta-Predictors by Stage 1 Model (Reduced Example)

Predictor	**Model 1** Salzburg, Female, 0-59 Stage 1 Estimate	**Model 2** Salzburg, Female, 60+ Stage 1 Estimate	**Model 3** Salzburg, Male, 0-59 Stage 1 Estimate	**Model 4** Salzburg, Male, 60+ Stage 1 Estimate
cb_v1.l1	0.03	0.01	-0.09	-0.07
cb_v1.l2	-0.10	-0.06	0.14	-0.03
cb_v1.l3	-0.06	0.04	-0.13	0.09
cb_v2.l1	0.34	-0.02	-0.01	0.01
cb_v2.l2	-0.45	-0.02	0.29	-0.02
cb_v2.l3	0.06	0.10	-0.01	0.06
cb_v3.l1	-0.04	-0.03	-0.18	-0.03
cb_v3.l2	0.00	-0.02	0.09	-0.03
cb_v3.l3	-0.03	0.03	0.04	0.05
Meta-Predictors				
Federal State	Salzburg	Salzburg	Salzburg	Salzburg
Sex	Female	Female	Male	Male
Age Group	0-59	60+	0-59	60+
Numeric Age	29	83	29	83

Notes: The table displays the cross-basis coefficient estimates from Stage 1 distributed lag non-linear models (DLNM), fitted separately for each combination of federal state, sex and age group using the reduced dataset. Model 2 corresponds to the full model results shown in Table 6. Numeric Age represents the midpoint of each age group. For the 60+ age group, the national total life expectancy at age 60 is used instead. Source: Own computation based on Bundesamt für Eich- und Vermessungswesen (2024), GeoSphere Austria (2021), Statistik Austria (2023), Statistik Austria (2024a), Statistik Austria (2025a) and Statistik Austria (2025c)

6.4 Stage 2 Analysis

In the second stage, a multivariate meta-analysis is computed. From its results, the best linear unbiased predictor (BLUP) can be calculated, and the subset-specific coefficients are recalculated.

6.4.1 Formula for Meta-Regression and BLUP calculation

The used formula for the meta-analysis is

$$\hat{\theta} = \alpha + \beta_1 \text{age} + \beta_2 \text{sex} + u_{\text{federal state}}$$

where $\hat{\theta}$ is a vector of subset-specific cross-basis coefficients from Stage 1 and α is the intercept.

The *federal state* variable is included as a random effect to capture between-federal states variability. *age group* and *sex* combinations are included as fixed effects to capture age- and sex-specific differences.

Basagaña and Ballester (2024) recommended to add the two meta-predictors mean and interquartile range of temperature from each of the models in the formula. It explains heterogeneity across models, but it performed worse than the model without them. The differences are likely already captured by the random effects of federal states.

EXAMPLE

The estimates are displayed in separate tables for each cross-basis dimension. As an example from the analysis with the reduced dataset for Salzburg, Table 8 shows the results for v1.l1 and v2.l2.

Table 8: Stage 2 Meta-Regression Results for Selected Cross-Basis Terms (Reduced Example)

	cb_v1.l1			***cb_v2.l2***		
	Estimate	**Std. Error**	**p-value**	**Estimate**	**Std. Error**	**p-value**
Fixed Effects						
Intercept	0.02	0.14	0.91	-0.10	0.23	0.67
Age (numeric)	0.00	0.00	0.97	0.00	0.00	0.81
Sex: Male (baseline: Female)	-0.09	0.06	0.17	0.08	0.10	0.41
Random Effect						
Federal State	0.001			0.001		
Model Diagnostics						
AIC = 50.97, BIC = 58.07, logLik = 10.51						

Notes: The table displays Stage 2 mixed-effects meta-regression results for two selected cross-basis dimensions (v1.l1 and v2.l2) using the reduced dataset. Female serves as reference category for sex. AIC = Akaike Information Criterion, BIC = Bayesian Information Criterion, logLik = log-likelihood. Source: Own computation based on Bundesamt für Eich- und Vermessungswesen (2024), GeoSphere Austria (2021), Statistik Austria (2023), Statistik Austria (2024a), Statistik Austria (2025a) and Statistik Austria (2025c)

The results are not individually interpretable. They are recombined in a subsequent step to produce predictions. Since the random effect is specified at the federal state level and only data from a single federal state (Salzburg) is included in the reduced dataset used in this example, the random effect variance is near zero, as there is no between-state variance estimable.

Using the results of the meta-regression, the best linear unbiased predictors (BLUPs) for each model can be extracted. They combine information from each federal state's data, derived through the stage 1 analysis, with pooled estimates so that strength is borrowed effectively from related groups. This additional approach leads to more robust results compared to the Stage 1 analysis alone. Subgroups that have smaller sample sizes and higher uncertainty are pulled more strongly toward the overall mean, while subgroups with larger sample sizes tend to stay closer to the Stage 1 results. This leads to more reliable estimates across subgroups.

EXAMPLE

The cross-basis coefficients are estimated with the goal of explaining variation by age group and sex, but also to account for variation across federal states. The resulting BLUPs are displayed in Table 9.

Table 9: Stage 2 Best Linear Unbiased Predictions (BLUPs) by Model (Reduced Example)

Predictor	**Model 1** Salzburg, Female, 0-59 BLUP Estimate	**Model 2** Salzburg, Female, 60+ BLUP Estimate	**Model 3** Salzburg, Male, 0-59 BLUP Estimate	**Model 4** Salzburg, Male, 60+ BLUP Estimate
cb_v1.l1	0.01	0.01	-0.07	-0.07
cb_v1.l2	0.01	-0.07	0.07	-0.01
cb_v1.l3	-0.11	0.05	-0.09	0.08
cb_v2.l1	0.20	-0.01	0.18	-0.03
cb_v2.l2	-0.08	-0.04	0.01	0.04
cb_v2.l3	0.13	0.11	0.06	0.04
cb_v3.l1	-0.13	-0.03	-0.14	-0.04
cb_v3.l2	0.06	-0.02	0.05	-0.03
cb_v3.l3	0.00	0.03	0.02	0.05

Notes: The table displays the Best Linear Unbiased Predictions (BLUPs) derived from the results of the Stage 2 meta-regression for each model using the reduced dataset for Salzburg. Source: Own computation based on Bundesamt für Eich- und Vermessungswesen (2024), GeoSphere Austria (2021), Statistik Austria (2023), Statistik Austria (2024a), Statistik Austria (2025a) and Statistik Austria (2025c)

To get the results for different levels of stratification, the BLUP coefficients are pooled, and population weights are calculated for the respective aggregation level.

The pooled coefficient vector is calculated as:

$$\hat{\theta}_{\text{pooled}} = \sum_i w_i \times \hat{\theta}_{i,\text{BLUP}}$$

where w_i represents the populations weight for subgroup i and $\theta_{i,BLUP}$ is the BLUP coefficient vector for subgroup i.

EXAMPLE

In this example, the pooling is performed at the federal state level. The population weights for Salzburg are displayed in Table 10.

Table 10: Population Weights by Demographic Subgroup for Salzburg (Reduced Example)

Sex	Female	Female	Male	Male
Age Group	0-59	60+	0-59	60+
Weight	0.37	0.14	0.38	0.11

Notes: Weights reflect each subgroup's average share of the total population in 2011-2025. Source: Own computation based on Statistik Austria (2025a)

The resulting pooled estimator for Salzburg is displayed in Table 11.

Table 11: Pooled BLUP Estimates for Salzburg (Reduced Example)

Predictor	**Salzburg** Pooled BLUP Estimator
cb_v1.l1	-0.03
cb_v1.l2	0.02
cb_v1.l3	-0.06
cb_v2.l1	0.14
cb_v2.l2	-0.03
cb_v2.l3	0.09
cb_v3.l1	-0.11
cb_v3.l2	0.04
cb_v3.l3	0.02

Notes: The table displays the population-weighted pooled cross-basis coefficients for Salzburg, derived from the subgroup-specific BLUPs (Table 9) and population weights (Table 10). Source: Own computation based on Bundesamt für Eich- und Vermessungswesen (2024), GeoSphere Austria (2021), Statistik Austria (2023), Statistik Austria (2024a), Statistik Austria (2025a) and Statistik Austria (2025c)

The variance-covariance matrix is approximated as:

$$V_{pooled} \approx \sum_{i} w_i^2 \times V_{i,BLUP}$$

where $V_{i,BLUP}$ is the variance-covariance matrix of the BLUP coefficients for subgroup i.

Using the pooled BLUP coefficients and their corresponding variance-covariance matrices, predictions are redone. A new cross-basis matrix is created for each aggregation level, using the same specifications as in Stage 1 to match with the pooled estimates. They included a natural cubic spline for the exposure-response dimension with knots at the 10^{th}, 75^{th} and 90^{th} percentiles of the national temperature distribution and a natural cubic spline for the lag-response dimension with knots on the logarithmic scale, with a maximum lag of 21 days. In combination with the BLUP coefficients, the exposure-response and lag-response curves are created for each aggregation level.

6.4.2 National Level Analysis

The national level analysis captures the overall association of mortality and temperature in Austria. For this, results are pooled across federal states as well as across demographic groups. In the pooling process, population-weighted averaging is applied. The result is a single exposure-response curve to show the overall association of mortality and temperature for Austria. Therefore, a change in age structure of the population could potentially change this curve. An additional curve is created using European Standard Population’s weights to adjust for differences in age structure and enable standardised comparisons to single federal state results. European Standard Population (ESP) values to compute weights were received from Eurostat (2013).

6.4.3 Federal State Level Analysis

To capture regional differences, an analysis similar to the national level analysis is done for each federal state. In this calculation, results are pooled across age group and sex combinations using population-weighted averaging. Exposure-response curves were calculated to show the actual response curves for each federal state. Additional curves were computed using weights of the European Standard Population (ESP) to provide standardised results by age group and sex, enabling comparison across federal states with different age structures.

6.4.4 Demographic Analysis by Age Group and Sex

The demographic analysis aims to examine how mortality and temperature are associated across demographic groups, defined by sex and age group, across Austria. The approach is analogous to the federal state level analysis. In this case, the pooling is done across federal states, again using population weights. In the first scenario the actual exposure-response curve for each age group and sex combination is calculated, reflecting the true geographic distribution of each subgroup.

6.5 Predictions and Minimum Mortality Temperature

As described in the literature, the relationship of mortality and temperature is non-linear. To present the results, average relative mortality values are predicted for the 5th to the 95th percentile as temperature range at 0.1° resolution. The predictions are centred at overall median temperature first to ensure comparability across models.

The temperature with lowest average relative mortality is the minimum mortality temperature. In related literature this is computed by calculating the global minimum (Basagaña & Ballester, 2024). In this analysis, both global and local minima are calculated. For models with sufficient data, they are usually identical. When the data is stratified into smaller subsets and the models for those are created, some results, mostly for the youngest age group in smaller federal states, had unreasonable heavy tails, which then influenced the global minimum. In these cases, using local minimum was used to obtain minimum mortality temperature with reasonable results. If multiple local minima existed, the one closest to median temperature was used. This is decided due to the assumption that minimum mortality occurs at the most frequent moderate temperature, which the population is adapted to (Yin et al., 2019). If no local minimum could be identified, the global minimum was used.

After identifying the minimum mortality temperature, all average relative mortality values are normalised so that minimum mortality temperature has the baseline value of 1. The resulting values are referred to as relative mortality as they express mortality risk at a given temperature relative to the risk at the optimum temperature. Relative mortality can then be interpreted as mortality risk at a certain temperature compared with the risk at the minimum mortality temperature. Confidence intervals were rescaled relative to the new baseline. After receiving the best linear unbiased predictions (BLUP), predictions and the minimum mortality temperature calculations and corresponding confidence intervals are recalculated with the same process.

EXAMPLE

The prediction results at the federal state level for Salzburg, using the reduced dataset and cross-basis with reduced dimensions, are shown in Table 12.

Table 12: Predicted Relative Mortality by Temperature and Lag for Salzburg (Reduced Example)

Temperature (°C)	**Lag (Days after exposure)**										
	0	**2**	**4**	**6**	**8**	**10**	**12**	**14**	**16**	**18**	**20**
1	0.94	0.97	0.99	1.01	1.02	1.03	1.03	1.03	1.02	1.02	1.01
4	0.95	0.97	0.99	1.01	1.02	1.02	1.03	1.02	1.02	1.01	1.00
7	0.96	0.98	1.00	1.01	1.02	1.02	1.02	1.02	1.01	1.01	1.00
10	0.97	0.99	1.00	1.01	1.01	1.01	1.01	1.01	1.01	1.00	1.00
13	0.99	0.99	1.00	1.00	1.01	1.01	1.01	1.00	1.00	1.00	1.00
16 (MMT)	1.00	1.00	1.00	1.00	1.00	1.00	1.00	1.00	1.00	1.00	1.00
19	1.00	1.00	1.00	1.00	1.00	1.00	1.00	1.00	1.00	1.01	1.01
22	1.00	1.00	0.99	0.99	0.99	1.00	1.00	1.00	1.01	1.02	1.02

Notes: The table displays predicted relative mortality by temperature (weighted by population density) and lag (days after exposure) for Salzburg, derived from the pooled BLUP estimates (Table 11). Values are expressed relative to the minimum mortality temperature (MMT) of 16 °C. Source: Own computation based on Bundesamt für Eich- und Vermessungswesen (2024), GeoSphere Austria (2021), Statistik Austria (2023), Statistik Austria (2024a), Statistik Austria (2025a) and Statistik Austria (2025c)

It is visible that the relative mortality for 16 °C is at 1 across all lags, as this represents the minimum mortality temperature. The predicted mortality at any other temperature is expressed relative to the mortality at this reference temperature.

Figure 5 shows the exposure-lag-response surface for Salzburg using the reduced dataset and reduced cross-basis dimensions. Visualisations of this relationship either show the exposure-response dimension, where estimates are averaged across lag days, or the lag-response dimension, where specific temperatures are selected to show the relationship across lags. For the lag-response curves, results are log-transformed, before being centred at the minimum mortality temperature.

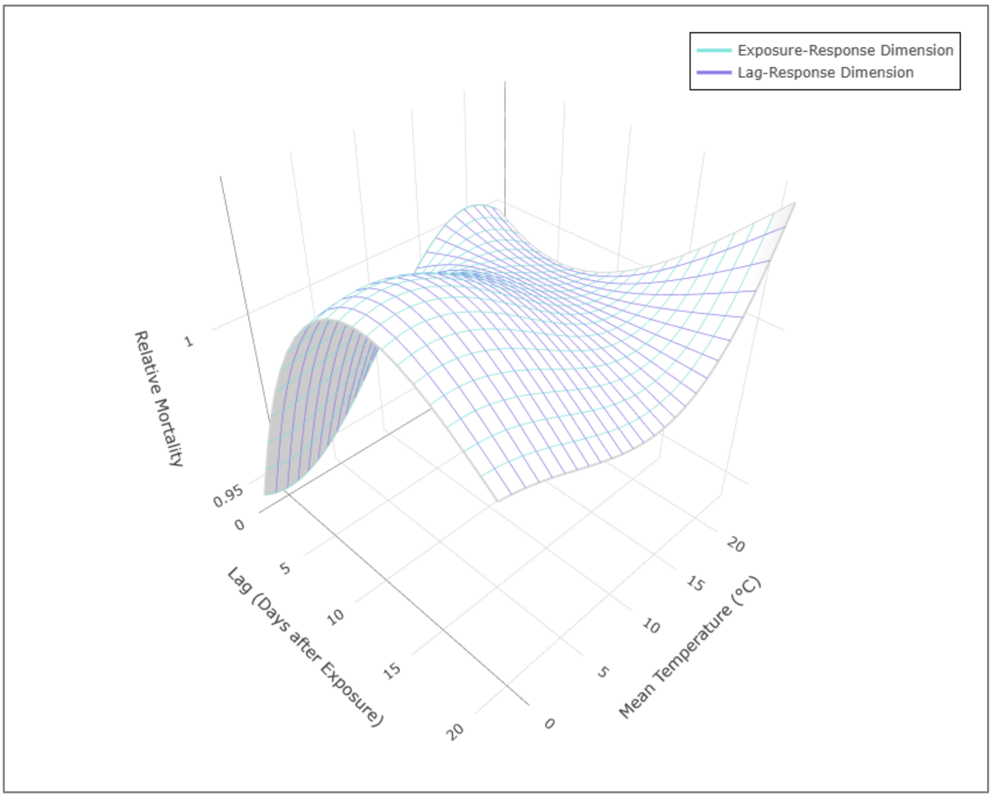

Figure 5: Exposure-Lag-Response Surface for Salzburg (Reduced Example)

Notes: The figure displays the three-dimensional exposure-lag-response relationship for Salzburg, derived from the pooled BLUP estimates, using the reduced dataset and cross-basis with reduced dimensions (3x3). The results shown in this figure are associated with wide confidence intervals. Source: Own computation based on Bundesamt für Eich- und Vermessungswesen (2024), GeoSphere Austria (2021), Statistik Austria (2023), Statistik Austria (2024a), Statistik Austria (2025a) and Statistik Austria (2025c)

6.6 Calculation of Attributable Mortality

Attributable mortality is calculated to quantify the relationship between mortality and temperature in population counts. The attributable fraction of deaths to certain temperatures are calculated using the minimum mortality temperature as a reference baseline. The methodology for calculating attributable fractions and attributable numbers follows an approach by Gasparrini and Leone (2014), which was also used by Basagaña and Ballester (2024).

Deaths are categorised into four temperature exposure categories based on percentiles of the temperature distribution to define extreme temperatures and the minimum mortality temperature to divide cold and heat:

Table 13: Temperature Category Definitions for Attributable Fractions

Extreme cold	Below the 2.5th percentile
Moderate cold	2.5th percentile - minimum mortality temperature
Moderate heat	Minimum mortality temperature - 97.5th percentile
Extreme heat	Above the 97.5th percentile

Notes: Temperature categories are defined based on percentiles of the temperature distribution and minimum mortality temperature, following the approach by Gasparrini and Leone (2014).

For each observed temperature, the relative mortality, also called relative risk (RR), was obtained through predicting for the exposure-response curves with minimum mortality temperature as the centre value. The attributable fraction (AF) is then calculated as:

$$AF = max\left(0, \frac{RR-1}{RR}\right)$$

AF ≥ 0 is necessary in this case to ensure that no negative attributable fractions are obtained, which are logically impossible, as deaths cannot be negative. However, they could arise in subgroups with sparse data, where local minima are used as minimum mortality temperature. This is due to unstable tails with implausibly low risks in the exposure-response curves.

The attributable number (AN) is calculated for each of the four categories as:

$$\mathrm{AN} = \sum_{t \in respective\ category} AF_t \times D_t$$

For each day *t* where the respective temperature category (e.g., moderate cold) was observed, the attributable fraction *AF* of that day's temperature is multiplied with the total deaths *D* of that day. The result then is the total number of deaths that are attributable to the temperature category.

6.7 Assumptions Checks

Due to the combination of weekly death counts and daily temperature values, standard errors and corresponding confidence intervals, as well as p-values, are recomputed using clustered covariance matrix estimation after fitting the model. This allows for within-cluster dependence within the same week. The clusters are defined by the variable *week_id*, labelling each week across all years of observation. A sensitivity check with Newey-West standard errors, which account for autocorrelation, confirms that remaining autocorrelation has little influence on the estimates. The mean ratio of Newey-West to cluster-robust standard errors is close to 1 (mean: 1.02, IQR: 0.96-1.06), indicating that the clustering approach adequately addresses the dependence within weeks in the data.

After aggregating predictions and residuals to the weekly level, further model diagnostics are performed. The appropriateness of quasi-Poisson distribution is evaluated by calculating the dispersion parameter, whose distribution across all 90 models is summarised in Table 20 in the Appendix. It indicates mild under- or overdispersion for most of the models, which confirmed the use of quasi-Poisson distribution to account for small deviations from the Poisson assumption. For the smaller federal states by population, the youngest age group shows some structures in the residual plots against fitted values (Figure 26 in the Appendix) and temperature (Figure 27 in the Appendix). This is expected given the data sparsity. Seasonal trends are adequately controlled for by the natural spline over time. Sensitivity analyses adjusting for relative humidity showed negligible impact on effect estimates (Table 21 in the Appendix), indicating that confounding by humidity does not bias the results.

In the meta-analysis, the heterogeneity between federal states seems to be well captured by the model (Figure 28 in the Appendix), while variation in age groups and sex could not be adequately explained in the youngest age group 0-39 and to some extent in the age groups 40-59 and 90+ (Figure 29 in the Appendix). Apart from this, diagnostics indicate only minor issues overall. Results, particularly for the youngest age group, should be interpreted with caution due to low event counts and sparse data. The full set of meta-regression coefficient estimates is reported in Table 22, provided in the Appendix.

6.8 Computational Environment

All statistical analyses were done using R programming (R Core Team, 2022) within the RStudio development environment (Posit Team, 2025). In the following all used packages are listed, sorted alphabetically and grouped by purpose.

Data cleaning and aggregation:

- *lubridate* (Grolemund & Wickham, 2011): To smoothly aggregate dates to weekly intervals
- *ncdf4* (Pierce, 2023): To handle meteorological data that was stored in NetCDF format
- *RANN* (Arya et al., 2019): To apply nearest-neighbour algorithm to link the differently gridded datasets

- *sf* (Pebesma & Bivand, 2023): For operations including coordinate reference system transformations and spatial joins

Analysis:

- *car* (Fox & Weisberg, 2019): For calculation of variance inflation factors to evaluate model
- *dlnm* (Gasparrini, 2011): For distributed lag non-linear modelling
- *lmtest* (Zeileis & Hothorn, 2002): To recompute the coefficient table using clustered variance-covariance matrix
- *mixmeta* (Sera et al., 2019): To compute meta-analysis in Stage 2
- *sandwich* (Zeileis et al., 2020): For calculation of cluster-robust standard errors
- *splines* (R Core Team, 2022): To add natural splines to the models

Visualisation and general utilities:

- *cowplot* (Wilke, 2024): To arrange plots
- *plotly* (Sievert, 2024): To create 3-dimensional plots
- *tidyverse* (collection of R packages) (Wickham et al., 2019): For data structuring, transformation and visualisations. (Used packages: *dplyr*, *tidyr*, *ggplot2*, *stringr*, *forcats*, *readr*, *tibble*)

7 Results

Following the methodology described in the previous chapter, this chapter presents the findings of the analysis. It starts with the descriptive analysis to summarise and highlight the main patterns of the data. This is followed by the section for the statistical analysis, which shows the results obtained by applying the described methodology to the cleaned dataset.

The results are shown on the national, federal state and population subgroup level. The most relevant visualisations have been included in this chapter. There are additional visualisations for each level in the appendix. Throughout this chapter, temperature values refer to the population-weighted daily mean air temperature at 2 metres, averaged across each region from 1 x 1 km gridded hourly data.

7.1 Descriptive Analysis

Although the median daily temperature in the observed period, from March 2011 to March 2025, is at 10.5 °C, the most frequent daily mean temperatures cluster around 3 °C and 16 °C. This is because the warm and cold seasons each have normally distributed temperatures around their respective means, which differ considerably. During the transitional seasons of spring and autumn, temperatures show more variance and therefore have a flatter distribution. The distributions for each season are visualised in Figure 30 in the Appendix.

The combination of all seasons, showing the distribution of the whole year, is shown in Figure 6. It has the two peaks, which correspond to summer and winter. The median temperature of 10 °C is between them. The minimum observed national mean daily temperature is -12 °C (February 3, 2012) and the maximum is 28.1 °C (July 28, 2013). It needs to be taken into consideration that these values are based on population-weighted national averages of daily mean temperatures rather than daily maximum or minimum temperatures that were seen in weather forecasts at the time. They therefore reflect the single coldest and warmest days within the analysed period in terms of this specific metric, which aims to reflect the temperatures that are most relevant to the population's health outcomes.

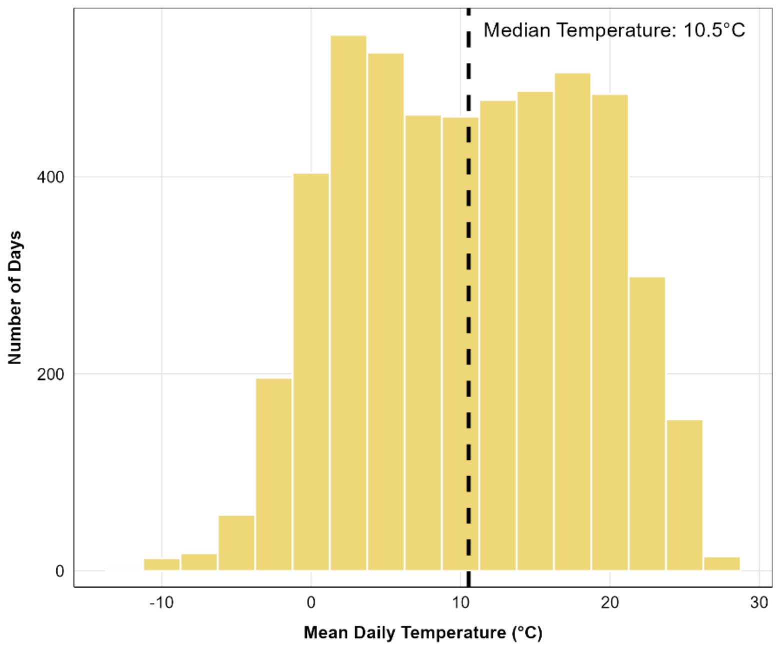

Figure 6: Distribution of Daily Mean Temperature in Austria

Notes: The figure displays the distribution of population density-weighted daily mean temperatures aggregated at the national level. The dashed line indicates the median temperature. The study period covers March 2011 to March 2025. Source: Own computation based on Bundesamt für Eich- und Vermessungswesen (2024), GeoSphere Austria (2021) and Statistik Austria (2024a)

Figure 7 shows the average monthly pattern of temperature across all years of observation and the corresponding average number of deaths. The national mean number of daily deaths is at approximately 230 during the winter months of December, January and February.

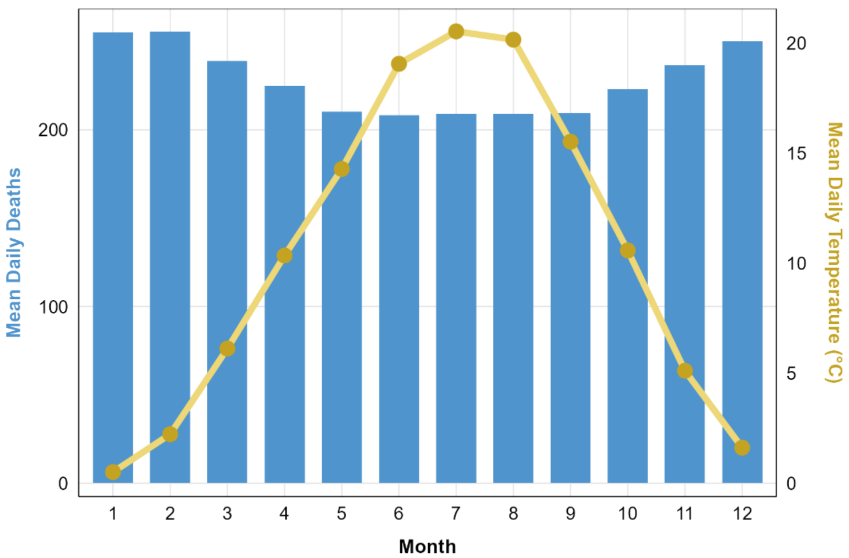

Figure 7: Mean Daily Deaths and Temperature by Month in Austria

Notes: The figure displays the mean monthly pattern of daily deaths and population-weighted daily mean temperature, averaged across all years of observation (March 2011 to March 2025) at the national level. Numbers on the x-axis represent months (from 1 = January to 12 = December). Own computation based on Bundesamt für Eich- und Vermessungswesen (2024), GeoSphere Austria (2021), Statistik Austria (2024a) and Statistik Austria (2025c)

In the summer months of June, July and August, it remains just above 200, while in the transitional months it rises and falls gradually toward the respective summer or winter level (Figure 7). Mean daily temperature shows an almost inverse pattern, but with more pronounced fluctuations from month to month. December, January and February are the three coldest months with mean temperatures between 0 °C and 2.5 °C, while June, July and August are the warmest with mean temperatures around 20 °C. In the spring months, temperatures gradually increase, while in autumn they gradually decline.

The distribution of temperature varies across federal states. The mean daily temperature, weighted by population, is lowest in Tyrol at 9 °C, followed by its eastern neighbours Salzburg and Carinthia, which are both just above 9 °C. The highest mean temperature is found in Vienna at 12 °C, followed by Burgenland at 11.4 °C and Lower Austria at 10.8 °C. These values reveal a clear east-west gradient, with higher temperatures in the eastern federal states and lower ones in the western federal states.

Minimum and maximum temperatures follow a similar spatial pattern, with Tyrol recording the lowest minimum temperature of -14.6 °C and Vienna the highest maximum temperature of 30.3 °C. The standard deviation of daily mean temperatures is approximately 8 °C for all federal states. Vorarlberg has the lowest value at 7.5 °C, indicating a narrower spread of temperature around its mean, while Burgenland, Carinthia and Vienna share the highest value at 8.1 °C, suggesting somewhat more pronounced temperature variability across days.

The mean daily temperature variance was derived by first calculating the variance across hours within each day and then averaging these daily variances. This approximates the mean variation throughout each day. This value is lowest in Vienna, followed by Vorarlberg and Upper Austria, and is highest in Carinthia.

Although relative humidity was not included in the statistical analysis, it is reported in Table 14 for reference. Mean relative humidity across all of Austria ranges from 70% to 79%. Vienna has the lowest value just above 70%, while Upper Austria and Salzburg have the highest values, both exceeding 78%. Interestingly, relative humidity does not follow an east-west gradient. Instead, lower values are found in both the eastern and western federal states and higher values in the states in between.

The temperature percentiles for each federal state using mean daily temperatures are provided in Table 23 in the Appendix. They overall show a similar temperature range. The interquartile ranges, which are the difference between the 25th and 75th percentile, lie between 12.6 to 14.0 °C. The interdecile ranges, which are the differences between the 10th and 90th percentile, are between 19.7 to 21.4 °C. The distribution of temperatures seems therefore to be similar across federal states.

Histograms showing the temperature distribution by federal state and season are provided in Figure 31 in the Appendix to further illustrate the relationship. The normal distribution of temperature by season, as described earlier on the national level, is visible for every federal state, with no outliers apparent. Median temperatures range from 9.1 °C in Tyrol and Salzburg to 11.4 °C in Burgenland and 12.0 °C in Vienna. This again reflects, as expected, the east-west gradient across federal states. The annual evolution of mean temperatures by federal state is shown in Figure 32 in the Appendix, confirming the consistency of this gradient over time.

Table 14: Summary of Meteorological Data by Federal State

Federal State	**Mean Daily Temperature**	**Minimum Temperature (of Daily Means)**	**Maximum Temperature (of Daily Means)**	**Standard Deviation Temperature (of Daily Means)**	**Mean Daily Temperature Variance**	**Mean Relative Humidity**
	°C	**°C**	**°C**	**°C**	**°C²**	**%**
AUSTRIA	10.5	-12.0	28.1	7.9	10.5	74.9
Burgenland	11.4	-11.4	29.8	8.1	10.8	73.4
Carinthia	9.5	-11.5	27.4	8.1	12.5	77.9
Lower Austria	10.8	-13.0	28.6	8.0	11.1	75.2
Salzburg	9.2	-14.1	26.5	7.7	11.1	78.1
Styria	10.2	-11.6	27.5	7.9	12.0	75.3
Tyrol	9.0	-14.6	26.4	7.6	12.3	74.5
Upper Austria	10.1	-13.0	28.1	7.9	9.9	78.3
Vienna	12.1	-11.7	30.3	8.1	8.5	70.1
Vorarlberg	10.4	-13.7	27.9	7.5	8.9	76.4

Notes: All temperature values refer to population density-weighted temperatures in °C from March 2011 to March 2025. "AUSTRIA" represents the national aggregates. Source: Own computation based on Bundesamt für Eich- und Vermessungswesen (2024), GeoSphere Austria (2021) and Statistik Austria (2024a)

In terms of total numbers in the observed time period, Vienna has the largest population with more than 1.8 million inhabitants, followed by Lower Austria, Upper Austria and Styria. However, the highest number of total deaths is found in Lower Austria, followed by Vienna, Upper Austria and Styria. Vienna ranks higher in population share, but lower in mortality compared to Lower Austria, likely due to Vienna's comparatively younger population.

After looking at the values in Table 15, it can be confirmed that the population size and the age distribution is affecting mortality counts. Burgenland has the highest mean annual crude death rate at 10.76 deaths per 1000 persons, followed by Carinthia, Lower Austria and Styria. To account for these demographic differences, an age-standardised death rate was computed, using the population distribution of Austria. This adjustment narrows the gap between states considerably. The range from lowest to highest mean annual crude death rate is at 3.48 (7.28-10.76), whereas for the age-standardised values it is only 1.46 (8.00-9.46). Even after adjusting for the age structure, Burgenland remains the state with the highest death rate, which is followed by Lower Austria and Vienna, showing an east-west gradient. Vorarlberg is the westernmost federal state with the second-smallest population, just after Burgenland, with 390,246.6 inhabitants on average. Yet it ranks lowest in mean annual crude death rates and age-standardised death rates and also records the lowest total number of deaths. Figure 33 in the Appendix displays the mean weekly age-specific death rate by sex and federal state, showing that the age-specific patterns are largely consistent across federal states.

Table 15: Population and Mortality by Federal State

Federal state	**Mean Annual Population**	**Total Deaths**	**Mean Annual Crude Death Rate**	**Age-Standardised Death Rate**
AUSTRIA	8,780,385.7	1,179,251	8.90	8.90
Burgenland	292,912.4	47,564	10.76	9.46
Carinthia	561,076.7	86,141	10.16	8.88
Lower Austria	1,667,684.0	248,440	9.88	9.35
Salzburg	550,550.7	65,872	7.95	8.20
Styria	1,237,296.0	180,530	9.65	8.89
Tyrol	745,182.6	85,736	7.66	8.07
Upper Austria	1,470,751.0	192,642	8.68	8.84
Vienna	1,864,687.0	229,624	8.16	9.17
Vorarlberg	390,246.6	42,702	7.28	8.00

Notes: Mean population was derived from annual mean population values from 2011-2025. The crude death rate is expressed per 1,000 persons per year. The age-standardised death rate uses Austria's national average population distribution as weights. "AUSTRIA" represents the national aggregate. Source: Own computation based on Statistik Austria (2024b), Statistik Austria (2024c), Statistik Austria (2025c)

Aggregated on the national level, deaths follow a seasonal pattern. They peak during winter months and get to their lowest point in summer, as shown in Figure 7. Deaths gradually fall in spring and rise in autumn. In the observed period from March 2011 to March 2025, a total of 1,179,251 deaths were recorded in Austria. The daily average therefore is approximately at 230.5 deaths.

When looking at the seasonal distribution by federal state in Figure 8, one notable difference is found. In all federal states. where mean monthly temperatures exceed 20 °C in summer months, a small bump in deaths is visible for the hottest months. The overall share of annual deaths is highest in winter for all federal states, declining in spring and rising in autumn. During summer, some federal states, including Burgenland, which is known to experience among the highest temperatures, show an increase in deaths toward midsummer before declining again toward autumn, creating more of a W-shaped than a U-shaped seasonal pattern. In contrast, Salzburg shows an opposite pattern for the summer months. There is a more pronounced dip in deaths during midsummer, forming a clear U-shaped pattern. Most federal states show only small fluctuations or nearly stagnant death shares across the summer months.

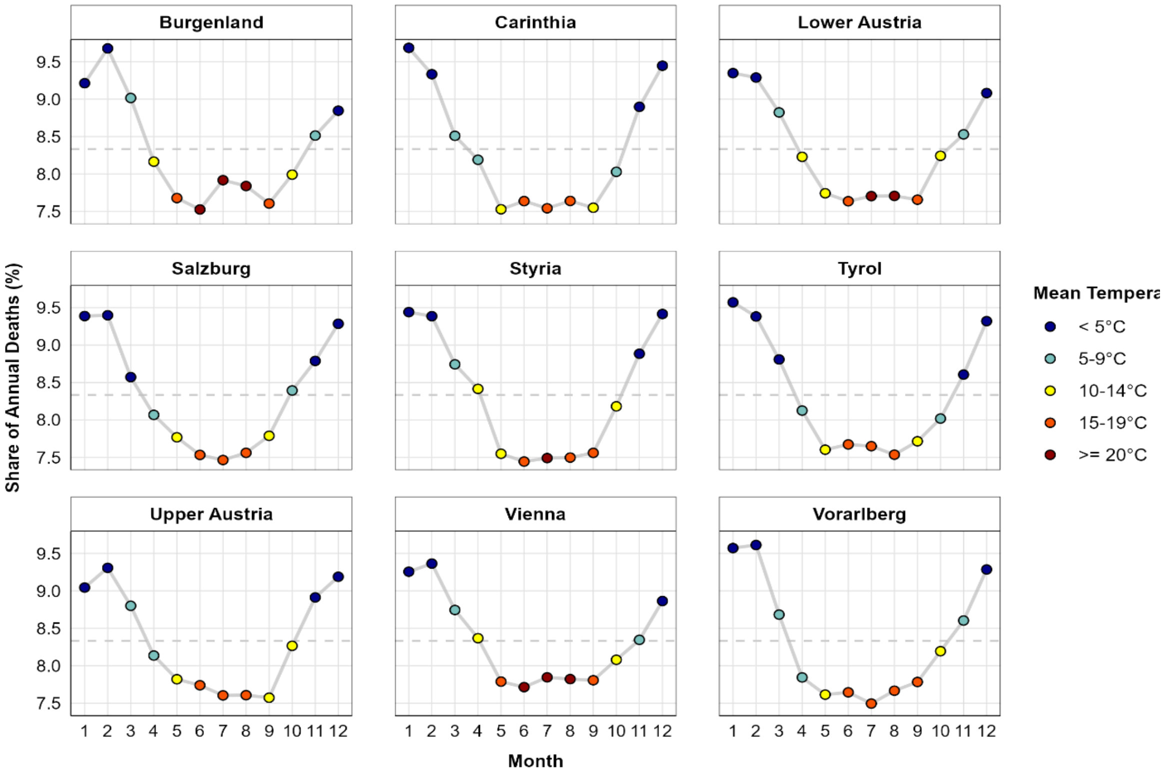

Figure 8: Monthly Share of Annual Deaths and Temperature by Federal State

Notes: The figure displays the mean monthly share of annual deaths (in %) and population density-weighted daily mean temperature for each federal state, averaged across the study period (March 2011 to March 2025). Numbers on the x-axis represent months (from 1 = January to 12 = December). Source: Own computation based on Bundesamt für Eich- und Vermessungswesen (2024), GeoSphere Austria (2021), Statistik Austria (2024a), Statistik Austria (2025a) and Statistik Austria (2025c)

Figure 9, showing a scatterplot of mean daily temperature against daily crude death rate, including a smoothed trend line, reveals the expected U-shaped pattern in most federal states. Death rates are higher at both ends of the temperature scale and lowest at moderate temperatures. A deviation from this pattern is visible in Vorarlberg, where mortality appears to decline at the coldest temperatures. However, this plot neither captures the lagged relationship between mortality and temperature, nor does it account for differences in age structure across federal states or other confounding variables.

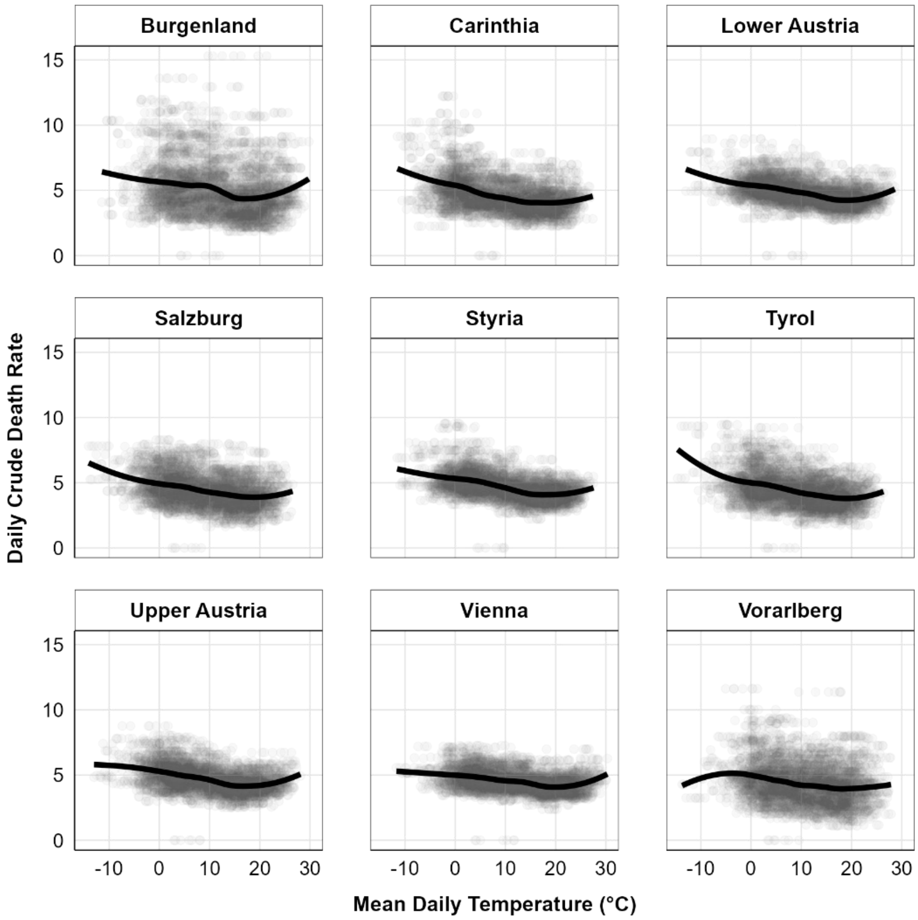

Figure 9: Daily Mean Temperature and Crude Death Rate by Federal State

Notes: The figure displays a scatterplot of population density-weighted daily mean temperature against the daily crude death rate for each federal state, with a smoothed trend line. Source: Own computation based on Bundesamt für Eich- und Vermessungswesen (2024), GeoSphere Austria (2021), Statistik Austria (2024a), Statistik Austria (2025a) and Statistik Austria (2025c)

Table 16 shows that the mean annual population in the observed time period is larger for females than males overall, mainly due to a higher share of females in the age groups at 60 and above. In the age group 40-59, the difference between sexes is marginal, while in the youngest age group, 0-39, males outnumber females. It is important to note that the age groups are not equal in size, as the youngest age group includes 40 single years, followed by an age group covering 20 years and two including 15 single years each thereafter. This grouping is applied in the statistical analysis due to the low counts of deaths in younger age groups.

The population pyramids for 2018 (Figure 3), the middle year of the analysis, clearly show an urn shape, as 5-year age groups are used. Figure 34 and Figure 35 in the Appendix confirm this structure for the years 2012 and 2024, which are close to the start and the end date of this analysis. Table 16 presents the population and mortality data using the aggregated age groups chosen for the statistical analysis, which differ from the 5-year age groups used in the population pyramids. The highest absolute number of deaths is observed in the age group 75-89 for both males and females (Table 16). Up to the age of 74, more males than females die in each age group. Beyond that age, more females die in absolute terms, although this is due to higher mortality of men at younger ages, which leaves fewer men in the older age groups. In relative terms, male mortality exceeds female mortality across all age groups, which is reflected in the mean annual age-specific death rate in Table 16.

Table 16: Population and Mortality by Age Group and Sex

Age Group	Sex	Mean Annual Population	Total Deaths	Mean Annual Age-Specific Death Rate
0-39	female	1,960,824.0	7,633	0.28
0-39	male	2,047,327.0	15,060	0.53
40-59	female	1,287,920.0	32,984	1.83
40-59	male	1,283,014.0	60,822	3.38
60-74	female	739,409.4	93,155	8.99
60-74	male	666,934.8	153,439	16.43
75-89	female	426,712.7	293,075	49.03
75-89	male	292,493.4	269,844	65.87
90+	female	55,925.1	181,097	231.19
90+	male	19,825.9	72,142	259.79

Notes: Mean annual population is averaged across the study period (March 2011 to March 2025). The age-specific death rate is expressed per 1,000 persons per year. Age groups correspond to the aggregated ones used in the statistical analysis. Source: Own computation based on Statistik Austria (2024b), Statistik Austria (2024c), Statistik Austria (2025c)

Looking at the distribution of deaths for each age group throughout the year in Figure 10, it is noticeable that older age groups show more seasonal fluctuations than younger ones. The share of annual deaths for the youngest age group shows peaks in February and July but remains relatively stable throughout the year. The observed pattern of more deaths in winter months and fewer in summer months becomes more pronounced with increasing age. The only exceptions to this pattern are the two oldest age groups, which nearly overlap, but, by a narrow margin, reverse order in October and December. As a result of this pattern, in April and October the shares of annual deaths nearly align for all age groups. When disaggregated by sex (Figure 36 in the Appendix), the monthly shares vary little between females and males, though females show slightly higher shares in winter months and lower ones in summer months.

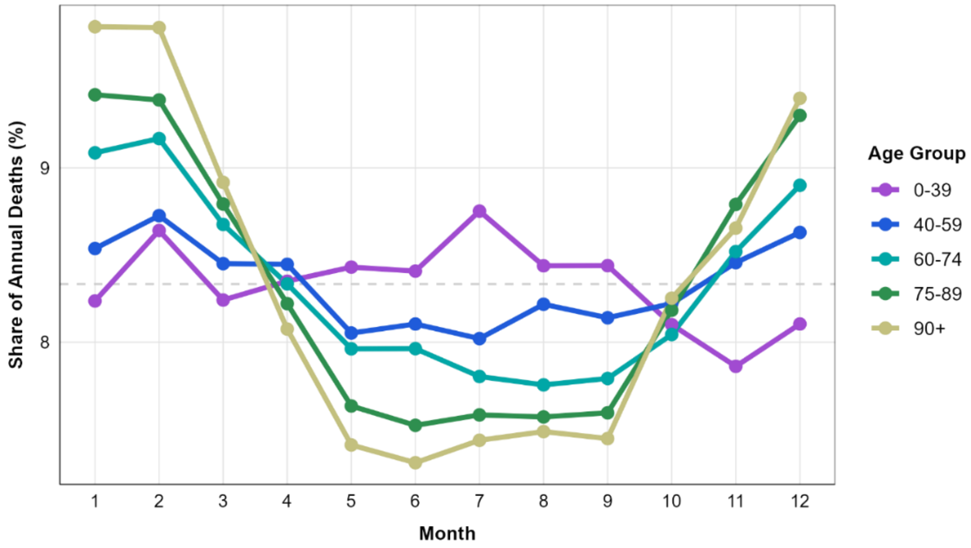

Figure 10: Monthly Share of Annual Deaths by Age Group

Notes: The figure displays the mean monthly share of annual deaths (in percent) for each age group, averaged across the study period (March 2011 to March 2025). Numbers on the x-axis represent months (from 1 = January to 12 = December). Source: Own computation based on Bundesamt für Eich- und Vermessungswesen (2024), GeoSphere Austria (2021), Statistik Austria (2024a), Statistik Austria (2025a) and Statistik Austria (2025c)

Figure 11 shows a scatterplot of daily mean temperature and age-specific death rate by age group and sex. The smoothed trend line reveals the expected U-shaped pattern for the oldest age groups. For younger age groups, and especially for females, this pattern is less pronounced, and the lines appear relatively flat. The most counterintuitive pattern is observed for males aged under 40, which looks M-shaped, caused by heavy tails on both ends. This may still reflect a similar underlying structure, but the limited data in this group makes the trends at the temperature extremes less reliable. A similarly heavy tail at cold temperatures is also visible for females in the same age group. However, as with Figure 9, this plot neither captures the lagged relationship between mortality and temperature nor accounts for confounding variables.

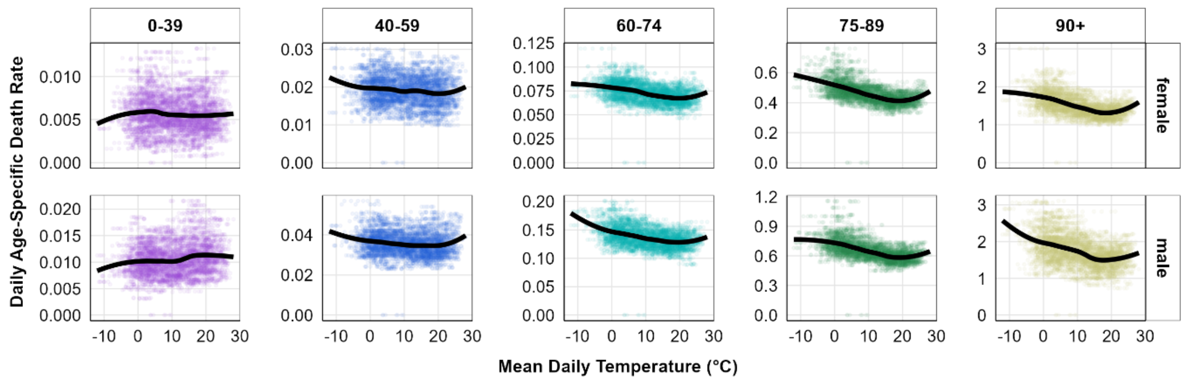

Figure 11: Daily Mean Temperature and Age-Specific Death Rate by Age Group and Sex

Notes: The figure displays a scatterplot of population density-weighted daily mean temperature against the age-specific death rate for each combination of age group and sex, with a smoothed trend line. Source: Own computation based on Bundesamt für Eich- und Vermessungswesen (2024), GeoSphere Austria (2021), Statistik Austria (2024a), Statistik Austria (2025a) and Statistik Austria (2025c)

7.2 Statistical Analysis

After fitting models for each federal state, sex and age group combination, the multivariate meta-regression model is computed. Using the best linear unbiased predictors (BLUP), results are pooled at different aggregation levels, and the exposure-response and lag-response curve values are recalculated. Based on these results, minimum mortality temperatures and attributable numbers are derived.

7.2.1 National Level Analysis

The exposure-response curve in Figure 12 describes the relationship between mortality and temperature, taking federal state-, age- and sex-specific differences into consideration and summarising deaths, not only on the days of temperature exposure, but also for the days thereafter. Seasonal effects and temporal trends were accounted for. The resulting curve shows mortality relative to the mortality at the minimum mortality temperature. It follows a reversed J-shape. If mortality had been predicted for higher temperatures, the curve is expected to follow a U-shape. However, the predictions were restricted to temperatures between the 5th and 95th percentiles of mean daily temperatures at the national level in the observed period.

The minimum mortality temperature in the national level analysis is 16.56 °C. It is the local and global minimum of the curve (Figure 12). Although mortality increases at cold and hot temperatures and the slope is similarly steep toward both ends, the area under the curve is clearly larger on the cold side. This is because the minimum mortality temperature lies closer to the upper end of the displayed temperature range and the curve not much steeper at the hot end. At the coldest visualised mean daily temperature of -1.94 °C (5th percentile), the relative mortality is 1.104, indicating that the risk is 10.4% higher compared to the mortality at the minimum mortality temperature. At the hottest visualised temperature of 22.66 °C (95th percentile), the relative mortality is 1.038, reflecting 3.8% higher mortality.

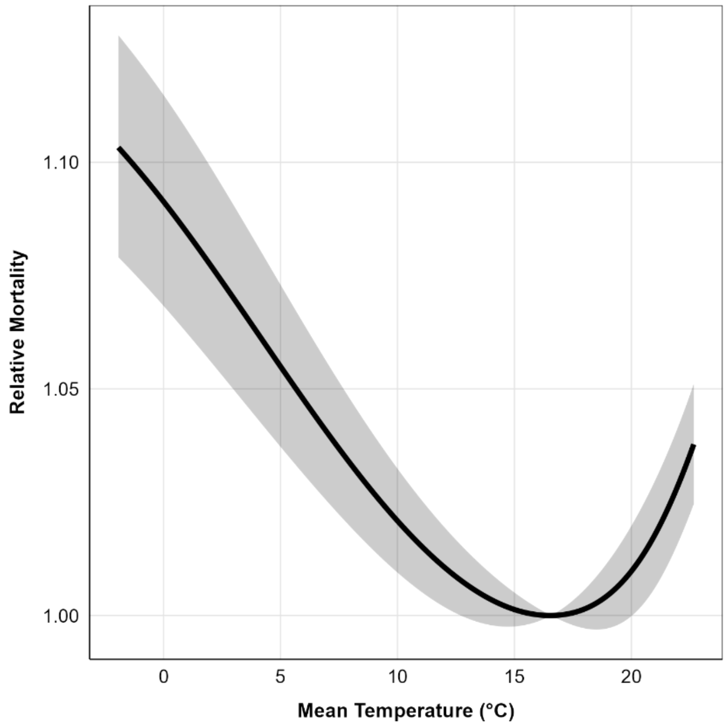

Figure 12: Exposure-Response Curve (National Level)

Notes: The figure displays the estimated relationship between population density-weighted daily mean temperature and relative mortality at the national level, averaged across all lags (0-21 days). Mortality is expressed relative to the minimum mortality temperature (MMT) of 16.56 °C. Predictions are restricted to the 5th to 95th percentile range of the national temperature distribution. Source: Own computation based on Bundesamt für Eich- und Vermessungswesen (2024), GeoSphere Austria (2021), Statistik Austria (2023), Statistik Austria (2024a), Statistik Austria (2025a) and Statistik Austria (2025c)

As mentioned before, the exposure-response curve summarises only two of the three dimensions, which are relative mortality and temperature. Days after exposure, which shows the lagged response, is the third dimension. It is aggregated by summing the effects of each lag, which are days after exposure and shows the resulting relationship between mortality and temperature.

Figure 13 shows the exposure-response curves decomposed for specific lags. The y-axis, again, indicates the relative mortality compared to the mortality at minimum mortality temperature. The sum of all these lag-lines results in the line shown before in Figure 12, which describes the summarised exposure-response of all lags.

At lag 0, meaning the day of exposure, the relative mortality is notably high for the hottest temperatures, reaching approximately 2% higher mortality compared to mortality at the minimum mortality temperature. On the day of exposure, colder temperatures fall below one in relative mortality, meaning the mortality is even lower on day one for the coldest temperatures compared to the minimum mortality temperature on that day. While the association of heat and mortality diminishes rapidly over subsequent days, the link with cold temperatures intensifies. Among the displayed lags (days after exposure), the effects of cold are most pronounced 5 days after exposure. By days 10 and 15, all relative mortality values have declined.

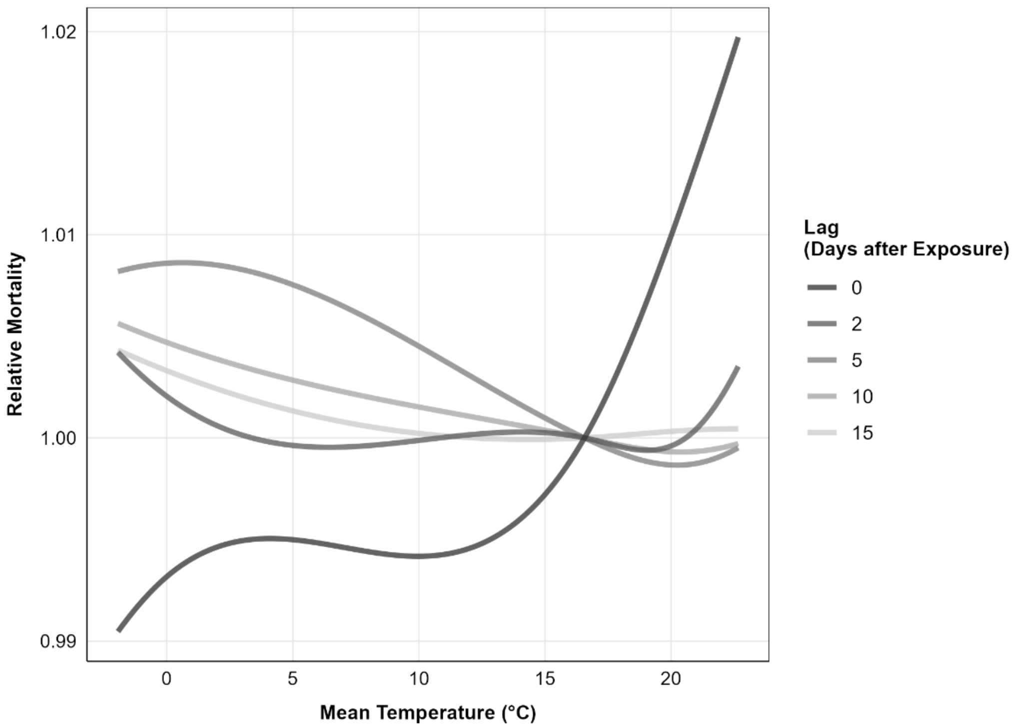

Figure 13: Exposure-Response Curves at Specific Lags (National Level)

Notes: The figure displays exposure-response curves decomposed by specific days after exposure. Relative mortality is expressed relative to the minimum mortality temperature. Source: Own computation based on Bundesamt für Eich- und Vermessungswesen (2024), GeoSphere Austria (2021), Statistik Austria (2023), Statistik Austria (2024a), Statistik Austria (2025a) and Statistik Austria (2025c)

Figure 14 presents the third dimension, days after exposure, from another dimension by showing lines for every temperature from the 5th to the 95th percentile of the temperature distribution. The baseline mortality is, as before, defined at the minimum mortality temperature of 16.56 °C for every lag. Values on the y-axis are logarithmised. The highest temperatures are associated with the strongest values on the day of exposure and decline close to 0 from day 5 onward. Cold temperatures show values below zero on the first day and increase steeply, reaching their peak on day 5, after which, they decline slowly again. Beyond day 14 after exposure, the effects do not fully disappear for some temperatures and even seem to slightly increase again. This is likely not a real pattern but rather a result from using sparse weekly data.

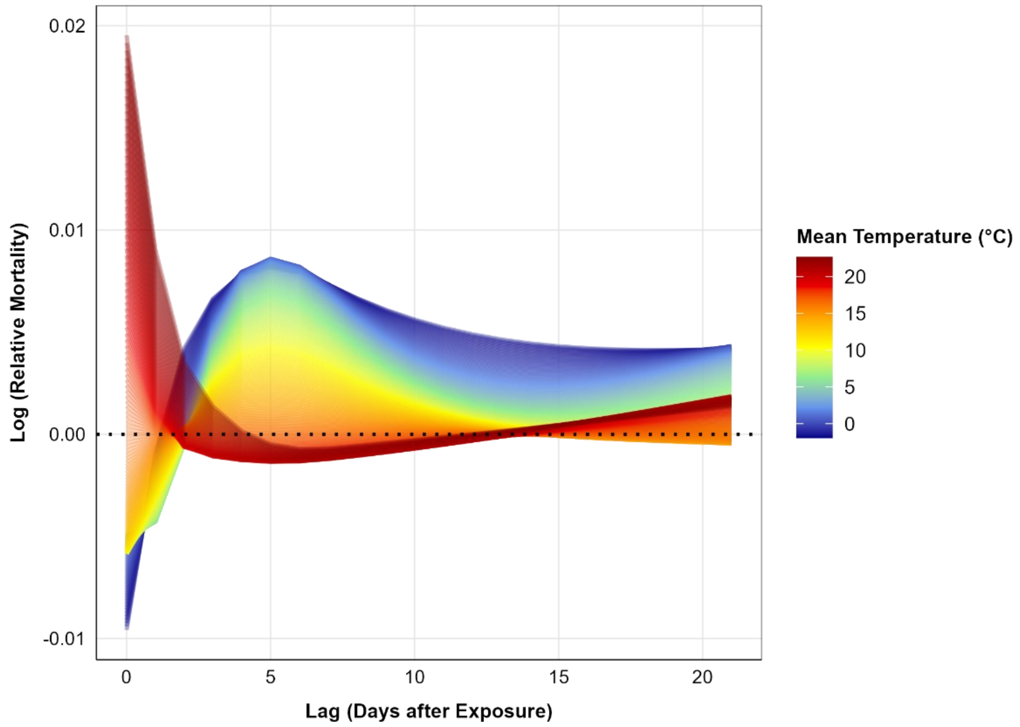

Figure 14: Lag-Response Curves (National Level)

Notes: The figure displays the lag-response relationship for temperatures ranging from the 5th to the 95th percentile of the national temperature distribution. Values on the y-axis are log-transformed relative mortality, with the minimum mortality temperature (16.56 °C) as the reference at each lag. Source: Own computation based on Bundesamt für Eich- und Vermessungswesen (2024), GeoSphere Austria (2021), Statistik Austria (2023), Statistik Austria (2024a), Statistik Austria (2025a) and Statistik Austria (2025c)

7.2.2 Federal State Level Analysis

Similar dynamics as at the national level were also observed on the federal state level, with only minor differences between federal states. Figure 15 shows the exposure-response curves for each federal state. Carinthia has the highest relative mortality at the coldest temperature compared to its minimum mortality temperature, followed by Burgenland and Upper Austria. The lowest relative mortality at the coldest temperatures is visible in Lower Austria and Tyrol. The highest displayed temperature is 22 °C and compared to mortality at their minimum mortality temperatures, Vienna and Tyrol have the highest relative mortality.

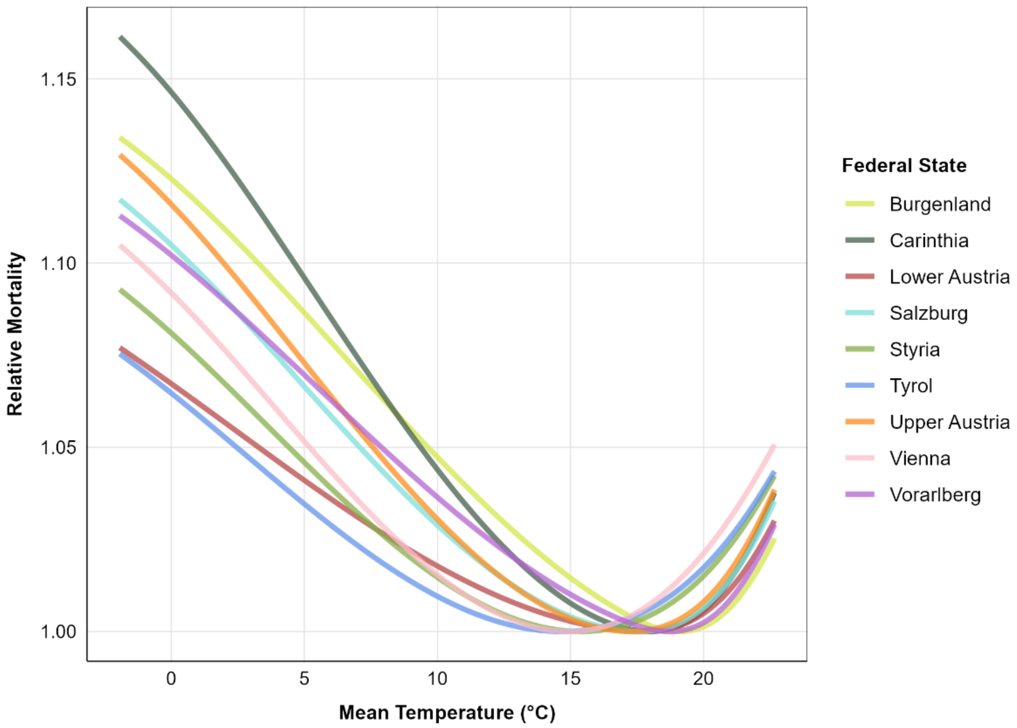

Figure 15: Exposure-Response Curves by Federal State

Notes: The figure displays the estimated relationship between population density-weighted daily mean temperature and relative mortality at the federal state level, averaged across all lags (0-21 days). Mortality is expressed relative to the minimum mortality temperature (MMT) of the corresponding federal state. Predictions are restricted to the 5th to 95th percentile range of the national temperature distribution.

Source: Own computation based on Bundesamt für Eich- und Vermessungswesen (2024), GeoSphere Austria (2021), Statistik Austria (2023), Statistik Austria (2024a), Statistik Austria (2025a) and Statistik Austria (2025c)

It needs to be taken into consideration that relative mortality is computed in relation to each federal state's minimum mortality temperature, which ranges from 14.7 °C in Tyrol to 19.1 °C in Burgenland (Table 17). The difference between minimum mortality temperature and mean temperature is smallest for Vienna, where the two values are only 2.9 °C apart (minimum mortality temperature: 15.0 °C; mean temperature: 12.1 °C). Mean temperatures are presented in Table 14. The largest differences are found in Carinthia (difference of 8.5 °C), Salzburg (difference of 8.4 °C) and Vorarlberg (difference of 8.4 °C). Tyrol has both, the lowest mean temperature and the lowest minimum mortality temperature, with a difference of 5.7 °C. Therefore, no clear pattern emerges.

Table 17: Minimum Mortality Temperature by Federal State (°C)

Federal State	**MMT** **(Minimum Mortality Temperature)**
Burgenland	19.1
Carinthia	18.0
Lower Austria	17.7
Salzburg	17.6
Styria	15.4
Tyrol	14.7
Upper Austria	17.3
Vienna	15.0
Vorarlberg	18.8

Notes: The minimum mortality temperature (MMT) represents the temperature at which predicted mortality is lowest for each federal state. Source: Own computation based on Bundesamt für Eich- und Vermessungswesen (2024), GeoSphere Austria (2021), Statistik Austria (2023), Statistik Austria (2024a), Statistik Austria (2025a) and Statistik Austria (2025c)

Figure 16 shows the exposure-response curves of each federal state, calculated with European Standard Population (ESP) weights alongside curves using actual population weights. Both curves allow for comparison across federal states but have different interpretations. The ESP-weighted curves reflect the temperature-mortality relationship independent of the federal state's age structure, while the population-weighted curves capture the actual demographic composition, showing the relationship as it emerges in the real population. The black striped line represents the exposure-response curve at the national level, and the black solid lines show the curves calculated with ESP weights. The coloured line represents the federal state's actual-population-weighted curve, aligning with the curves shown in Figure 15.

At higher temperatures, most federal states align with the national curve, although Vienna and Tyrol are slightly above it. For cold temperatures, there is more variation between federal states. The steepest increase is found in Carinthia, with the curve rising most toward colder temperatures. Burgenland and Upper Austria are also slightly above the national curve for cold temperatures, while Tyrol, Lower Austria and Styria fall below. It is important to note, that the confidence intervals displayed are large and, for all federal states at almost all temperatures, overlap with the national curve. Interestingly, the differences between the approaches of population weighted pooling and ESP-weighted pooling are minimal. Burgenland and Carinthia exhibit the largest divergences but are still almost fully overlapping.

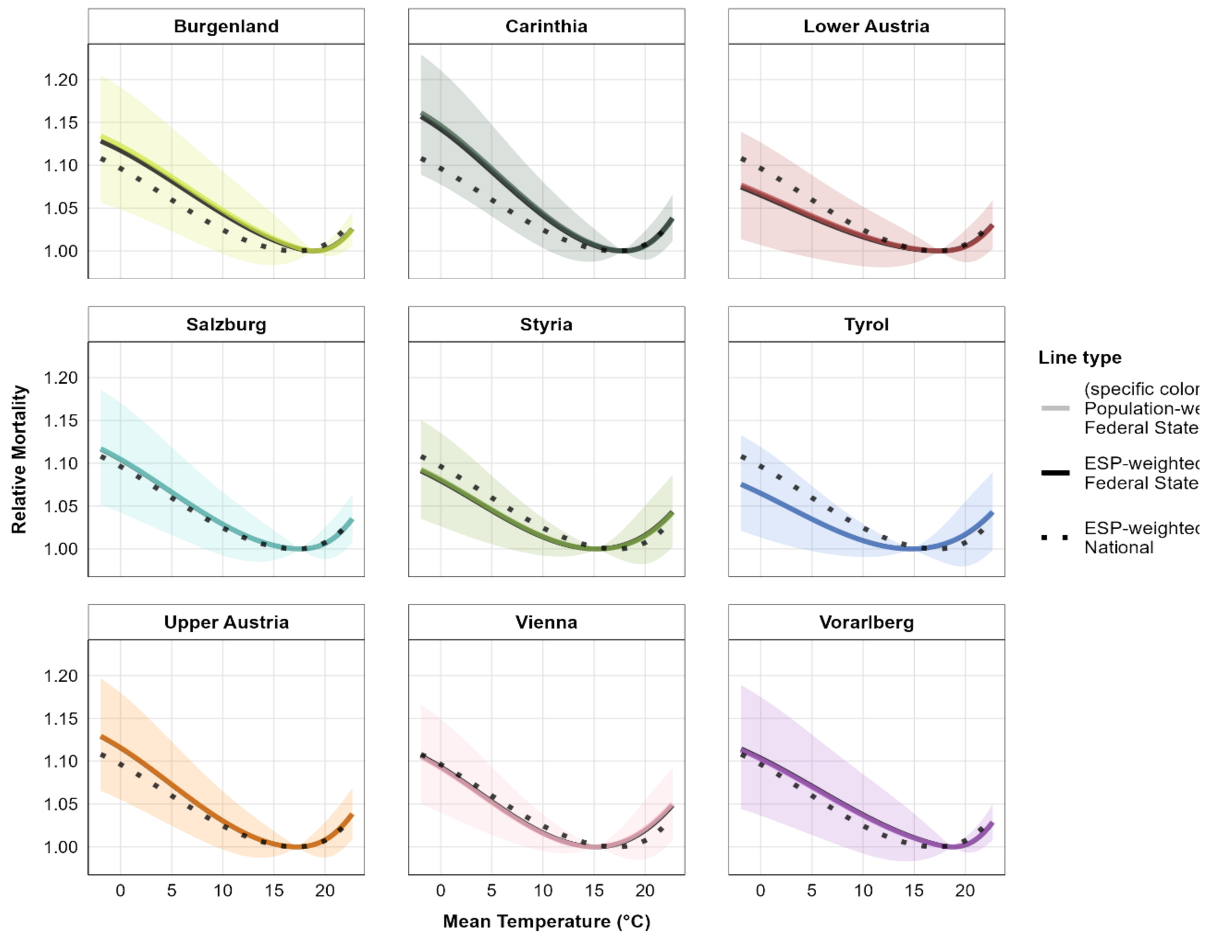

Figure 16: Exposure-Response Curves by Federal State with ESP and Population Weights

Notes: The figure displays the estimated relationship between population density-weighted daily mean temperature and relative mortality for each federal state using both actual population weights (coloured) and European Standard Population (ESP) weights (black solid). The national-level curve using ESP weights is shown as a black dashed line. Confidence intervals correspond to the federal state-specific curves. Mortality is expressed relative to the minimum mortality temperature (MMT) of 16.56 °C. Predictions are restricted to the 5th to 95th percentile range of the national temperature distribution. Source: Own computation based on Bundesamt für Eich- und Vermessungswesen (2024), GeoSphere Austria (2021), Statistik Austria (2023), Statistik Austria (2024a), Statistik Austria (2025a) and Statistik Austria (2025c)

For better readability and comparability, the lag-response curves at the federal state level are shown only for the temperature at the 5th and 95th percentile of the national temperature distribution in Figure 17. It is visible that all federal states have similar trends as already described for the national level. For hot temperatures, the first day is associated with higher mortality compared to the minimum mortality temperature on the first day, while for the coldest temperature, the first day shows even lower values. The logarithmised relative mortality decreases quickly and stays close to zero after a few days. For the colder temperature, a peak is reached around day 5. Depending on the federal state, the subsequent decline occurs at different speeds, but an initial decline can be observed in all federal states. At more than 14 days after exposure, small fluctuations appear, occasionally going slightly upward again. This is rather unrealistic and likely caused by the use of weekly data. Figure 37 shows the population-weighted lag-response curves for each federal state, while Figure 38 visualises the 5th and 95th percentiles of the temperature distribution using ESP-weights, both are provided in the Appendix for reference, though they do not yield additional insights beyond the findings presented in Figure 17.

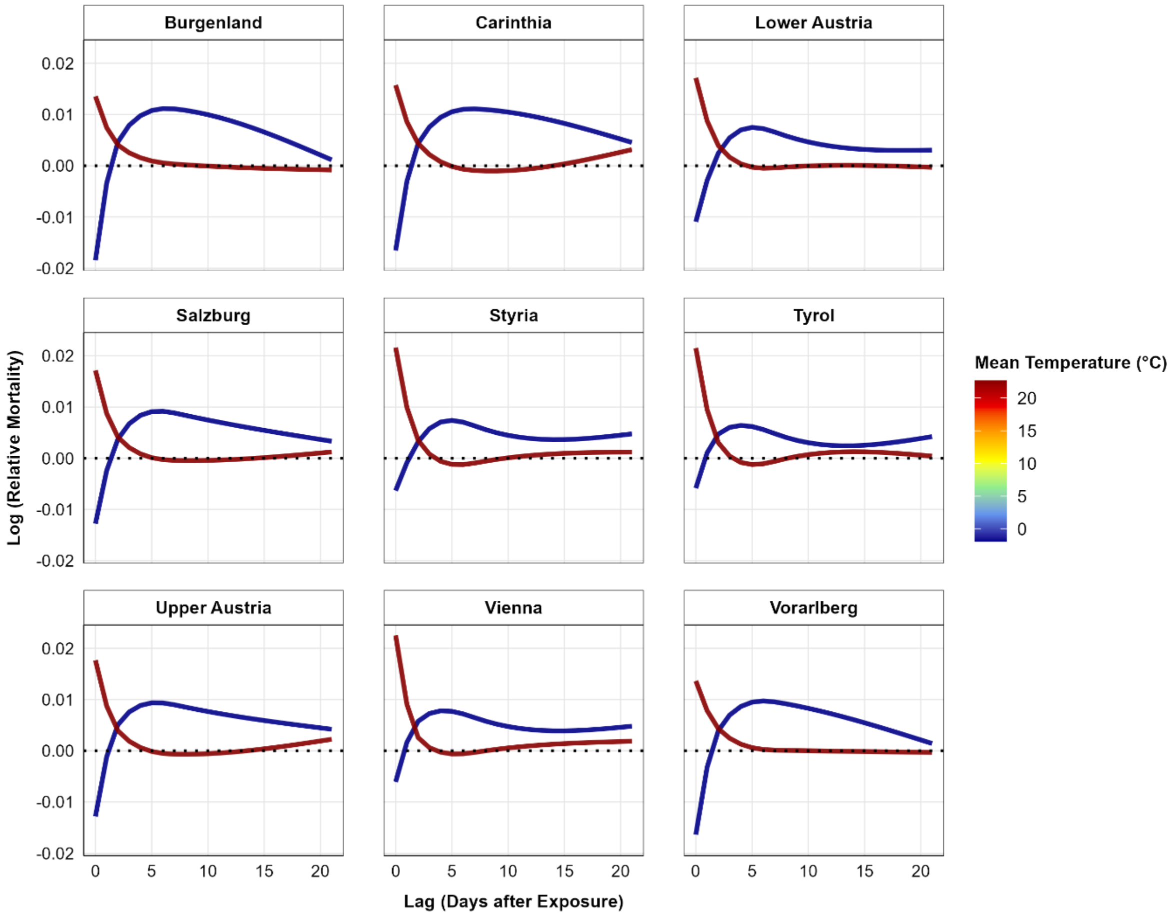

Figure 17: Lag-Response Curves at 5th and 95th Percentiles by Federal State

Notes: The figure displays lag-response curves for each federal state at the 5th and 95th percentiles of the national temperature distribution. The BLUP was pooled using population weights. Values on the y-axis are log-transformed relative mortality with the minimum mortality temperature as reference. Source: Own computation based on Bundesamt für Eich- und Vermessungswesen (2024), GeoSphere Austria (2021), Statistik Austria (2023), Statistik Austria (2024a), Statistik Austria (2025a) and Statistik Austria (2025c)

7.2.3 Demographic Analysis by Age Group and Sex

Figure 18 shows the exposure-response curves for the different age groups. There appears to be a clear pattern, where the oldest age group is affected most by the coldest temperatures and the youngest the least. For warmer temperatures it is almost inverse, although the age groups nearly overlap. When interpreting these curves, one needs to consider the minimum mortality temperature again, as the curves display the relative mortality in relation with it as a reference point.

Table 18: Minimum Mortality Temperature by Age Group and Sex (°C)

	0-39	40-59	60-74	75-89	90+
Female	13.9	16.9	18.5	19.3	19.7
Male	13.9	18.6	19.7	20.1	20.3

Notes: The minimum mortality temperature (MMT) represents the temperature at which predicted mortality is lowest for each age group and sex combination. Source: Own computation based on Bundesamt für Eich- und Vermessungswesen (2024), GeoSphere Austria (2021), Statistik Austria (2023), Statistik Austria (2024a), Statistik Austria (2025a) and Statistik Austria (2025c)

The minimum mortality temperature is lower for younger age groups. Across all ages the minimum mortality temperatures are higher for males and increase with age regardless of sex. Overall sex-specific differences in the exposure-response curves are not fundamental, but the curves for females are nonetheless clearly steeper at colder and hotter temperatures across all age groups.

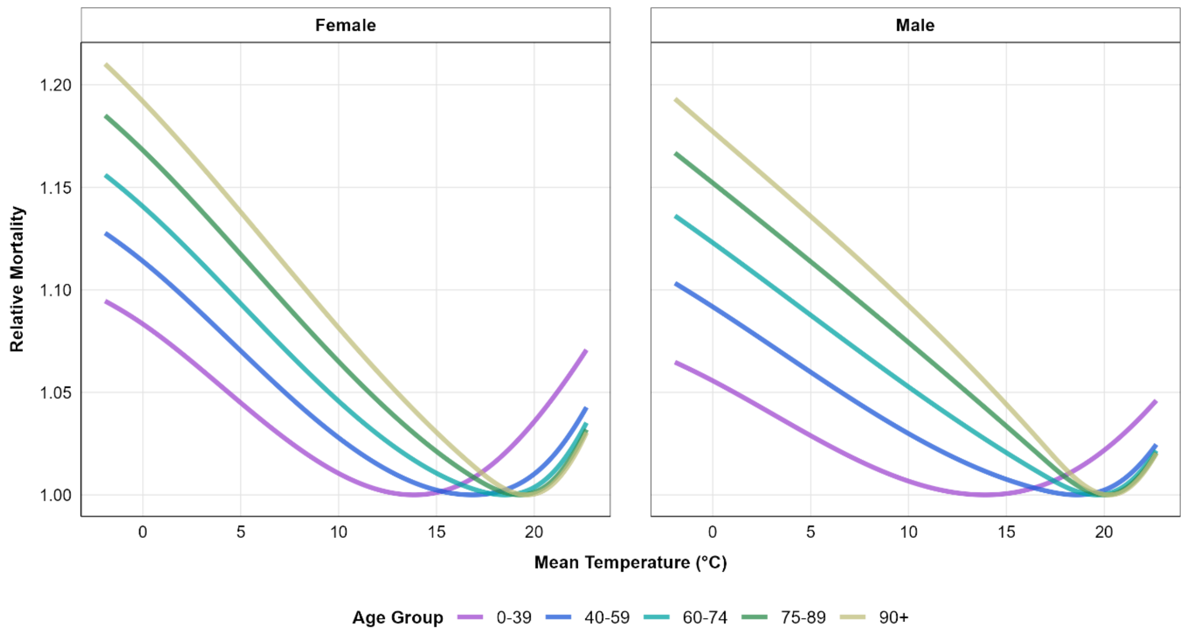

Figure 18: Exposure-Response Curves by Age Group and Sex

Notes: The figure displays the estimated relationship between population density-weighted daily mean temperature and relative mortality at the demographic subgroup level, averaged across all lags (0-21 days). Mortality is expressed relative to the minimum mortality temperature (MMT) of the corresponding demographic subgroup. Predictions are restricted to the 5th to 95th percentile range of the national temperature distribution. Source: Own computation based on Bundesamt für Eich- und Vermessungswesen (2024), GeoSphere Austria (2021), Statistik Austria (2023), Statistik Austria (2024a), Statistik Austria (2025a) and Statistik Austria (2025c)

The lag-response curves at the 5th and 95th percentile show the relationship for each age group and sex combination, as previously shown for the federal state level. Overall, cold-related mortality appears to strengthen with age, while the curves for heat mostly stay the same across ages. Especially males in the youngest age group have a relatively flat curve after being exposed to cold temperature. Interestingly, females in all age groups of age 40 and above show a cold temperature trend where, as usual, the first days show little association with mortality before increasing steeply to a peak on day 5. After that, the curve for females decreases more rapidly than for males, but then shows a small increase, whereas for all males the curve keeps declining. This secondary increase could reflect a steeper decline in mortality at the minimum mortality temperature for females, as the lag-response curves are shown relative to this temperature. If mortality drops more steeply at this reference point for females, this could create the observed rise. It is also possible that this reflects data sparsity, given the fewer female deaths in most age groups and the use of weekly data. Figure 39, provided in the Appendix, shows the distribution for each federal state across all temperatures.

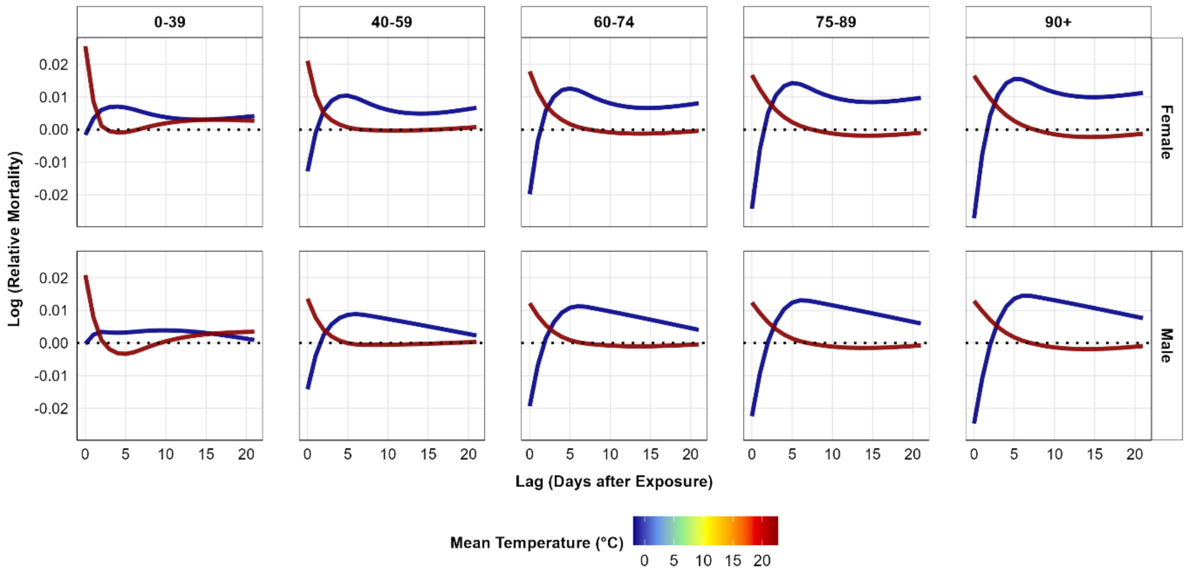

Figure 19: Lag-Response Curves at 5th and 95th Percentiles by Age Group and Sex

Notes: The figure displays lag-response curves for each demographic subgroup at the 5th and 95th percentiles of the national temperature distribution. Values on the y-axis are log-transformed relative mortality with the minimum mortality temperature as reference. Source: Own computation based on Bundesamt für Eich- und Vermessungswesen (2024), GeoSphere Austria (2021), Statistik Austria (2023), Statistik Austria (2024a), Statistik Austria (2025a) and Statistik Austria (2025c)

7.2.4 Attributable Mortality

Attributable numbers are computed based on the same data as the exposure-response and lag-response curves. They measure the impact associated with temperature ranges, always in comparison with the minimum mortality temperature. This data is combined with the actual number of deaths and the percentage of deaths attributable to non-optimal temperatures is calculated.

The number of deaths occurring at the minimum mortality temperature is taken as baseline. It is assumed that this number of deaths would have occurred at any temperature. The deaths that exceed this baseline are defined as excess deaths and therefore mortality that is attributable to temperature. The temperature thresholds for extreme cold and extreme heat are defined as temperatures below the 2.5th percentile and above the 97.5th percentile. Moderate cold and moderate heat are defined as temperatures between the 2.5th or 97.5th percentile and the minimum mortality temperature.

The attributable fractions obtained using ESP weights closely mirror those derived from population weights, with only small differences across all levels of the analysis. Table 19 shows the attributable fractions of mortality by temperature category. While extreme cold, moderate heat and extreme heat each account for between 0.25% and 0.3% of deaths on the national level using the population's weights, moderate cold is standing out with 2.92% of deaths being associated with this temperature category. The highest fractions for attributable mortality in the national, federal state and demographic analysis are in all cases found for moderate cold. For attributable numbers, the actual exposure becomes more relevant. Although the relative mortality for moderate cold appears modest in the exposure-response curves (Figure 12), its high attributable fraction reflects the fact that temperatures in this range occur most frequently, thus leading to a disproportionately higher contribution to overall mortality.

On the federal state level, Carinthia has the highest fractions for cold-attributable mortality, followed by Burgenland. Overall, cold appears to affect mortality least in Lower Austria and Vienna. This pattern holds for both moderate and extreme cold, though attributable fractions are generally low across all federal states.

Mortality attributable to moderate and extreme heat is highest in Vienna. For moderate heat, it is followed by Burgenland, Styria and Lower Austria. In extreme heat, the pattern is similar, although Styria has lower values and Upper Austria has slightly higher values, resulting in minor shifts across federal states. Heat-attributable mortality consistently shows the smallest fractions in Salzburg.

Attributable fractions across demographic groups show a distinct pattern. Cold-attributable fractions increase with age for both moderate and extreme cold. Moderate and extreme heat, by contrast, show the highest attributable fractions in the youngest age group. For moderate heat, it initially decreases before rising again in older age groups. Among females, the increase in attributable fractions for extreme heat with age is steeper than for males. In relative terms, women seem to be more affected by both heat and cold compared to men, despite men having a higher baseline mortality rate.

Table 19: Attributable Fractions of Mortality by Temperature Category (%)

	Extreme cold		Moderate cold		Moderate heat		Extreme heat		Not attributable	
National Level										
	Pop.-W.	ESP-W.	Pop.-W.	ESP-W.	Pop.-W.	ESP-W.	Pop.-W.	ESP-W.	Pop.-W.	ESP-W.
AUSTRIA	0.29	0.30	2.92	3.16	0.30	0.26	0.25	0.25	96.23	96.03
Federal State Level										
	Pop.-W.	ESP-W.	Pop.-W.	ESP-W.	Pop.-W.	ESP-W.	Pop.-W.	ESP-W.	Pop.-W.	ESP-W.
Burgenland	0.36	0.34	4.17	3.93	0.35	0.36	0.25	0.24	94.88	95.13
Carinthia	0.46	0.45	5.32	5.14	0.17	0.18	0.16	0.16	93.88	94.06
Lower Austria	0.24	0.24	2.18	2.08	0.29	0.30	0.21	0.21	97.07	97.18
Salzburg	0.35	0.35	3.94	3.93	0.10	0.10	0.12	0.12	95.49	95.50
Styria	0.29	0.28	2.58	2.52	0.35	0.36	0.17	0.17	96.62	96.67
Tyrol	0.25	0.25	2.23	2.24	0.19	0.19	0.12	0.12	97.20	97.20
Upper Austria	0.36	0.36	3.91	3.90	0.25	0.25	0.20	0.20	95.29	95.30
Vienna	0.30	0.30	2.22	2.27	0.97	0.92	0.30	0.30	96.21	96.20
Vorarlberg	0.31	0.32	3.63	3.70	0.13	0.13	0.18	0.18	95.74	95.67
Demographic Subgroup Level										
	Female	Male	Female	Male	Female	Male	Female	Male	Female	Male
0-39	0.23	0.15	2.36	1.54	0.82	0.56	0.36	0.27	96.23	97.48
40-59	0.32	0.27	3.73	3.33	0.32	0.17	0.29	0.23	95.34	96.00
60-74	0.38	0.37	4.73	4.70	0.25	0.15	0.30	0.24	94.34	94.55
75-89	0.49	0.44	5.98	5.85	0.21	0.14	0.31	0.24	93.01	93.33
90+	0.55	0.50	6.67	6.48	0.20	0.15	0.32	0.26	92.26	92.61

Notes: The table displays the share of deaths attributable to each temperature category at the national, federal state and demographic subgroup level. Temperature categories are defined based on the 2.5th and the 97.5th percentiles of the temperature distribution and the minimum mortality temperature. At the national and federal state level, results are shown using both actual population weights (abbreviated: Pop.-W.) and European Standard Population Weights (abbreviated: ESP-W.). At the demographic subgroup level, results are shown by age group and separately for females and males. Source: Own computation based on Bundesamt für Eich- und Vermessungswesen (2024), GeoSphere Austria (2021), Statistik Austria (2023), Statistik Austria (2024a), Statistik Austria (2025a) and Statistik Austria (2025c)

8 Discussion

There is a clear association between mortality and temperature. Overall, mortality is most pronounced at the coldest temperatures, particularly in older age groups. At warmer temperatures, mortality tends to decline, although, it increases again at the highest temperatures. The exposure-response curves, visualising this relationship of mortality and temperature, align with expected patterns. The national curve aligns with the “reversed J-shape” described by Masselot et al. (2023). The federal state level curves as well as the curves by demographic group align with this pattern, although the youngest age group of 0-39-year-olds is, partially due to their lower minimum mortality temperature, already close to the more often in literature described U-shaped curve (e.g. Achebak et al., 2019; Ballester et al., 2016; Conte Keivabu, 2022). Exposure-response curves with the minimum mortality temperature on the higher end of the range, are more likely to show a reversed J-shape. If the exposure-response curve had predicted the relative mortality for even higher temperatures as well, it likely would have resembled more the U-shape. However, this was not meaningful, since the 95th percentile of the temperature distribution is at 22.66 °C, which was chosen as the upper limit of the prediction range.

Lag-response curves reveal where the average relative mortality in the exposure-response curve results from. At both the national and the federal state levels, results were consistent. High temperatures have the highest relative mortality on the day of exposure and quickly decline thereafter. Cold temperatures, by contrast, show their peak four to five days after exposure and decrease more slowly afterward. This results, in the exposure-response curves, in a higher average relative mortality for cold temperatures compared to heat. Basagaña and Ballester (2024) demonstrate that the peak of cold-related mortality in the lag-response curve shifts when weekly, rather than daily, mortality data is paired with daily temperature data. This may explain the present results, given that cold-related mortality is generally reported to peak around the third day after exposure (Gasparrini et al., 2010). The true peak for Austria therefore might also occur on day three, but the use of weekly data potentially blurs this pattern.

While the curves for each federal state using population-weighted pooling model the locally observed temperature-mortality association, the curves on the federal state level using ESP weights allow for direct comparison of effects across federal states, independent of their age distribution. The two methods yielded similar results and the relative differences between federal states remained largely consistent.

Relative mortality is expressed relative to mortality at the minimum mortality temperature. As this reference point varies between federal states, comparisons across federal states need to consider this differing baseline. Tyrol, with a comparatively low minimum mortality temperature, may show higher relative mortality at a given temperature, above the minimum mortality temperature, than Burgenland, for instance. At 22 °C, mortality in Tyrol is expressed relative to the baseline mortality at 14.7 °C, whereas for Burgenland the baseline is at 19.1 °C.

Minimum mortality temperatures show no clear association with the mean temperature of each federal state. Carinthia, for instance, has one of the lowest mean temperatures, but one of the highest minimum mortality temperatures. Vienna shows the opposite pattern, while Tyrol records the lowest values across federal states for both. This pattern contradicts the findings of Achebak et al. (2019), who reported a high correlation between the two variables across regions and over time.

In the present analysis the minimum mortality temperature is rising with age and is consistently higher for males compared to females. In an analysis of Czech data by Vésier and Urban (2023) minimum mortality temperature was lower for women compared to men and the findings of an analysis of Spanish data suggest that women had lower minimum mortality temperatures than men as well, with the exception of one age group (Achebak et al., 2019). Therefore, the result for sex-specific minimum mortality temperatures found in this analysis are in line with the literature, as through physiological differences women are more vulnerable to heat (Mehnert et al., 2002), and men to cold temperatures (Graham, 1988).

For age groups, there is no consistent pattern found in the literature. In the first analysis, with increasing age, minimum mortality is oscillating for both males and females (Vésier & Urban, 2023). Achebak et al. (2019) found that minimum mortality decreases for older age groups. This is opposite to the findings of the present analysis, where minimum mortality temperatures increase with age. However, the confidence intervals of the exposure-response curves overlap considerably. Nevertheless, even in the descriptive analysis, younger age groups appeared less vulnerable to temperature-related mortality, while still exhibiting a subtle rise during the hottest months.

Overall, the lag-response curves of the age- and sex-specific analysis have a similar pattern as observed at the national level, but for younger age groups, the peaks for cold temperatures are less pronounced. The secondary increase in cold-related mortality for females that is observed in the lag-response curves has no obvious explanation. It could reflect biological differences between sexes, but is more likely a statistical artefact, resulting from insufficient data, as it is also visible in some federal states that do not have disproportionately higher female population counts.

At the national level, cold temperatures are attributable to 3.21% of deaths (extreme cold: 0.29%; moderate cold: 2.92%) and hot temperatures to 0.55% of deaths (extreme heat: 0.25%; moderate heat: 0.3%). The proportion of cold-attributable deaths is mostly driven by moderate cold, reflecting not so much the mortality response at those temperatures, but primarily the high frequency of exposure to this temperature range. A similar distribution in attributable numbers of deaths was found as well by Gasparrini et al. (2015a), with the biggest fraction for moderate cold and smaller ones for all other categories in all countries included in their analysis. The authors found that the fractions vary by country. Moderate cold-attributable fraction is between just above 2% in Brazil and Thailand and at 9% in China and Japan. One neighbouring country to Austria, Italy, was included in this analysis. It has just above 8% attributable fraction to moderate cold. Values for extreme cold, moderate heat and extreme heat were between 0.5% and 1% in Italy (Gasparrini et al., 2015a), all of which are higher than the corresponding values found for Austria.

Masselot et al. (2023) analysed cold- and attributable fractions for more European regions. Values for Austria for cold were at around 4.43% and values for heat were at 0.69%, which are slightly higher for both heat- and cold-attributable fractions compared to this analysis. Their analysis focused on urban areas rather than rural areas, which may explain this discrepancy. Fastl et al. (2024) describe different challenges for heat and cold in rural and urban areas. Nevertheless, the results for Vienna, with 2.52% for cold and 1.27% for heat, diverge even further from the values found by Masselot et al. (2023), but their analysis also included other Austrian urban areas in addition to Vienna, which might cause these differing values.

In the national level analysis, the attributable numbers result in a cold-to-heat-related death ratio of 5.8:1. Compared to the 8.3:1 ratio of cold-to-heat-related deaths, found by García-León et al. (2024) for Europe, this seems rather low. Their analysis examined European regions including Austria, using data from 1991 to 2020. Using their national-level results of attributable numbers, the resulting cold-to-heat-related death ratio is 5.9:1 for Austria. This almost perfectly aligns with the ratio found in the present analysis. Austria's cold-to-heat ratio is consistently lower than the European average. However, since García-León et al. (2024) did not provide attributable fractions, it cannot be determined whether this reflects a smaller cold burden, a larger heat burden or both.

García-León et al. (2024) find that Northern Europe has lower risks of heat-related deaths than Southern Europe and the risk of cold-related death is higher in the east compared to the west. For the present analysis, when looking at the federal state level, there is no north-to-south gradient visible, neither for cold- nor for heat-attributable fractions, but federal states differ in their temperature exposure. An east-west gradient is visible for heat-attributable fractions, with the easternmost federal states of Vienna, Burgenland and Lower Austria having the highest attributable fractions. These are followed by the central federal states Styria and Upper Austria. Exposure to high temperatures is overall higher in eastern federal states. Vienna’s exceptionally high heat-attributable fractions can be largely explained by the overall greater exposure to high temperatures in comparison with all other federal states. Additionally, since all-cause mortality data was used in this analysis, differences in cardiovascular disease prevalence across federal states may also partially explain this gradient, as there is a higher share of cardiovascular patients in eastern states (Stein et al., 2011), who are more vulnerable to temperature extremes (Fastl et al., 2024). For cold-attributable fractions, the highest values were found in federal states in the centre of Austria as well as Burgenland, specifically in Carinthia, Burgenland, Salzburg and Upper Austria. Carinthia, which has an especially high value for deaths attributable to moderate cold, has the highest exposure to cold temperatures. The lowest cold-attributable fractions were found in Lower Austria and Vienna, which are, apart from Burgenland, the federal states with the highest mean daily temperature.

Vienna was expected to show the most distinct pattern of all federal states, as it is a city-state. It has the highest heat-attributable fraction, among the lowest cold-attributable fraction and the within-day temperature variance was lowest in Vienna at 8.5. This is consistent with the urban heat island effect discussed by Fastl et al. (2024), where urban areas experience higher temperatures and, during summer nights, the temperatures do not decrease as much. Even after controlling for the age structure in the exposure-response curve, Vienna shows slightly higher effects for heat and lower ones for cold.

In this analysis the heat- and cold-attributable fractions were higher for women in all age groups, despite men having a higher baseline mortality, indicating greater female vulnerability to temperature extremes. Cold-attributable fractions increased with age for both moderate and extreme cold, while heat showed a more complex pattern. Attributable fractions were highest in the youngest age group, with moderate heat initially decreasing before rising again in older age groups. Among females, the increase in attributable fractions for extreme heat with age was steeper than for males. In an analysis of Spanish data, women also showed higher heat-attributable mortality across all age groups, but men showed higher cold-attributable mortality, except in their youngest age group 60-74. Their analysis had a focus on cardiovascular mortality (Achebak et al., 2019), which might explain these differences to some degree, as this could reshape the vulnerability. European data, from the summer of 2022, revealed that the heat burden increases with age, which is contrary to the present findings (Ballester et al., 2023).

8.1 Limitations

This analysis relies on weekly mortality data rather than daily observations. As Huber et al. (2024) demonstrates, analyses based on weekly data may underestimate heat-related mortality compared to daily data. In addition, Basagaña and Ballester (2024) recommend specific minimum dataset sizes for analyses combining weekly mortality data and daily temperature data. The present dataset falls slightly below these recommendations, which likely introduces imprecision in the estimated associations. The present 14-year study period is shorter than the 20 years recommended in the literature for unbiased estimation of minimum mortality temperature when weekly mortality data is combined with daily temperature data (Basagaña & Ballester, 2024).

Spatial limitations affect the accuracy of temperature estimates. Mortality records only indicate the place of residence of the deceased, not the exact location of death. Kollanus et al. (2021) found differences between people living at home or in care facilities. Even when temperatures were weighted by population density, individuals within federal states likely experienced heterogeneous exposures to temperature. Some federal states represent large geographic areas that show variation, meaning that the assigned temperature values may not accurately reflect individual-level exposures. This analysis could also not control for urban-rural differences within federal states, even though these may shape temperature exposure and vulnerability (Fastl et al., 2024).

The analysis uses mean values of hourly temperatures, which may capture temperatures with different relevance to physiological exposure. Nighttime temperatures may have different health implications than midday temperatures, but they are all given the same weight. Moreover, this analysis uses ambient outdoor temperatures rather than body temperature or indoor thermal conditions.

Relative humidity was tested but excluded from the analysis due to not having substantial effects on the model. Still, weather conditions are shaped by more than temperature and humidity, such as air pressure, wind patterns and sunlight. Certain temperatures might covary with specific weather conditions such as air pressure or sunlight duration that could influence mortality.

Another limitation is the lack of information on causes of death in the mortality data. It could provide additional explanatory insight and would have likely influenced the temperature mortality relationship. It is well established that people with cardiovascular or respiratory diseases are more vulnerable to temperature (Fastl et al., 2024), and there is an east-west gradient in cardiovascular diseases in Austria (Stein et al., 2011). Moreover, socioeconomic differences were not controlled for, which can modify vulnerability to temperature (Visser et al., 2022).

The Stage 1 analysis models include seasonal adjustment, consistent with approaches used in related studies. However, because temperature and seasonality are highly correlated, controlling may lead to underestimation of direct effects of temperature on mortality. The seasonality variable captures broader seasonal mortality patterns, including influenza waves and the COVID-19 pandemic, which may overlap with temperature-driven effects. Therefore, the true temperature-mortality relationship may be different to what the estimates capture.

The dataset spans a relatively limited number of years. Therefore, it is not possible to capture cohort effects or long-term adaptation patterns to temperature. Furthermore, particularly younger populations have sparse mortality counts and produce therefore potentially less reliable estimates.

Additionally, the demographic composition of age groups may confound the age- and sex-specific results. Women are over-represented in the oldest age groups, which show the highest vulnerability, potentially contributing to the higher female attributable fractions beyond physiological differences. Similarly, the youngest age group has the highest proportion of residents in Vienna, where heat exposure is greatest, which may partly explain the elevated heat-attributable fractions observed in this group.

The meta-analysis across federal states and demographic groups pools estimates, following standard practise in the temperature-mortality research (Basagaña & Ballester, 2024; Gasparrini et al., 2015b). While this approach is well-established, the pooling process might affect the precision, especially that of pooled standard errors and confidence intervals. Additionally, through pooling, estimates are pulled towards the overall mean. While this approach enhances statistical robustness, it may lose heterogeneity in the association. The Stage 1 analysis, while less statistically robust, shows greater variability that may more accurately reflect heterogeneity. It is a trade-off between statistical robustness and potential effect loss, which is especially relevant when working with sparse data.

Austria has a spatial pattern of heat exposure with more heat days in flatter eastern regions than in the more mountainous western regions (Fastl et al., 2024). This might not be as visible in the results as one might expect, since these results show relative fractions of heat- and cold. Federal states that are experiencing higher temperatures might have working mitigation strategies, which is not accounted for in this analysis.

Age-standardised all-cause mortality is lower in regions with higher altitudes, which is also causing an east-west gradient in Austria (Burtscher et al., 2021). This is also likely not reflected in the results of the statistical analysis, as they show relative mortality compared to mortality at minimum mortality temperatures, but it can explain the differences in the age-standardised death rates shown in the descriptive analysis.

Also, population projections were used for parts of the 2024 and 2025 data, which also introduce some uncertainty into the denominator and therefore the estimated mortality rates.

9 Conclusion

This thesis aimed to assess how temperature-related mortality in Austria varies across federal states and demographic groups, addressing a gap in regional temperature-mortality research in Central Europe. The analysis confirms that mortality and temperature are linked through a reverse J-shaped relationship, with higher mortality at the cold and hot ends of the temperature distribution. Cold-related mortality peaks four to five days after exposure and diminishes slowly thereafter, whereas heat-related mortality peaks on the day of exposure and declines rapidly. Cold-attributable deaths exceed heat-attributable deaths, with moderate cold accounting for the highest fractions. Nonetheless, approximately 95% of deaths are not attributable to temperature. The heat- and cold-attributable fractions estimated for Austria are somewhat lower than those reported in some Europe-wide analyses (e.g. Masselot et al., 2023), yet the cold-to-heat-related ratio of 5.8:1 aligns almost perfectly with the finding of García-León et al. (2024) for Austria, who also report a more unbalanced ratio for Europe overall.

Exposure-response relationships are broadly similar across federal states, suggesting that differences in attributable mortality are driven less by varying temperature vulnerability and more by differences in exposure to certain temperature ranges. A notable east-west gradient emerges for heat-attributable mortality, with Vienna, Burgenland and Lower Austria exhibiting the highest fractions. Vienna, the only city-state among the federal states, shows the highest heat-attributable and lowest cold-attributable mortality. This is consistent with the urban heat island effect, whereby urban areas tend to exhibit higher temperatures than their surroundings (Fastl et al., 2024). Carinthia shows notably high cold-attributable mortality, reflecting its higher exposure to cold temperatures compared to other federal states. The minimum mortality temperature varies across federal states but shows no clear association with mean temperature.

The heat-attributable mortality fractions appear to decrease with age, while cold-attributable mortality increases. Both trends are likely linked to age-related differences in the minimum mortality temperature, which rises with age and is consistently higher for males than for females across all age groups. Although males have overall higher mortality rates, females seem to be more sensitive to temperature variation at both cold and hot temperatures.

Given the high uncertainty of estimates in the present analysis, differences between federal states or demographic groups should be treated with caution.

Looking ahead, as population ageing unfolds alongside global warming, the number of older individuals exposed to rising temperatures is likely to increase. Heat vulnerability may become a greater concern in the oldest age groups, given their steeper exposure-response curves for heat. The health burden associated with extreme heat may grow disproportionately in the Austrian population, which is in line with other literature (Chen et al., 2024; Masselot et al., 2023). García-León et al. (2024) predict that under a 3 °C global warming scenario, consistent with current climate policies, the heat-to-cold mortality ratio in Europe could shift to 2.6:1 by 2100, while for Austria this ratio is projected to be at 2.0:1, indicating that cold-attributable deaths would only be twice as high as heat-attributable deaths by 2100.

This thesis shows that temperature-related mortality in Austria is shaped by a complex interplay of climate, regional differences and demographic factors. As temperatures continue to rise, understanding these patterns across regions and population groups is essential for effective adaptation.

10 References

Achebak, H., Devolder, D., & Ballester, J. (2019). Trends in temperature-related age-specific and sex-specific mortality from cardiovascular diseases in Spain: A national time-series analysis. *The Lancet Planetary Health*, *3*(7), e297–e306. https://doi.org/10.1016/S2542-5196(19)30090-7

Arya, S., Mount, D., Kemp, S. E., & Jefferis, G. (2019). *RANN: Fast Nearest Neighbour Search (Wraps ANN Library) Using L2 Metric* (Version 2.6.1) [R; R]. https://cran.r-project.org/package=RANN

Austrian Federal Ministry for European and International Affairs. (n.d.). *Geography*. Austrian Federal Ministry for European and International Affairs (BMEIA). Retrieved 25 January 2026, from https://www.bmeia.gv.at/oev-wien/about-austria/geography

Balaj, M., Henson, C. A., Aronsson, A., Aravkin, A., Beck, K., Degail, C., Donadello, L., Eikemo, K., Friedman, J., Giouleka, A., Gradeci, I., Hay, S. I., Jensen, M. R., Mclaughlin, S. A., Mullany, E. C., O'connell, E. M., Sripada, K., Stonkute, D., Sorensen, R. J. D., … Gakidou, E. (2024). Effects of education on adult mortality: A global systematic review and meta-analysis. *The Lancet Public Health*, *9*(3), e155–e165. https://doi.org/10.1016/S2468-2667(23)00306-7

Balas, M., Lindinger, H., Offenzeller, M., & Völler, S. (2024). *The Austrian Strategy for Adaptation to Climate Change*. Federal Ministry Republic of Austria Climate Action, Environment, Energy, Mobility, Innovation and Technology (BMK).

Ballester, J., Quijal-Zamorano, M., Méndez Turrubiates, R. F., Pegenaute, F., Herrmann, F. R., Robine, J. M., Basagaña, X., Tonne, C., Antó, J. M., & Achebak, H. (2023). Heat-related mortality in Europe during the summer of 2022. *Nature Medicine*, *29*(7), 1857–1866. https://doi.org/10.1038/s41591-023-02419-z

Ballester, J., Robine, J.-M., Herrmann, F. R., & Rodó, X. (2011). Long-term projections and acclimatization scenarios of temperature-related mortality in Europe. *Nature Communications*, *2*(1), 358. https://doi.org/10.1038/ncomms1360

Ballester, J., Rodó, X., Robine, J.-M., & Herrmann, F. R. (2016). European seasonal mortality and influenza incidence due to winter temperature variability. *Nature Climate Change*, *6*(10), 927–930. https://doi.org/10.1038/nclimate3070

Bär, S., Bundo, M., de Schrijver, E., Müller, T. J., & Vicedo-Cabrera, A. M. (2022). Suicides and ambient temperature in Switzerland: A nationwide time-series analysis. *Swiss Medical Weekly*, *152*, w30115.

Basagaña, X., & Ballester, J. (2024). Unbiased temperature-related mortality estimates using weekly and monthly health data: A new method for environmental epidemiology and climate impact studies. *The Lancet Planetary Health*, *8*(10), e766–e777. https://doi.org/10.1016/S2542-5196(24)00212-2

Brauer, M., Roth, G. A., Aravkin, A. Y., Zheng, P., Abate, K. H., Abate, Y. H., Abbafati, C., Abbasgholizadeh, R., Abbasi, M. A., Abbasian, M., Abbasifard, M., Abbasi-Kangevari, M., Abd ElHafeez, S., Abd-Elsalam, S., Abdi, P., Abdollahi, M., Abdoun, M., Abdulah, D. M., Abdullahi, A., … Gakidou, E. (2024). Global burden and strength of evidence for 88 risk factors in 204 countries and 811 subnational locations, 1990–2021: A systematic analysis for the Global Burden of Disease Study 2021. *The Lancet*, *403*(10440), 2162–2203. https://doi.org/10.1016/S0140-6736(24)00933-4

Bundesamt für Eich- und Vermessungswesen. (2022). *Digitales Geländemodell—Höhenraster 5m Stichtag 31.12.2022* [Data set]. https://data.bev.gv.at/geonetwork/srv/ger/catalog.search#/metadata/2f9fe78a-eefb-43c2-8688-b5acfa0d132f

Bundesamt für Eich- und Vermessungswesen. (2024). *Verwaltungsgrenzen (VGD) BEV Stichtag 01.10.2024* [Data set]. https://doi.org/10.48677/f7b698de-7f87-482c-97dd-33ebaf32fe40

Burtscher, J., Millet, G. P., & Burtscher, M. (2021). Does living at moderate altitudes in Austria affect mortality rates of various causes? An ecological study. *BMJ Open*, *11*(6), e048520. https://doi.org/10.1136/bmjopen-2020-048520

Chen, K., de Schrijver, E., Sivaraj, S., Sera, F., Scovronick, N., Jiang, L., Roye, D., Lavigne, E., Kyselý, J., Urban, A., Schneider, A., Huber, V., Madureira, J., Mistry, M. N., Cvijanovic, I., Gasparrini, A., & Vicedo-Cabrera, A. M. (2024). Impact of population aging on future temperature-related mortality at different global warming levels. *Nature Communications*, *15*(1), 1796. https://doi.org/10.1038/s41467-024-45901-z

Cheng, J., Xu, Z., Bambrick, H., Su, H., Tong, S., & Hu, W. (2019). Impacts of heat, cold, and temperature variability on mortality in Australia, 2000–2009. *Science of The Total Environment*, *651*, 2558–2565. https://doi.org/10.1016/j.scitotenv.2018.10.186

Conte Keivabu, R. (2022). Extreme Temperature and Mortality by Educational Attainment in Spain, 2012–2018. *European Journal of Population*, *38*(5), 1145–1182. https://doi.org/10.1007/s10680-022-09641-4

de Schrijver, E., Bundo, M., Ragettli, M. S., Sera, F., Gasparrini, A., Franco, O. H., & Vicedo-Cabrera, A. M. (2022). Nationwide Analysis of the Heat- and Cold-Related Mortality Trends in Switzerland between 1969 and 2017: The Role of Population Aging. *Environmental Health Perspectives*, *130*(3), 037001. https://doi.org/10.1289/EHP9835

de Schrijver, E., Folly, C. L., Schneider, R., Royé, D., Franco, O. H., Gasparrini, A., & Vicedo-Cabrera, A. M. (2021). A Comparative Analysis of the Temperature-Mortality Risks Using Different Weather Datasets Across Heterogeneous Regions. *GeoHealth*, *5*(5), e2020GH000363. https://doi.org/10.1029/2020GH000363

de Schrijver, E., Royé, D., Gasparrini, A., Franco, O. H., & Vicedo-Cabrera, A. M. (2023). Exploring vulnerability to heat and cold across urban and rural populations in Switzerland. *Environmental Research: Health*, *1*(2), 025003. https://doi.org/10.1088/2752-5309/acab78 de Schrijver, E., Sivaraj, S., Raible, C. C., Franco, O. H., Chen, K., & Vicedo-Cabrera, A. M. (2023). Nationwide projections of heat- and cold-related mortality impacts under various climate change and population development scenarios in Switzerland. *Environmental Research Letters*, *18*(9), 094010. https://doi.org/10.1088/1748-9326/ace7e1

Eurostat. (2013). *Revision of the European Standard Population: Report of Eurostat's task force (2013 edition)*. Publications Office of the European Union. https://data.europa.eu/doi/10.2785/11470

Eurostat. (2025). *Median age by sex* ([Eq_pop04]) [Data set]. https://ec.europa.eu/eurostat/databrowser/view/eq_pop04/default/table

Fastl, C., Arnberger, A., Gallistl, V., Stein, V. K., & Dorner, T. E. (2024). Heat vulnerability: Health impacts of heat on older people in urban and rural areas in Europe. *Wiener Klinische Wochenschrift*, *136*(17–18), 507–514. https://doi.org/10.1007/s00508-024-02419-0

Flynn, A., McGreevy, C., & Mulkerrin, E. C. (2005). Why do older patients die in a heatwave? *QJM*, *98*(3), 227–229. https://doi.org/10.1093/qjmed/hci025

Fox, J., & Weisberg, S. (2019). *An R Companion to Applied Regression* (Version Third edition) [R; R]. Sage. https://socialsciences.mcmaster.ca/jfox/Books/Companion/

Gallo, E., Quijal-Zamorano, M., Méndez Turrubiates, R. F., Tonne, C., Basagaña, X., Achebak, H., & Ballester, J. (2024). Heat-related mortality in Europe during 2023 and the role of adaptation in protecting health. *Nature Medicine*, *30*(11), 3101–3105. https://doi.org/10.1038/s41591-024-03186-1

Galobardes, B., Lynch, J., & Smith, G. D. (2007). Measuring socioeconomic position in health research. *British Medical Bulletin*, *81–82*(1), 21–37. https://doi.org/10.1093/bmb/ldm001

García-León, D., Masselot, P., Mistry, M. N., Gasparrini, A., Motta, C., Feyen, L., & Ciscar, J.-C. (2024). Temperature-related mortality burden and projected change in 1368 European regions: A modelling study. *The Lancet Public Health*, *9*(9), e644–e653. https://doi.org/10.1016/S2468-2667(24)00179-8

Gasparrini, A. (2011). *Distributed lag linear and non-linear models in R: the package dlnm* [R; R]. https://doi.org/10.18637/jss.v043.i08

Gasparrini, A., Armstrong, B., & Kenward, M. G. (2010). Distributed lag non-linear models. *Statistics in Medicine*, *29*(21), 2224–2234. https://doi.org/10.1002/sim.3940

Gasparrini, A., Guo, Y., Hashizume, M., Lavigne, E., Zanobetti, A., Schwartz, J., Tobias, A., Tong, S., Rocklöv, J., Forsberg, B., Leone, M., Sario, M. D., Bell, M. L., Guo, Y.-L. L., Wu, C., Kan, H., Yi, S.-M., Coelho, M. de S. Z. S., Saldiva, P. H. N., … Armstrong, B. (2015a). Mortality risk attributable to high and low ambient temperature: A multicountry observational study. *The Lancet*, *386*(9991), 369–375. https://doi.org/10.1016/S0140-6736(14)62114-0

Gasparrini, A., Guo, Y., Hashizume, M., Lavigne, E., Zanobetti, A., Schwartz, J., Tobias, A., Tong, S., Rocklöv, J., Forsberg, B., Leone, M., Sario, M. D., Bell, M. L., Guo, Y.-L. L., Wu, C., Kan, H., Yi, S.-M., Coelho, M. de S. Z. S., Saldiva, P. H. N., … Armstrong, B. (2015b). Mortality risk attributable to high and low ambient temperature: A multicountry observational study. *The Lancet*, *386*(9991), 369–375. https://doi.org/10.1016/S0140-6736(14)62114-0

Gasparrini, A., & Leone, M. (2014). Attributable risk from distributed lag models. *BMC Medical Research Methodology*, *14*(1), 55. https://doi.org/10.1186/1471-2288-14-55

GeoSphere Austria. (2021). *INCA Stundendaten* (Version 1) [Data set]. GeoSphere Austria. https://doi.org/10.60669/6AKT-5P05

Graham, T. E. (1988). Thermal, metabolic, and cardiovascular changes in men and women during cold stress. *Medicine and Science in Sports and Exercise*, *20*(5 Suppl), S185-92. https://doi.org/10.1249/00005768-198810001-00017

Grolemund, G., & Wickham, H. (2011). *Dates and Times Made Easy with lubridate* [R; R]. https://www.jstatsoft.org/v40/i03/

Guide of the World. (n.d.). *Austria Physical Map*. Guide of the World. Retrieved 19 October 2025, from https://www.guideoftheworld.com/wp-content/uploads/map/austria_physical_map.jpg

Haas, W., Moshammer, H., Muttarak, R., & Koland, O. (2019). *Österreichischer Special Report Gesundheit, Demographie und Klimawandel*. Verlag der Österreichischen Akademie der Wissenschaften. https://doi.org/10.1553/asr18

Huber, V., Breitner-Busch, S., He, C., Matthies-Wiesler, F., Peters, A., & Schneider, A. (2024). Heat-Related Mortality in the Extreme Summer of 2022. *Deutsches Ärzteblatt International*, *121*(3), 79–85. https://doi.org/10.3238/arztebl.m2023.0254

Huppmann, D., Keiler, M., Riahi, K., Rieder, H., Brad, A., Formayer, H., Fuchs, S., Kettner, C., Kranzl, L., Novy, A., Resch, G., Schinko, T., Schmidt, J., Schöniger, F., Steininger, K. W., Spittler, N., Donner, A., Holzinger, M., Hummel, E.-M., … Scheifinger, K. (2025). *Zweiter Österreichischer Sachstandsbericht zum Klimawandel | AAR2—Zusammenfassung für die politische Entscheidungsfindung*. Verlag der Österreichischen Akademie der Wissenschaften. https://doi.org/10.1553/aar2-spm-de

Hutter, H.-P., Moshammer, H., Wallner, P., Leitner, B., & Kundi, M. (2007). Heatwaves in Vienna: Effects on mortality. *Wiener Klinische Wochenschrift*, *119*(7–8), 223–227. https://doi.org/10.1007/s00508-006-0742-7

Janoš, T., Ballester, J., Čupr, P., & Achebak, H. (2024). Countrywide analysis of heat- and cold-related mortality trends in the Czech Republic: Growing inequalities under recent climate warming. *International Journal of Epidemiology*, *53*(1), dyad141. https://doi.org/10.1093/ije/dyad141

K.C., S., Dhakad, M., Potančoková, M., Adhikari, S., Yildiz, D., Mamolo, M., Sobotka, T., Zeman, K., Abel, G., Lutz, W., & Goujon, A. (2024). *Updating the Shared Socioeconomic Pathways (SSPs) Global Population and Human Capital Projections* (Working Paper WP-24-003). International

Institute for Applied Systems Analysis (IIASA). http://www.wittgensteincentre.org/dataexplorer

Kollanus, V., Tiittanen, P., & Lanki, T. (2021). Mortality risk related to heatwaves in Finland – Factors affecting vulnerability. *Environmental Research*, *201*, 111503. https://doi.org/10.1016/j.envres.2021.111503

Lowe, R., Ballester, J., Creswick, J., Robine, J.-M., Herrmann, F., & Rodó, X. (2015). Evaluating the Performance of a Climate-Driven Mortality Model during Heat Waves and Cold Spells in Europe. *International Journal of Environmental Research and Public Health*, *12*(2), 1279–1294. https://doi.org/10.3390/ijerph120201279

Lutz, W., Butz, W. P., & K.C., S. (2014). *World Population and Human Capital in the Twenty-First Century*. (Original work published Oxford University Press)

Martínez-Solanas, È., Quijal-Zamorano, M., Achebak, H., Petrova, D., Robine, J.-M., Herrmann, F. R., Rodó, X., & Ballester, J. (2021). Projections of temperature-attributable mortality in Europe: A time series analysis of 147 contiguous regions in 16 countries. *The Lancet Planetary Health*, *5*(7), e446–e454. https://doi.org/10.1016/S2542-5196(21)00150-9

Masselot, P., Mistry, M., Vanoli, J., Schneider, R., Iungman, T., Garcia-Leon, D., Ciscar, J.-C., Feyen, L., Orru, H., Urban, A., Breitner, S., Huber, V., Schneider, A., Samoli, E., Stafoggia, M., de'Donato, F., Rao, S., Armstrong, B., Nieuwenhuijsen, M., … Aunan, K. (2023). Excess mortality attributed to heat and cold: A health impact assessment study in 854 cities in Europe. *The Lancet Planetary Health*, *7*(4), e271–e281. https://doi.org/10.1016/S2542-5196(23)00023-2

Mehnert, P., Bröde, P., & Griefahn, B. (2002). Gender-related difference in sweat loss and its impact on exposure limits to heat stress. *International Journal of Industrial Ergonomics*, *29*(6), 343–351. https://doi.org/10.1016/S0169-8141(02)00073-2

OECD & European Observatory on Health Systems and Policies. (2025). *Country Health Profile 2025: Austria* (State of Health in the EU). OECD Publishing; European Observatory on Health Systems and Policies.

Pascal, M., Wagner, V., & Corso, M. (2023). Changes in the temperature-mortality relationship in France: Limited evidence of adaptation to a new climate. *International Journal of Biometeorology*, *67*(4), 725–734. https://doi.org/10.1007/s00484-023-02451-1

Pebesma, E., & Bivand, R. (2023). *Spatial Data Science: With Applications in R* [R; R]. Chapman and Hall/CRC. https://doi.org/10.1201/9780429459016

Pierce, D. (2023). *ncdf4: Interface to Unidata netCDF (Version 4 or Earlier) Format Data Files* (Version 1.22) [R; R]. https://cran.r-project.org/package=ncdf4

Posit Team. (2025). *RStudio: Integrated Development Environment for R* [Computer software]. Posit Software, PBC. http://www.posit.co/

R Core Team. (2022). *R: A language and environment for statistical computing* [Computer software]. R Foundation for Statistical Computing. https://www.R-project.org/

Rásky, É., Stolz, E., Burkert, N. T., & Großschädl, F. (2015). Potentially preventable premature deaths in women and men from the two leading causes of death in Austria, mortality statistics of the nine federal states 2010–2012. *BMC Public Health*, *15*(1), 1177. https://doi.org/10.1186/s12889-015-2502-y

Schifano, P., Leone, M., De Sario, M., de'Donato, F., Bargagli, A. M., D'Ippoliti, D., Marino, C., & Michelozzi, P. (2012). Changes in the effects of heat on mortality among the elderly from 1998–2010: Results from a multicenter time series study in Italy. *Environmental Health*, *11*(1), 58. https://doi.org/10.1186/1476-069X-11-58

Schmidt, A. E., Brugger, K., Csekits, C., Haslinger, K., Hollosi, B., Kaufmann, H., Knopper, M., Kovacs, B., Lampl, C., Niedermoser, B., & Richter, L. (2024). *Nationaler Hitzeschutzplan Österreich*. Bundesministerium für Soziales, Gesundheit, Pflege und Konsumentenschutz (BMSGPK).

Schuster, J. (2025). *Nicht-binäre Geschlechter in der Bevölkerungsstatistik* (Nr. 1; STATjournal). Statistik Austria. https://www.statistik.at/fileadmin/pages/406/STATjournal-1-2025_barrierefrei_AdPg_Geschlechter.pdf

Sera, F., Armstrong, B., Blangiardo, M., & Gasparrini, A. (2019). *An extended mixed-effects framework for meta-analysis* [R; R]. http://www.ag-myresearch.com/2019_sera_statmed.html

Sievert, C. (2024). *plotly: Create Interactive Web Graphics via 'plotly.js'* [R; R]. https://cran.r-project.org/package=plotly

Son, J.-Y., Liu, J. C., & Bell, M. L. (2019). Temperature-related mortality: A systematic review and investigation of effect modifiers. *Environmental Research Letters*, *14*(7), 073004. https://doi.org/10.1088/1748-9326/ab1cdb

Statistik Austria. (2023). *Ausführliche Sterbetafel für Österreich ab dem Alter von 35 Jahren nach höchster abgeschlossener Bildung* [Data set].

Statistik Austria. (2024a). *1 square km grid data from the Austrian population census 2021* (Version SDMX GenericMetadata XML (DataSetID: CENSUS_INS21ES_A). Prepared for ESTAT) [Data set]. https://ec.europa.eu/eurostat/web/gisco/geodata/population-distribution/population-grids

Statistik Austria. (2024b). *Bevölkerung im Jahresdurchschnitt ab 2002* [Data set]. https://statcube.at/statistik.at/ext/statcube/jsf/tableView/tableView.xhtml

Statistik Austria. (2024c). *Bevölkerung im Jahresdurchschnitt für Österreich und die Bundesländer* [Data set]. https://statcube.at/statistik.at/ext/statcube/jsf/tableView/tableView.xhtml

Statistik Austria. (2025a). *Bevölkerung zu Jahresbeginn ab 2002 (einheitlicher Gebietsstand 1.1.2025)* [Data set]. https://statcube.at/statistik.at/ext/statcube/jsf/tableView/tableView.xhtml

Statistik Austria. (2025b). *Gestorbene* [Data set]. https://statcube.at/statistik.at/ext/statcube/jsf/tableView/tableView.xhtml

Statistik Austria. (2025c). *Gestorbene in Österreich (ohne Auslandssterbefälle) ab 2000 nach Kalenderwoche und Altersgruppe* [Data set]. https://statcube.at/statistik.at/ext/statcube/jsf/tableView/tableView.xhtml

Statistik Austria. (2025d). *Lebenserwartung bei der Geburt 1970 bis 2024 nach Bundesländern und Geschlecht* [Data set]. https://www.statistik.at/statistiken/bevoelkerung-und-soziales/bevoelkerung/demographische-indikatoren-und-tafeln/sterbetafeln

Statistik Austria. (2025e). *Österreich. Zahlen. Daten. Fakten 24/25*. Statistik Austria. https://www.statistik.at/services/tools/services/publikationen/detail/2123

Statistik Austria. (2025f). *Österreichischer Zahlenspiegel—September 2025*. Statistik Austria. https://www.statistik.at/services/tools/services/publikationen

Stein, K. V., Rieder, A., & Dorner, T. E. (2011). East-West gradient in cardio-vascular mortality in Austria: How much can we explain by following the pattern of risk factors? *International Journal of Health Geographics*, *10*(1), 59. https://doi.org/10.1186/1476-072X-10-59

United Nations (Ed.). (2009). *World population prospects*. United Nations.

United Nations (Ed.). (2010). *World population ageing, 1950-2050*. United Nations.

Vésier, C., & Urban, A. (2023). Gender inequalities in heat-related mortality in the Czech Republic. *International Journal of Biometeorology*, *67*(8), 1373–1385. https://doi.org/10.1007/s00484-023-02507-2

Visser, M. de, Kunst, A. E., & Fleischmann, M. (2022). *Geographic and socioeconomic differences in heat-related mortality among the Dutch population: A time series analysis*. https://doi.org/10.1136/bmjopen-2021-058185

Wickham, H., Averick, M., Bryan, J., Chang, W., McGowan, L. D., François, R., Grolemund, G., Hayes, A., Henry, L., Hester, J., Huhn, M., Pedersen, T. L., Miller, E., Bache, S. M., Müller, K., Ooms, J., Robinson, D., Seidel, D. P., Spinu, V., … Yutani, H. (2019). *Welcome to the tidyverse* [R; R]. https://doi.org/10.21105/joss.01686

Wilke, C. O. (2024). *cowplot: Streamlined Plot Theme and Plot Annotations for 'ggplot2'* (Version 1.1.3) [R; R]. https://cran.r-project.org/package=cowplot

Winklmayr, C., Muthers, S., Niemann, H., Mücke, H.-G., & an der Heiden, M. (2022). Heat-Related Mortality in Germany From 1992 to 2021. *Deutsches Ärzteblatt International*, *119*(26), 451–457. https://doi.org/10.3238/arztebl.m2022.0202

Yin, Q., Wang, J., Ren, Z., Li, J., & Guo, Y. (2019). Mapping the increased minimum mortality temperatures in the context of global climate change. *Nature Communications*, *10*(1), 4640. https://doi.org/10.1038/s41467-019-12663-y

Yu, W., Xu, R., Ye, T., Han, C., Chen, Z., Song, J., Li, S., & Guo, Y. (2021). Temperature-mortality association during and before the COVID-19 pandemic in Italy: A nationwide time-stratified case-crossover study. *Urban Climate*, *39*, 100948. https://doi.org/10.1016/j.uclim.2021.100948

Zeileis, A., & Hothorn, T. (2002). *Diagnostic Checking in Regression Relationships* [R; R]. https://cran.r-project.org/doc/Rnews/

Zeileis, A., Köll, S., & Graham, N. (2020). *Various Versatile Variances: An Object-Oriented Implementation of Clustered Covariances in R* [R; R]. https://doi.org/10.18637/jss.v095.i01

Zhao, Q., Guo, Y., Ye, T., Gasparrini, A., Tong, S., Overcenco, A., Urban, A., Schneider, A., Entezari, A., Vicedo-Cabrera, A. M., Zanobetti, A., Analitis, A., Zeka, A., Tobias, A., Nunes, B., Alahmad, B., Armstrong, B., Forsberg, B., Pan, S.-C., … Li, S. (2021). Global, regional, and national burden of mortality associated with non-optimal ambient temperatures from 2000 to 2019: A three-stage modelling study. *The Lancet Planetary Health*, *5*(7), e415–e425. https://doi.org/10.1016/S2542-5196(21)00081-4

A Appendix

A.1 Abstract (English)

Despite Austria's exposure to a wide range of temperatures, comprehensive analyses of temperature-related mortality across regions, age groups and sex remain scarce. This thesis addresses that gap by examining the association between temperature and all-cause mortality for the period March 2011 to March 2025. Distributed lag non-linear models (DLNM) are fitted separately for each combination of federal state, age group and sex. Estimates are then combined using multivariate meta-analysis, based on which, temperature-attributable fractions are computed. The results confirm a reversed J-shaped temperature-mortality relationship, with a national minimum mortality temperature of approximately 16.6 °C. The temperature-mortality relationship remains broadly similar across federal states, but regional differences in temperature exposure lead to varying attributable burdens. An east-west gradient emerges for heat-attributable fractions, with Vienna, Burgenland and Lower Austria exhibiting the highest burdens. Females show consistently higher attributable fractions than males. Heat-attributable fractions are highest in the youngest age group, while cold-attributable fractions increase with age. Overall, cold-attributable mortality substantially exceeds heat-attributable mortality across all subgroups.

A.2 Abstract (German)

Obwohl Österreich eine große Bandbreite an Temperaturen aufweist, gibt es nach wie vor kaum umfassende Analysen zur temperaturbedingten Sterblichkeit über Regionen, Altersgruppen und Geschlechter hinweg. Die vorliegende Arbeit setzt an dieser Forschungslücke an und untersucht den Zusammenhang zwischen Temperatur und Gesamtmortalität für den Zeitraum von März 2011 bis März 2025. Für jede Kombination aus Bundesland, Altersgruppe und Geschlecht werden Distributed Lag Non-linear Modelle (DLNM) geschätzt. Die Ergebnisse werden anschließend mittels multivariater Meta-Analyse zusammengeführt und darauf aufbauend die auf Temperatur zurückführbaren Mortalitätsanteile berechnet. Die Ergebnisse bestätigen eine umgekehrt J-förmige Temperatur-Mortalitäts-Beziehung mit einem Sterblichkeitsminimum bei etwa 16,6 °C. Während diese Beziehung über die Bundesländer hinweg weitgehend konstant bleibt, führen Unterschiede in der regionalen Temperaturverteilung zu deutlichen regionalen Unterschieden in den temperaturbedingten Mortalitätsanteilen. Bei den hitzebedingten Anteilen zeigt sich ein Ost-West-Gradient, wobei Wien, das Burgenland und Niederösterreich die höchsten Belastungen aufweisen. Frauen weisen durchwegs höhere temperaturbedingte Mortalitätsanteile auf als Männer. Die hitzebedingten Anteile sind in der jüngsten Altersgruppe am höchsten, während die kältebedingten Anteile mit zunehmendem Alter steigen. Insgesamt übersteigt in allen Untergruppen die kältebedingte Mortalität die hitzebedingte erheblich.

A.3 Statement

All research, analysis and interpretation were conducted solely by myself. AI tools (Claude and ChatGPT) were used as assistive tools exclusively for language refinement to improve readability and phrasing, as well as for resolving technical issues in R.

A.4 Additional Figures and Tables

A.4.1 Data Sources and Grid Alignment

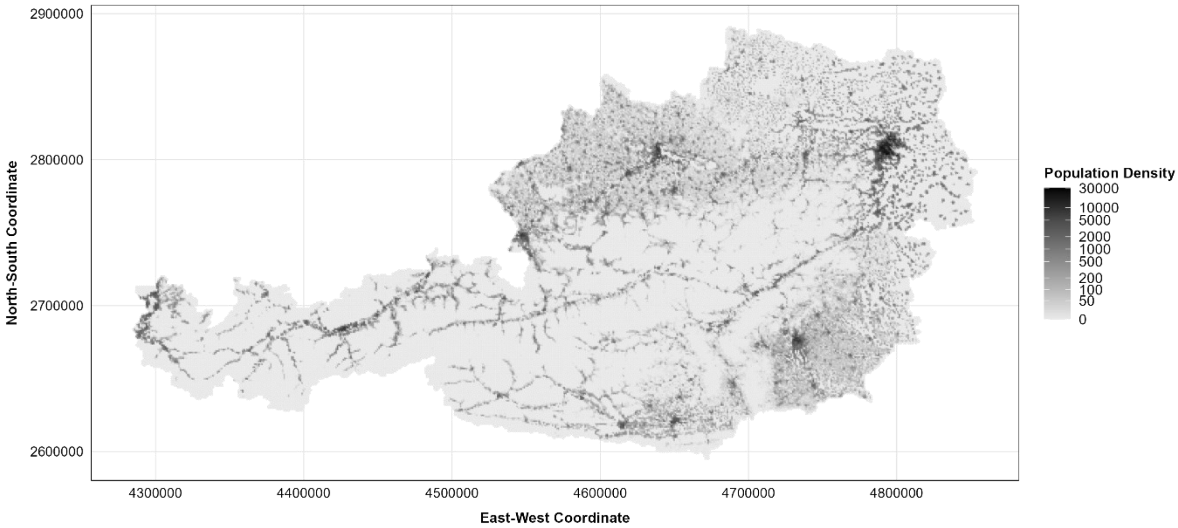

Figure 20: Population Density Grid of Austria

Notes: The figure displays the spatial distribution of population based on the 1 x 1 km grid from the Austrian population census. Source: Own visualisation based on Statistik Austria (2024a)

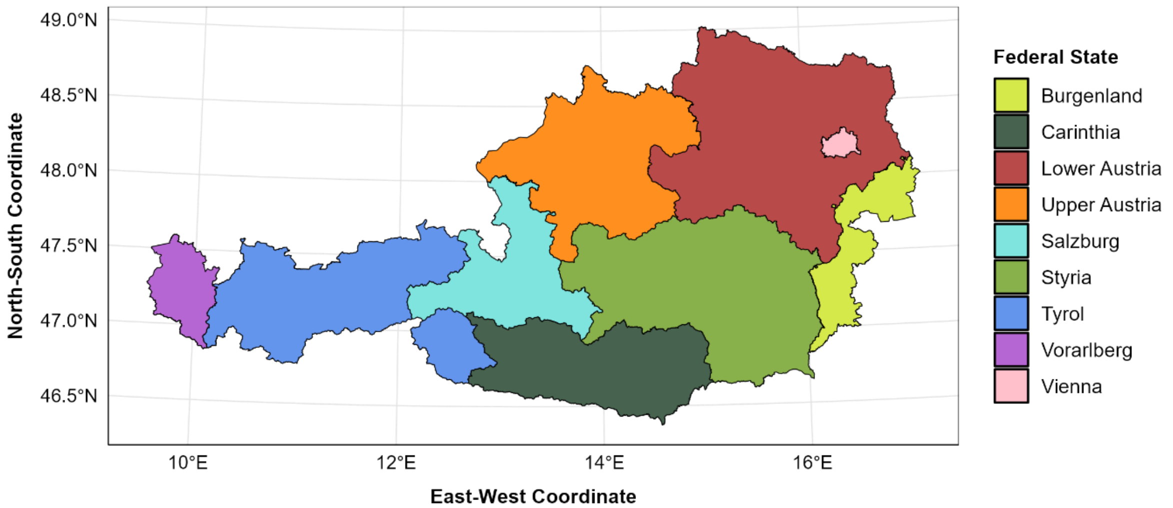

Figure 21: Federal State Borders of Austria (Shapefile)

Notes: The figure displays the administrative borders of Austria's nine federal states, derived from the official shapefile with reference date October 1, 2024. Source: Own visualisation based on Bundesamt für Eich- und Vermessungswesen (2024)

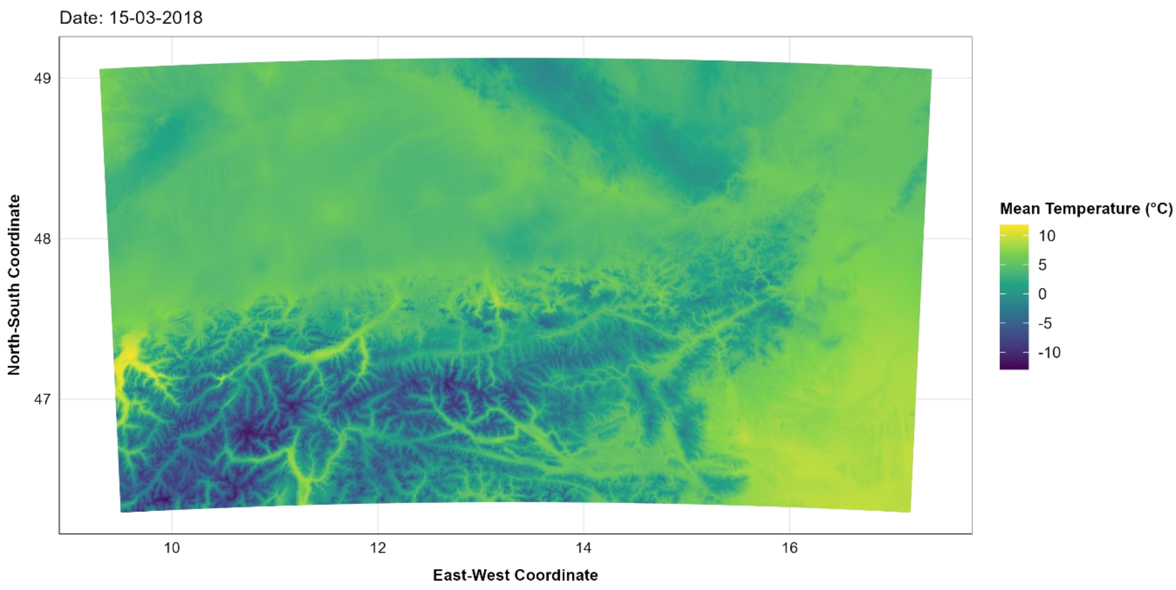

Figure 22: Spatial INCA Temperature Data for March 15, 2018

Notes: The figure displays the gridded air temperature at 2 metres height from the INCY analysis system at 1 x 1 km resolution for an example date. The data extends beyond Austria's borders. Source: Own visualisation based on GeoSphere (2021)

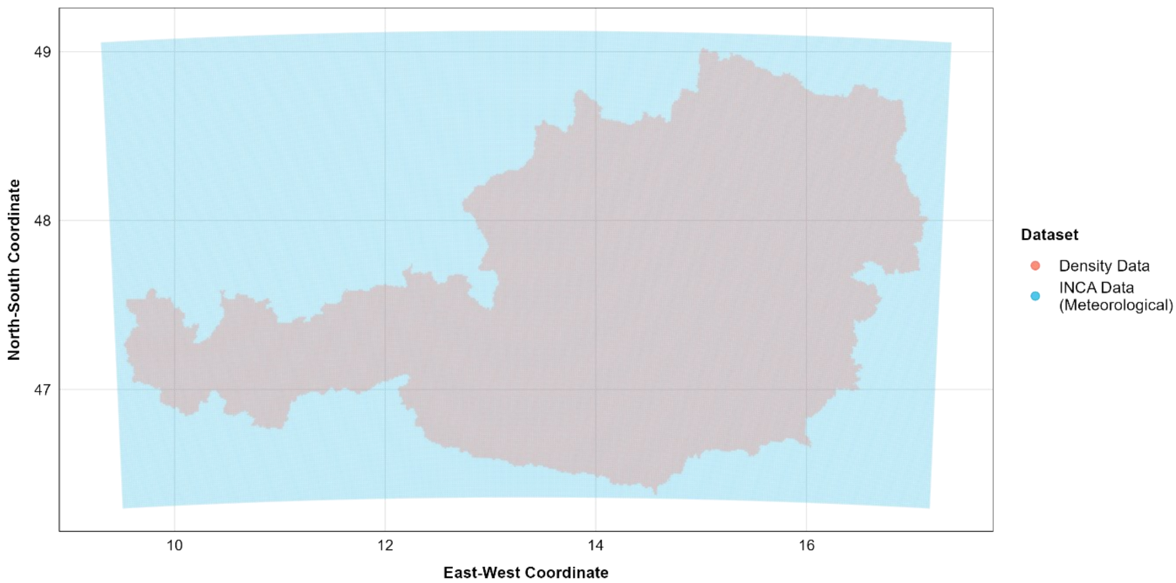

Figure 23: Overlap of INCA and Population Density Grid

Notes: The figure displays the spatial overlap between the INCA meteorological grid and the population density grid after projection onto a common coordinate reference system. Source: Own visualisation based on Bundesamt für Eich- und Vermessungswesen (2024), GeoSphere (2021) and Statistik Austria (2024a)

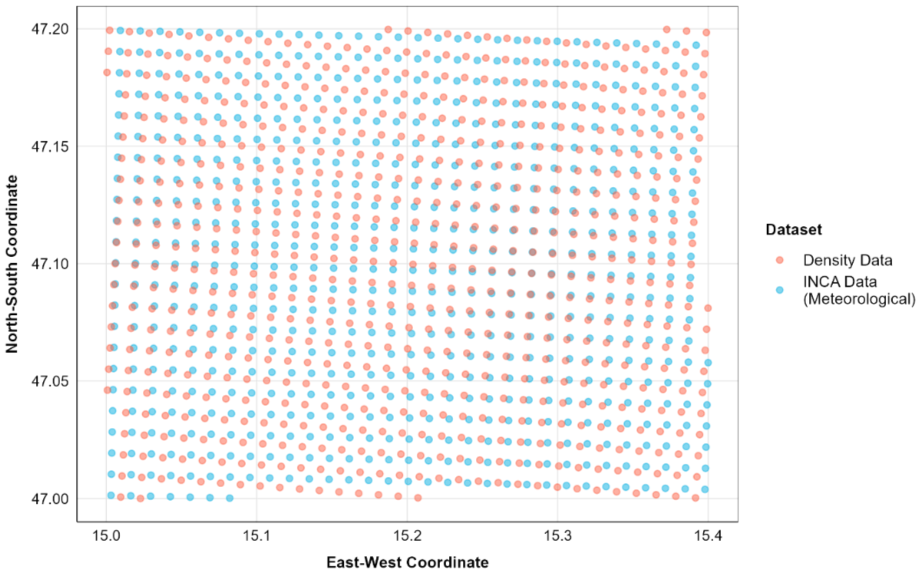

Figure 24: Overlap of INCA and Population Density Grid (Zoomed)

Notes: The figure displays a zoomed view of the spatial overlap between the INCA meteorological grid and the population density grid, illustrating the grid alignment at a local scale. Source: Own visualisation based on Bundesamt für Eich- und Vermessungswesen (2024), GeoSphere (2021) and Statistik Austria (2024a)

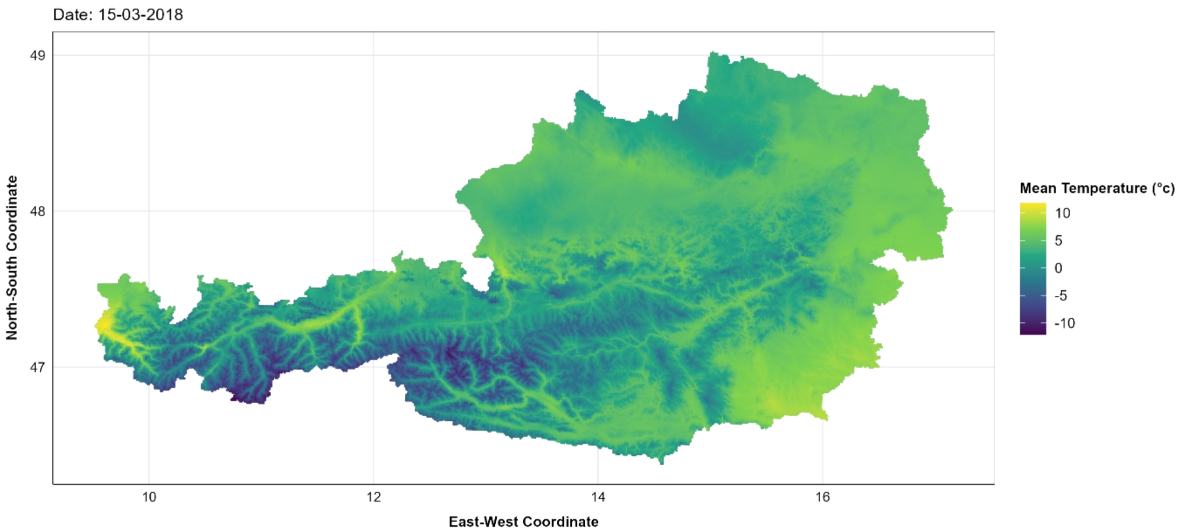

Figure 25: INCA Temperature Data Matched with Population Density for March 15, 2018

Notes: The figure displays the INCA temperature data after matching with the population density grid, restricting the data to populated areas within Austria. The example date is March 15, 2018. Source: Own visualisation based on Bundesamt für Eich- und Vermessungswesen (2024), GeoSphere (2021) and Statistik Austria (2024a)

A.4.2 Model Diagnostics and Sensitivity Analyses

Table 20: Dispersion Parameters of Stage 1 Models

Minimum	1st quartile	Median	Mean	3rd quartile	Maximum
0.71	0.85	0.89	0.90	0.93	1.13

Notes: The table summarises the distribution of dispersion parameters across all 90 Stage 1 models. Values closer to 1 indicate adequate model fit, values below 1 suggesting underdispersion and above 1 suggesting overdispersion. Source: Own computation based on Bundesamt für Eich- und Vermessungswesen (2024), GeoSphere Austria (2021), Statistik Austria (2024a), Statistik Austria (2025a) and Statistik Austria (2025c)

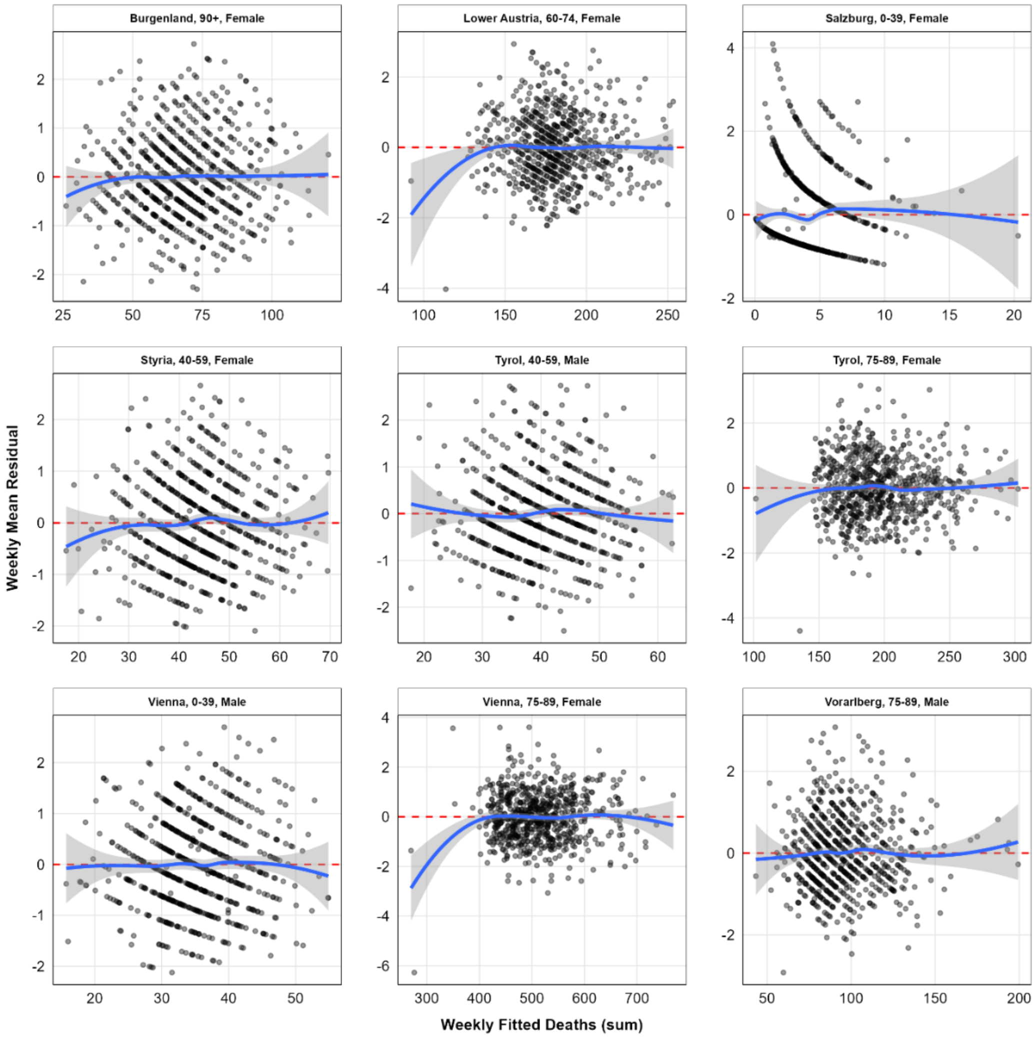

Figure 26: Residuals vs. Fitted Values (Stage 1)

Notes: The figure displays weekly mean Pearson residuals plotted against weekly summed fitted deaths for a representative subset of models, stratified by federal state, age group and sex. A smoothed trend line is included. If it is near zero, it indicates adequate specification of the mean structure. Source: Own computation based on Bundesamt für Eich- und Vermessungswesen (2024), GeoSphere Austria (2021), Statistik Austria (2024a), Statistik Austria (2025a) and Statistik Austria (2025c)

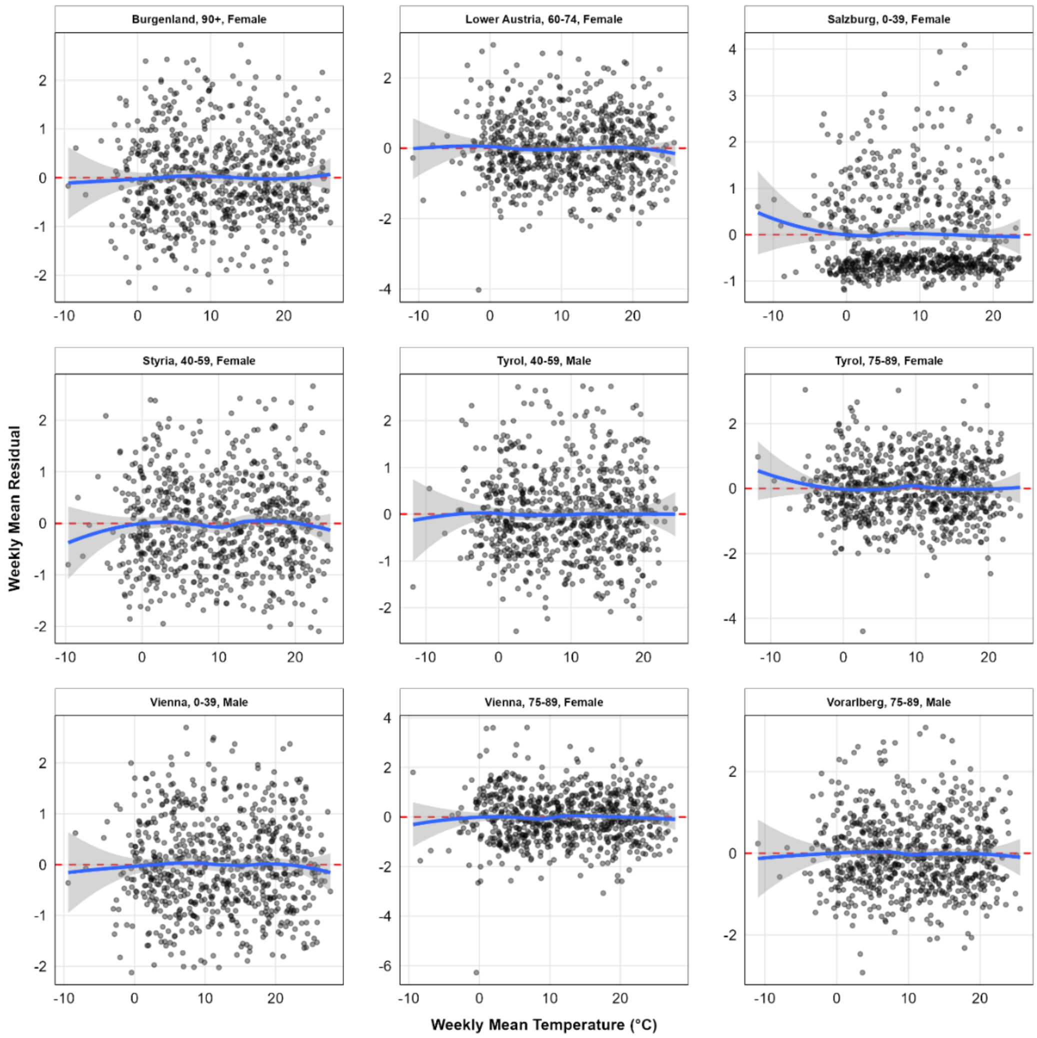

Figure 27: Residuals vs. Mean Temperature (Stage 1)

Notes: The figure displays weekly mean Pearson residuals plotted against weekly mean temperature for a representative subset of models, stratified by federal state, age group and sex. A smoothed trend line is included. If it is near zero, it indicates that the cross-basis adequately captures the exposure-response relationship. Source: Own computation based on Bundesamt für Eich- und Vermessungswesen (2024), GeoSphere Austria (2021), Statistik Austria (2024a), Statistik Austria (2025a) and Statistik Austria (2025c)

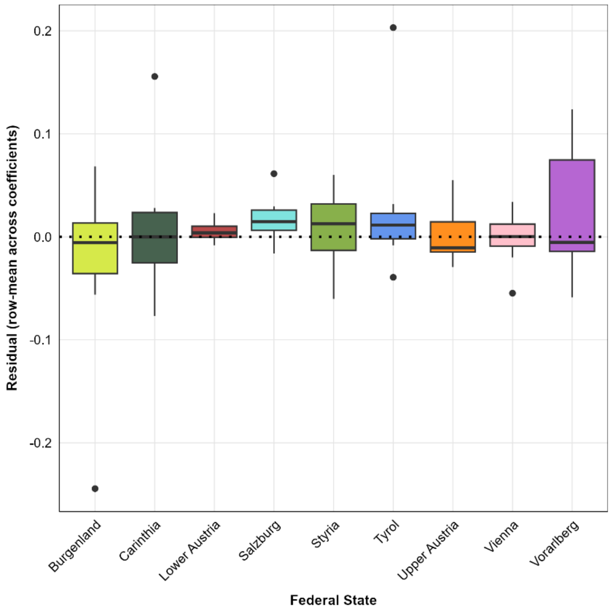

Figure 28: Meta-Regression Residuals by Federal State (Stage 2)

Notes: The figure displays the distribution of row-mean meta-regression residuals across federal states. Comparable spread and centring around zero indicate that the random-effects structure adequately accounts for between-state heterogeneity. Source: Own computation based on Bundesamt für Eich- und Vermessungswesen (2024), GeoSphere Austria (2021), Statistik Austria (2023), Statistik Austria (2024a), Statistik Austria (2025a) and Statistik Austria (2025c)

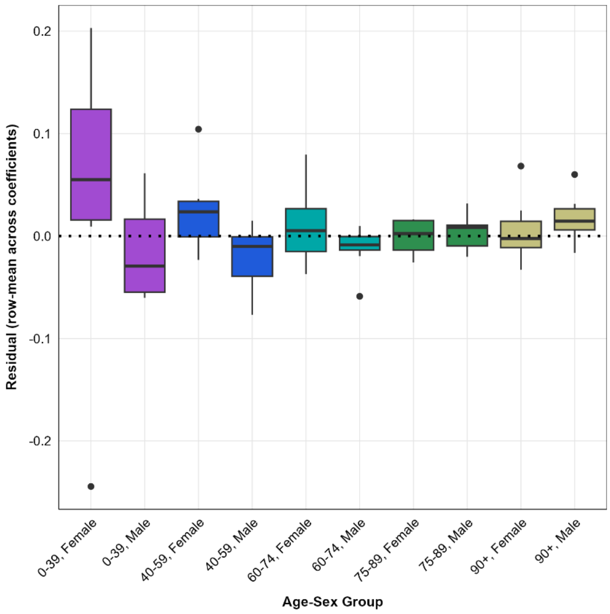

Figure 29: Meta-Regression Residuals by Age Group and Sex (Stage 2)

Notes: The figure displays the distribution of row-mean meta-regression residuals across sex and age groups. Similar variability and centring around zero suggest that the fixed and random effects adequately capture demographic heterogeneity in the temperature-mortality association. Source: Own computation based on Bundesamt für Eich- und Vermessungswesen (2024), GeoSphere Austria (2021), Statistik Austria (2023), Statistik Austria (2024a), Statistik Austria (2025a) and Statistik Austria (2025c)

Table 21: Sensitivity Analysis: Effect of Including Relative Humidity (Stage 1)

Model	**Mean MMT**	**Mean Relative Mortality at 5th percentile**	**Mean Relative Mortality at 95th percentile**
Base Model	14.822	1.120	0.972
Including Relative Humidity as Fixed Effect	14.950	1.121	0.968
Including Relative Humidity with Natural Spline	14.958	1.119	0.967

Notes: The table compares mean results across all 90 Stage 1 models for three specifications: The base model, a model including relative humidity as a fixed effect, and a model including relative humidity with a natural spline. MMT refers to the minimum mortality temperature. Relative mortality is evaluated at the 5th and 95th percentiles of the national temperature distribution. Source: Own computation based on Bundesamt für Eich- und Vermessungswesen (2024), GeoSphere Austria (2021), Statistik Austria (2024a), Statistik Austria (2025a) and Statistik Austria (2025c)

Table 22: Meta-Regression Results (Stage 2, Full Model)

	Intercept			**Age (numeric)**			**Sex: Male** (baseline: Female)		
	Estimate	**Conf. interval**	**p value**	**Estimate**	**Conf. interval**	**p value**	**Estimate**	**Conf. interval**	**p value**
cb_iv1.l1	-0.08	(-0.16, -0.01)	0.03	0.03	(-0.02, 0.08)	0.29	-0.04	(-0.10, 0.02)	0.16
cb_iv1.l2	0.02	(-0.06, 0.10)	0.64	-0.02	(-0.08, 0.04)	0.58	-0.06	(-0.12, 0.00)	0.03
cb_iv1.l3	0.01	(-0.03, 0.06)	0.62	-0.04	(-0.09, 0.02)	0.16	0.05	(-0.02, 0.12)	0.13
cb_iv1.l4	-0.02	(-0.07, 0.03)	0.36	-0.19	(-0.35, -0.03)	0.02	0.08	(-0.05, 0.21)	0.23
cb_iv1.l5	-0.11	(-0.25, 0.03)	0.13	0.13	(-0.06, 0.32)	0.17	-0.07	(-0.20, 0.07)	0.32
cb_iv2.l1	-0.01	(-0.08, 0.07)	0.87	-0.01	(-0.07, 0.05)	0.80	0.01	(-0.06, 0.07)	0.83
cb_iv2.l2	0.03	(-0.05, 0.12)	0.44	-0.02	(-0.09, 0.04)	0.45	0.00	(0.00, 0.00)	0.08
cb_iv2.l3	0.00	(0.00, 0.00)	0.10	0.00	(0.00, 0.00)	0.84	0.00	(0.00, 0.00)	0.84
cb_iv2.l4	0.00	(0.00, 0.00)	0.86	0.00	(0.00, 0.00)	0.13	0.00	(0.00, 0.00)	0.14
cb_iv2.l5	0.00	(0.00, 0.00)	0.87	0.00	(0.00, 0.00)	0.63	0.00	(0.00, 0.00)	0.81
cb_iv3.l1	0.00	(0.00, 0.00)	0.02	0.00	(0.00, 0.00)	0.20	0.00	(0.00, 0.00)	0.83
cb_iv3.l2	0.00	(0.00, 0.00)	0.98	0.00	(0.00, 0.00)	0.93	0.00	(0.00, 0.00)	0.07
cb_iv3.l3	0.00	(0.00, 0.00)	0.58	0.00	(0.00, 0.00)	0.01	0.00	(0.00, 0.00)	0.06
cb_iv3.l4	0.00	(0.00, 0.00)	0.01	-0.01	(-0.04, 0.02)	0.50	0.03	(0.01, 0.04)	0.01
cb_iv3.l5	0.00	(-0.02, 0.02)	0.91	-0.03	(-0.06, 0.00)	0.09	0.01	(-0.01, 0.04)	0.18
cb_iv4.l1	0.00	(-0.02, 0.02)	0.74	0.01	(-0.01, 0.03)	0.18	0.00	(-0.02, 0.02)	1.00
cb_iv4.l2	-0.02	(-0.04, 0.00)	0.11	0.01	(0.00, 0.03)	0.16	-0.03	(-0.09, 0.03)	0.38
cb_iv4.l3	0.04	(-0.01, 0.09)	0.09	0.01	(-0.04, 0.06)	0.63	-0.07	(-0.14, 0.00)	0.04
cb_iv4.l4	0.04	(-0.01, 0.09)	0.14	-0.02	(-0.05, 0.01)	0.22	0.01	(-0.02, 0.03)	0.63
cb_iv4.l5	0.00	(-0.02, 0.03)	0.87	-0.02	(-0.05, 0.02)	0.35	0.02	(-0.01, 0.04)	0.16

Notes: The table displays the Stage 2 meta-regression coefficient estimates, 95% confidence intervals and p-values for each cross-basis dimension. Female serves as the baseline category for sex. Values displayed as 0.00 are the result of rounding for display purposes and do not indicate zero effects. Source: Own computation based on Bundesamt für Eich- und Vermessungswesen (2024), GeoSphere Austria (2021), Statistik Austria (2024a), Statistik Austria (2025a) and Statistik Austria (2025c)

A.4.3 Descriptive Analysis

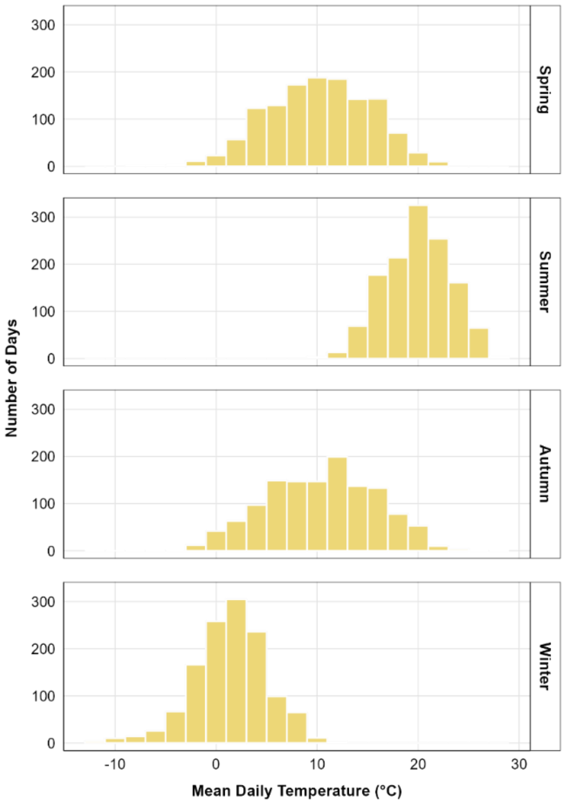

Figure 30: Distribution of Daily Mean Temperature by Season (National Level)

Notes: The figure displays the distribution of population density-weighted daily mean temperatures for each season, aggregated at the national level over the study period (March 2011 to March 2025). Source: Own computation based on Bundesamt für Eich- und Vermessungswesen (2024), GeoSphere (2021) and Statistik Austria (2024a)

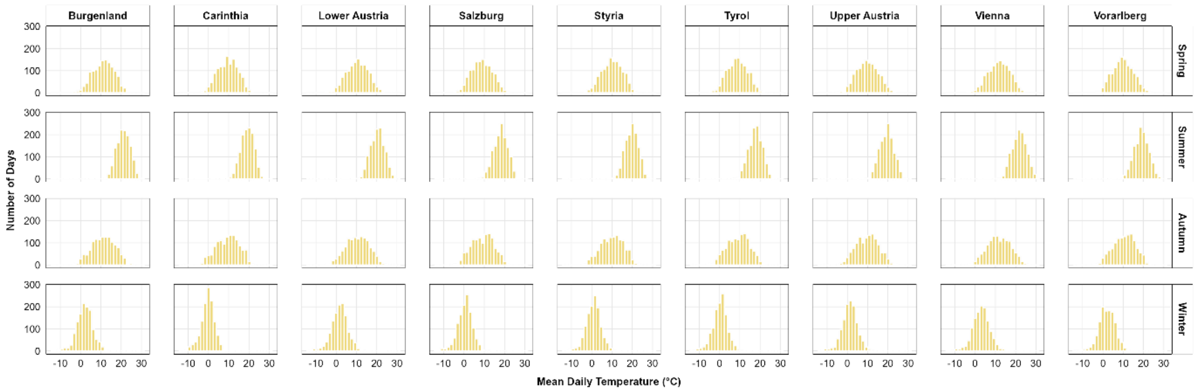

Figure 31: Distribution of Daily Mean Temperature by Federal State and Season

Notes: The figure displays the distribution of population density-weighted daily mean temperatures for each federal state, separated by season, over the study period. Source: Own computation based on Bundesamt für Eich- und Vermessungswesen (2024), GeoSphere (2021) and Statistik Austria (2024a)

Table 23: Percentiles of Daily Mean Temperature by Federal State (°C)

Federal State	p2.5	p10	p25	p50	p75	p90	p97.5
AUSTRIA	-2.9	0.4	3.9	10.5	17.0	21.0	24.2
Burgenland	-2.8	0.8	4.7	11.4	18.1	22.2	25.4
Carinthia	-4.5	-1.1	2.5	9.9	16.5	20.3	23.3
Lower Austria	-3.2	0.4	4.1	10.7	17.3	21.4	24.8
Salzburg	-4.2	-0.6	2.8	9.1	15.4	19.3	22.6
Styria	-3.5	-0.3	3.5	10.3	16.9	20.7	23.8
Tyrol	-4.4	-0.8	2.7	9.1	15.3	18.9	22.1
Upper Austria	-3.6	0.0	3.5	10.0	16.5	20.6	23.9
Vienna	-2.1	1.5	5.5	12.0	18.7	22.9	26.3
Vorarlberg	-2.7	0.5	4.4	10.4	16.5	20.3	23.6

Notes: The table displays selected percentiles of the population density-weighted daily mean temperature distribution for each federal state over the study period (March 2011 to March 2025). "AUSTRIA" represents the national aggregate. Source: Own computation based on Bundesamt für Eich- und Vermessungswesen (2024), GeoSphere (2021) and Statistik Austria (2024a)

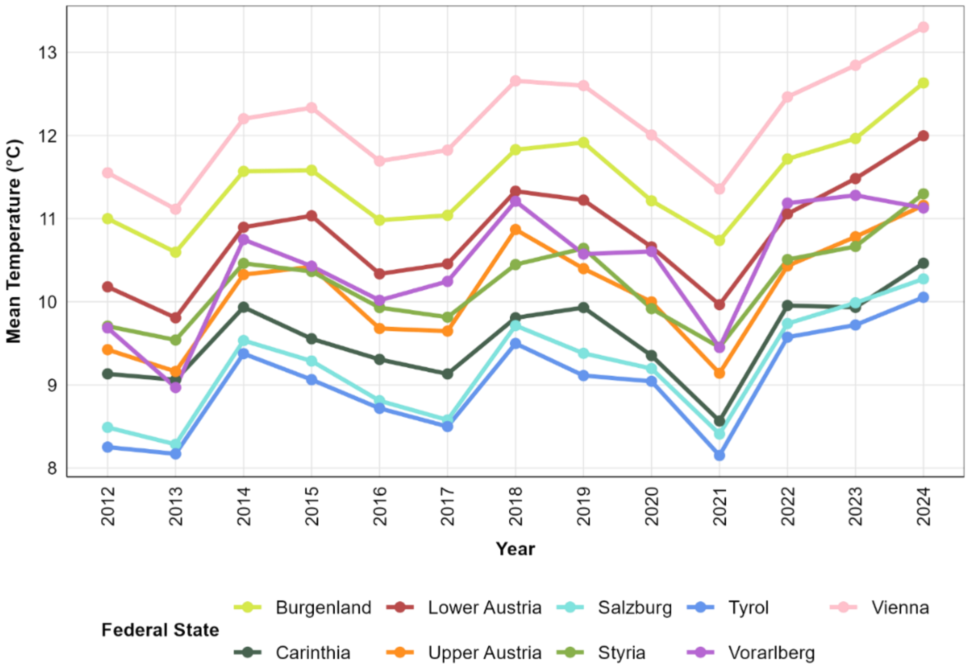

Figure 32: Annual Mean Temperature by Federal State (2012-2024)

Notes: The figure displays the population density-weighted annual mean temperature for each federal state for the years 2012 to 2024. Source: Own computation based on Bundesamt für Eich- und Vermessungswesen (2024), GeoSphere (2021) and Statistik Austria (2024a)

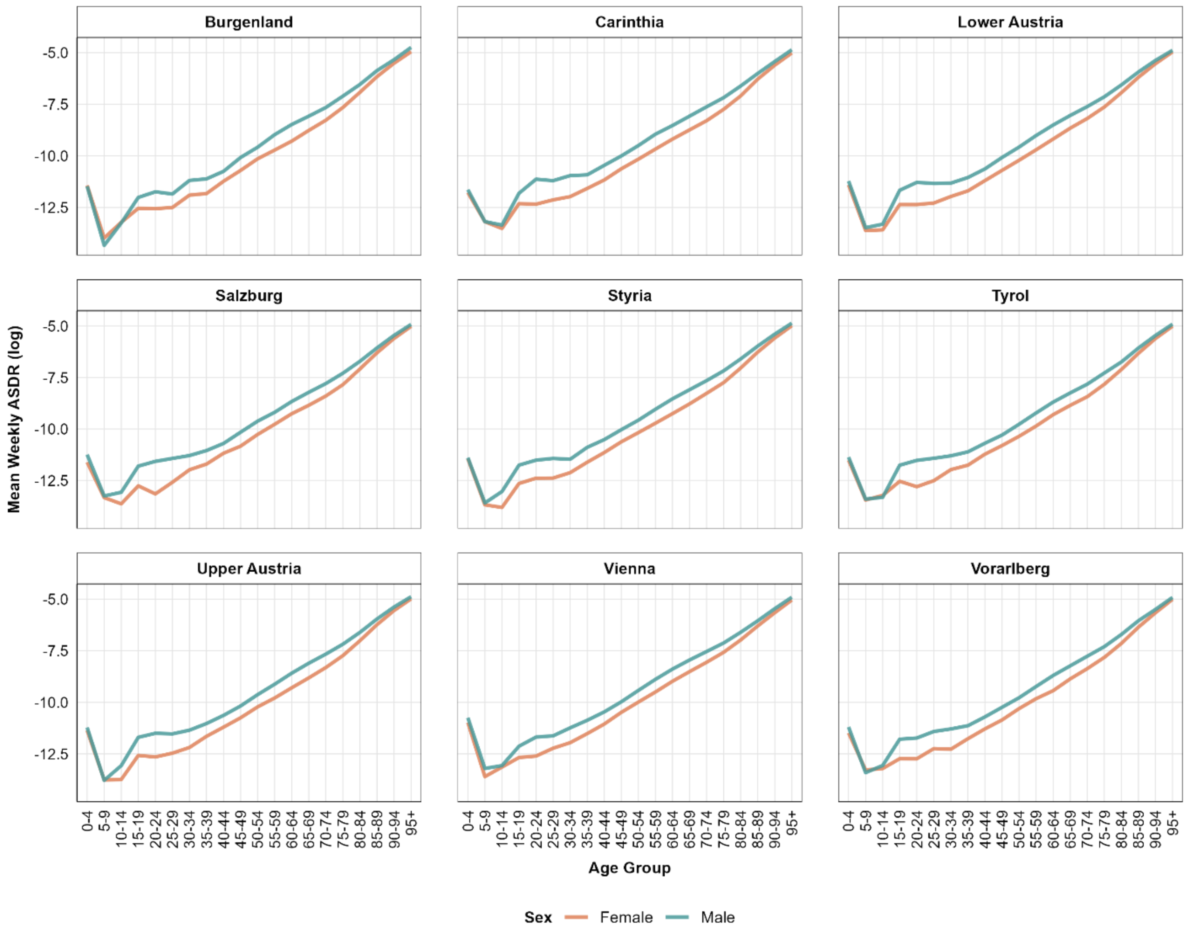

Figure 33: Mean Weekly Age-Specific Death Rate by Sex and Federal State (Log Scale)

Notes: The figure displays the mean weekly age-specific death rate (log-transformed) for 5-year age groups, separated by sex, for each federal state over the study period (March 2011 to March 2025). Source: Own computation based on Statistik Austria (2024b) and Statistik Austria (2025a)

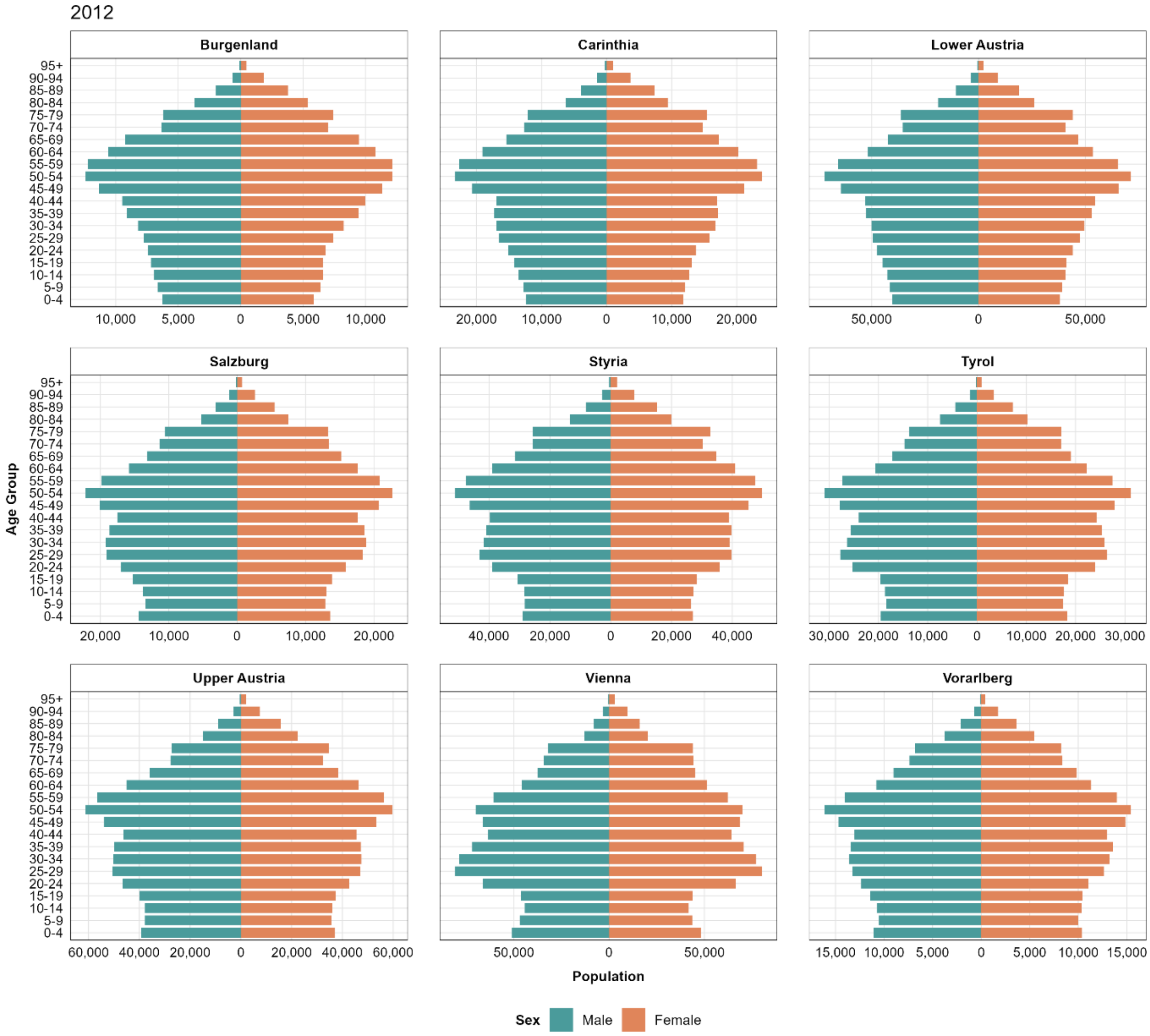

Figure 34: Population Pyramids by Federal State in 2012

Notes: Federal state-specific population by 5-year age group and sex. Source: Own visualisation based on Statistik Austria (2024b)

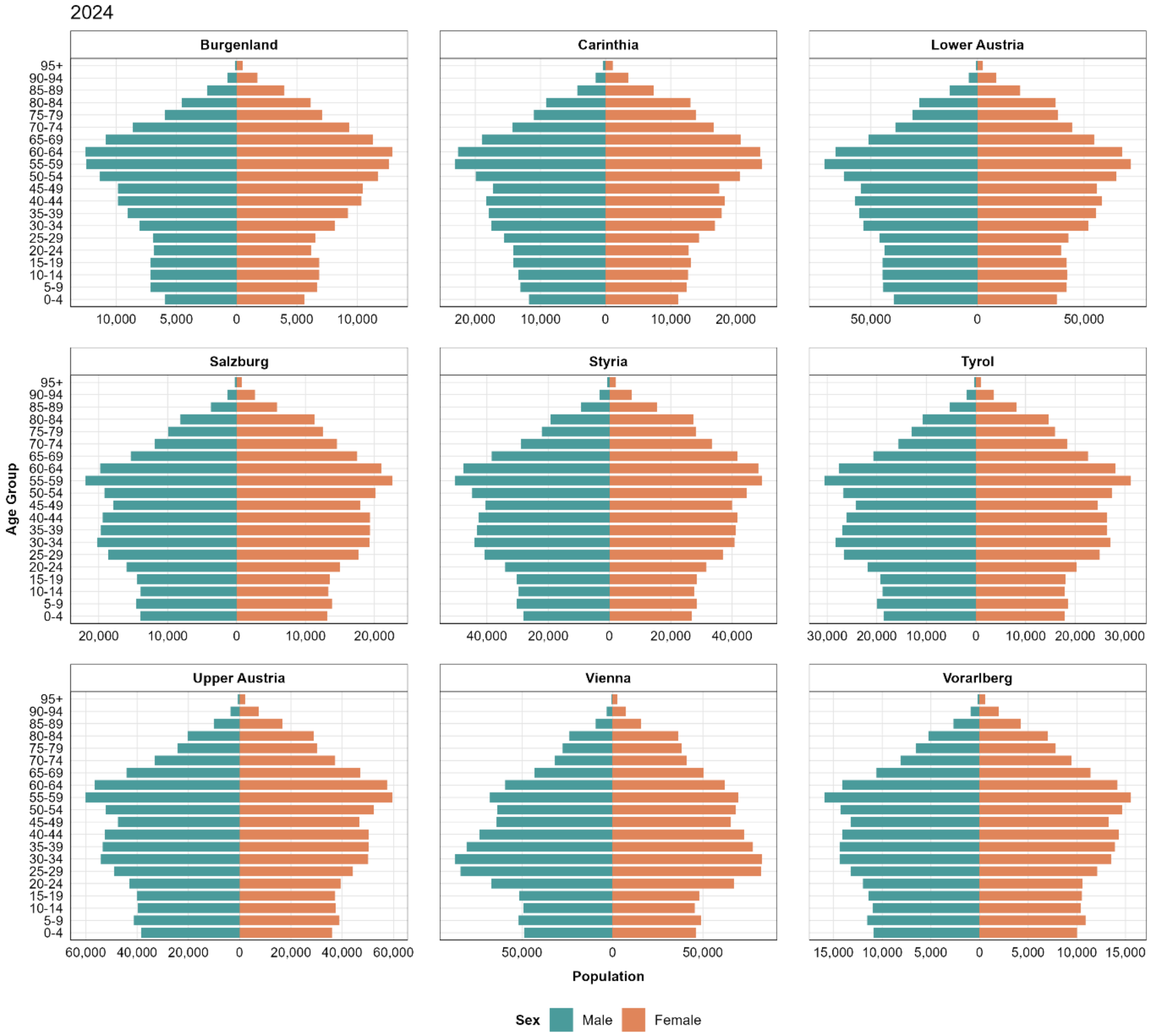

Figure 35: Population Pyramids by Federal State in 2024

Notes: Federal state-specific population by 5-year age group and sex. Source: Own visualisation based on Statistik Austria (2024b)

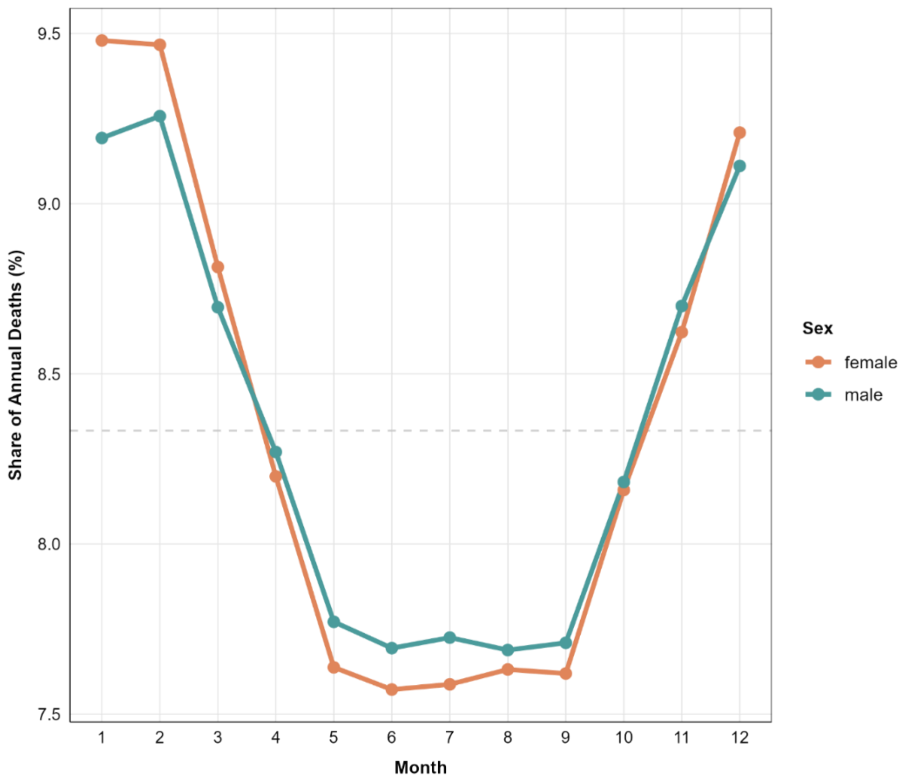

Figure 36: Monthly Share of Annual Deaths by Sex

Notes: The figure displays the mean monthly share of annual deaths (in percent) for each sex, averaged across the study period (March 2011 to March 2025). Numbers on the x-axis represent months (1 = January to 12 = December). Source: Own computation based on Statistik Austria (2025a) and Statistik Austria (2025c)

A.4.4 Statistical Analysis

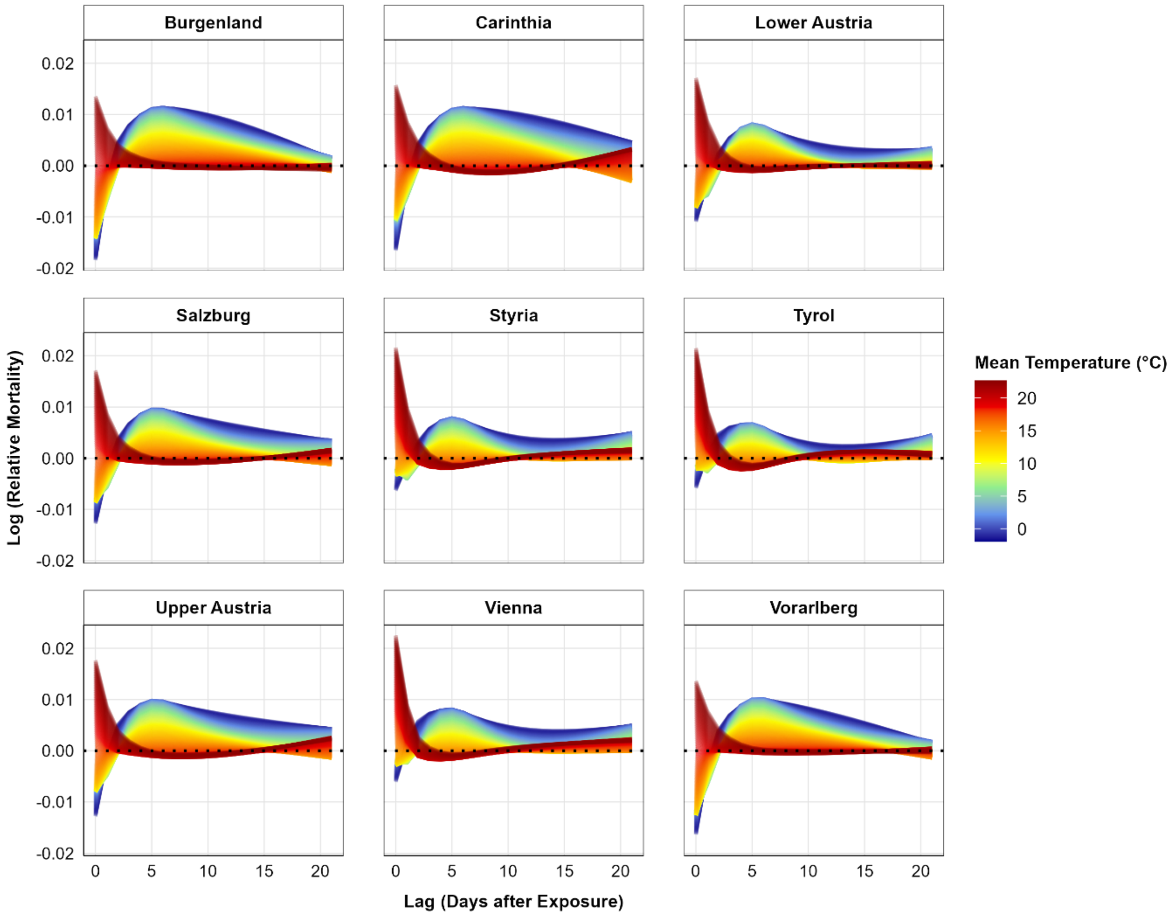

Figure 37: Lag-Response Curves by Federal State

Notes: The figure displays the lag-response relationship for each federal state for temperatures ranging from the 5th to the 95th percentile of the national temperature distribution. Values on the y-axis are log-transformed relative mortality, with the minimum mortality temperature of the corresponding federal state as the reference at each lag. Source: Own computation based on Bundesamt für Eich- und Vermessungswesen (2024), GeoSphere Austria (2021), Statistik Austria (2023), Statistik Austria (2024a), Statistik Austria (2025a) and Statistik Austria (2025c)

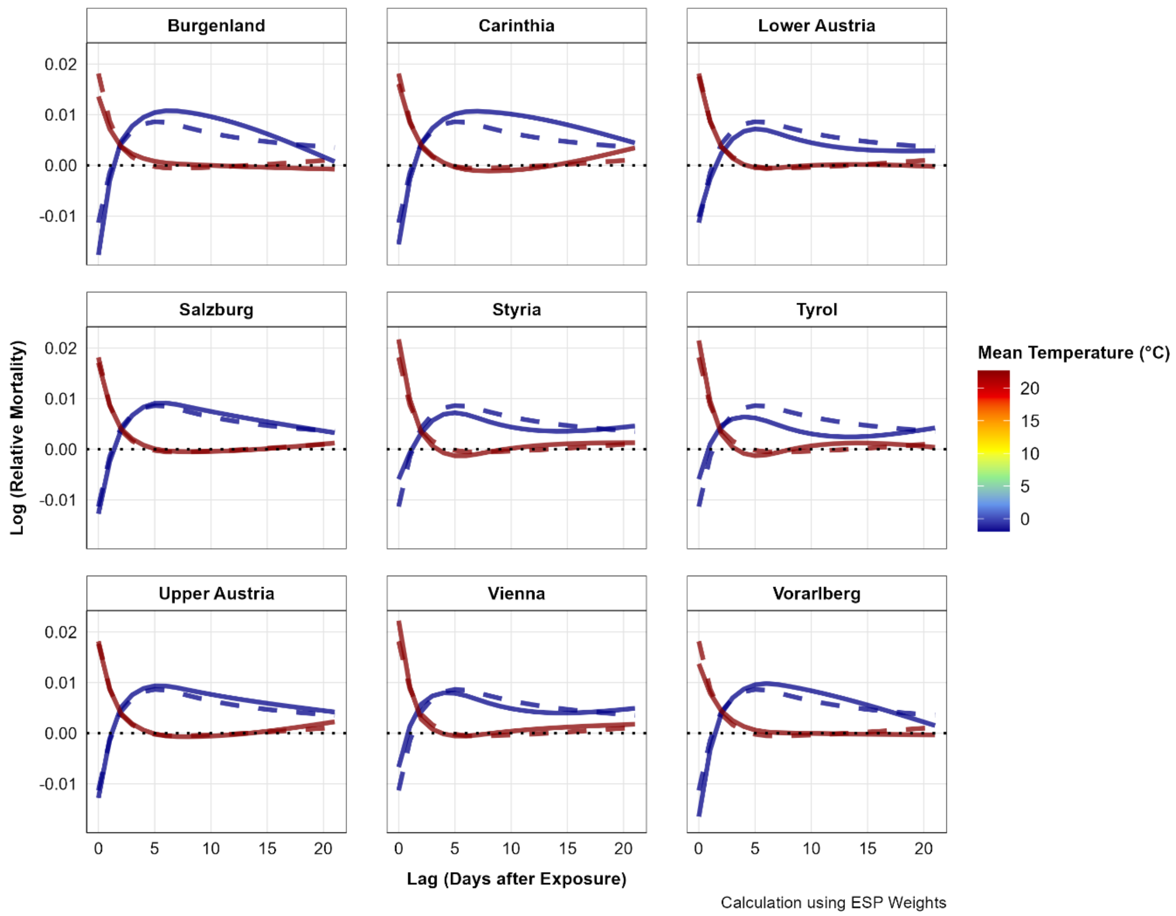

Figure 38: Lag-Response Curves at 5th and 95th Percentiles by Federal State with ESP Weights

Notes: The figure displays lag-response curves for each federal state at the 5th and 95th percentiles of the national temperature distribution, using European Standard Population (ESP) weights. Dashed lines represent the national-level estimates, solid lines represent ESP-weighted federal state estimates. Values on the y-axis are log-transformed relative mortality with the minimum mortality temperature as reference.

Source: Own computation based on Bundesamt für Eich- und Vermessungswesen (2024), GeoSphere Austria (2021), Statistik Austria (2023), Statistik Austria (2024a), Statistik Austria (2025a) and Statistik Austria (2025c)

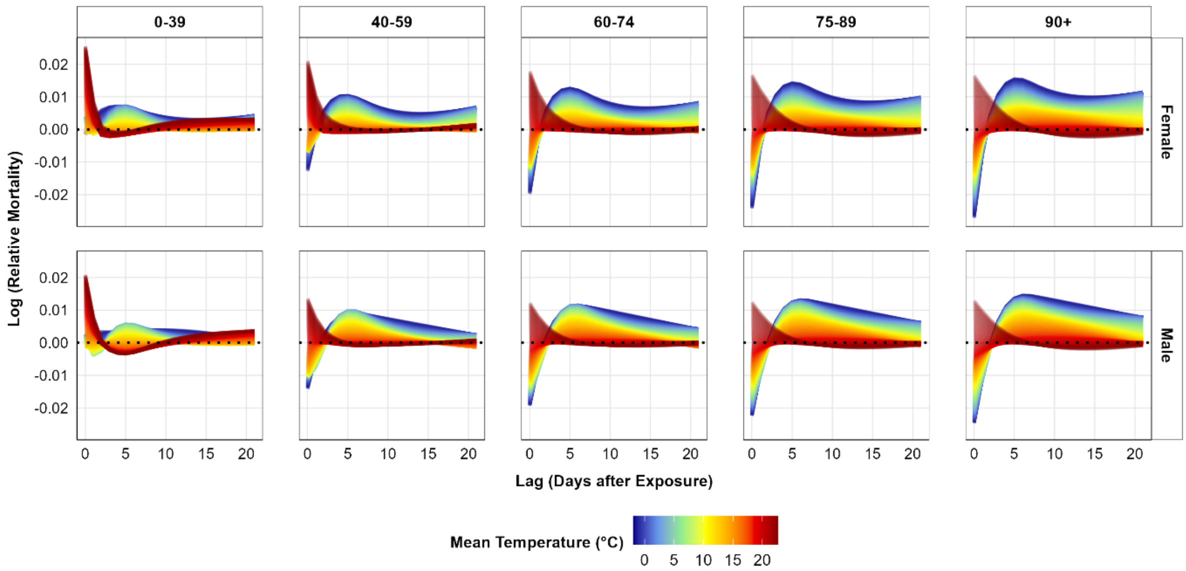

Figure 39: Lag-Response Curves by Age Group and Sex

Notes: The figure displays the lag-response relationship for each combination of age group and sex for temperatures ranging from the 5th to the 95th percentile of the national temperature distribution. Values on the y-axis are log-transformed relative mortality, with the minimum mortality temperature of the corresponding demographic subgroup as the reference at each lag. Source: Own computation based on Bundesamt für Eich- und Vermessungswesen (2024), GeoSphere Austria (2021), Statistik Austria (2023), Statistik Austria (2024a), Statistik Austria (2025a) and Statistik Austria (2025c)